The role of Angiotensin-(1-7) in a mouse model of renal fibrosis

Danielle Zimmerman

This thesis is submitted in partial fulfillment of the M.Sc. program in Cellular and Molecular Medicine

University of Ottawa

Ottawa, Ontario

Abstract

Angiotensin-(1-7) [Ang-(1-7)] is a heptapeptide component of the renin angiotensin system and the endogenous ligand for the Mas receptor. Ang-(1-7) is generated mainly via angiotensin converting enzyme 2 (ACE2)-dependent cleavage of Angiotensin (Ang) II. Studies suggest Ang-(1-7) may protect against progression of renal injury in experimental models of chronic kidney disease, although the responses may be dose dependent. The role of Ang-(1-7) in the progression of renal fibrosis in unilateral ureteral obstruction (UUO) remains unclear. We tested the hypothesis that endogenous Ang-(1-7) and low dose exogenous Ang-(1-7) would protect against renal injury in the UUO model, while high dose Ang-(1-7) would exacerbate renal injury. Male C57Bl/6 mice underwent UUO and received vehicle, the Ang-(1-7) antagonist A779, or one of three doses of Ang-(1-7) for 10 days. Treatment with A779 exacerbated renal injury as seen by increased fibronectin, transforming growth factor-β (TGF-β), and α-smooth muscle actin (α-SMA) expression, increased tubulointerstitial fibrosis scores, macrophage infiltration, apoptosis, and NADPH oxidase activity in obstructed kidneys. Paradoxically, delivery of exogenous Ang-(1-7) was associated with increased renal injury regardless of dose. Taken together, these data indicate the Mas receptor may be sensitive to concentrations of Ang-(1-7) within the obstructed kidney and that exogenous Ang-(1-7) stimulates pro-fibrotic and pro-inflammatory signalling through unclear pathways.

Table of Contents

List of Tables

List of Figures

List of Abbreviations

α-SMA	Alpha-smooth muscle actin
ACE	Angiotensin-converting enzyme
ACE2	Angiotensin-converting enzyme 2
AGT	Angiotensinogen
Ang I	Angiotensin I
Ang II	Angiotensin II
Ang-(1-4)	Angiotensin-(1-4)
Ang-(1-5)	Angiotensin-(1-5)
Ang-(1-7)	Angiotensin-(1-7)
ANOVA	One-way analysis of variance
APS	Ammonium persulfate
ARB	Angiotensin receptor blocker
AT1	Angiotensin Type 1
AT2	Angiotensin Type 2
BP	Blood pressure
BSA	Bovine serum albumin
CKD	Chronic kidney disease
CTGF	Connective tissue growth factor
EGTA	Ethylene glycol tetraacetic acid
EMT	Epithelial-to-mesenchymal transition
ERK	Extra-cellular related kinase
FBS	Fetal bovine serum
GFR	Glomerular filtration rate
GPCR	G-protein coupled receptor

IL-6	Interleukin – 6
JNK	c-Jun N-terminal kinase
KO	Knock out
MAPK	Mitogen activated protein kinase
MCP-1	Monocyte chemoattractant protein – 1
NADPH	Nicotinamide adenine dinucleotide phosphate
NF-kB	Nuclear factor-kappa B
NO	Nitric oxide
NRK	Rat kidney epithelial cells
PBS	Phosphate buffered saline
PCR	Polymerase chain reaction
PMA	Phorbol 12-myristate 13-acetate
PMSF	Phenylmethylsulphonyl fluoride
RAS	Renin Angiotensin System
SBP	Systolic blood pressure
SDS	Sodium dodecyl sulfate
SEM	Standard error of the mean
SHR	Spontaneously hypertensive rat
SHP-1	Src homology region 2 domain-containing phosphatase-1
TEMED	Tetramethulehtylenediamine
TGF-β	Transforming growth factor-β
TUNEL	Terminal deoxynucleotidyl trasferase dUTP nick end labelling
UUO	Unilateral ureteral obstruction
5/6 Nx	5/6 nephrectomy

Acknowledgments

I would like to thank my supervisor Dr. Kevin Burns for his continuous support and guidance throughout this project - even though I sometimes thought the biweekly meetings would drive us both nuts. I would also like to acknowledge my co-supervisor Dr. Rhian Touyz. Their knowledge, expertise, and patience made this both a productive and enjoyable experience.

I am also grateful to Dr. Chris Kennedy for being an integral part of my advisory committee and helping to shed light on the issues surrounding certain antibodies.

Members of the Kidney Research Centre including Joe Zimpelmann, Fengxia Xiao, Anthony Carter, and Alexi Gutsol have played important roles in this project and their assistance has been greatly appreciated.

Thank you also to the Italian Night Committee (Research Scholarship) for the financial assistance I received during my graduate studies.

Finally, I must thank my family who have provided endless encouragement and bottomless coffee throughout the entire process.

Statement of Contributions

All the experiments and assays described in this thesis were performed by Danielle Zimmerman except the following:

1. All UUO procedures and osmotic minipump implantations were performed by A. Carter. All osmotic minipumps were prepared for implantation by Danielle Zimmerman and she was present during surgical procedures.

2. Staining of histological sections was performed by A Gutsol. Analysis of TIF scores and F4/80 staining was also performed by A Gutsol.

3. Real time RT-PCR for the Mas receptor in Part 2 was performed by F. Xiao.

4. Immunoblotting for TGF-β in Part 1 and Part 2 were performed by J. Zimpelmann.

Parts of this thesis have been presented at International Conferences including the 2011 American Society of Nephrology Kidney Week (November, 12 2011: Endogenous Angiotensin-(1-7) Protects Against Tubulointerstitial Fibrosis in Mice with Unilateral Ureteral Obstruction, SA-PO2771) and the High Blood Pressure Research Conference (September 23 2011: The Angiotensin-(1-7) antagonist A779 increases kidney AT1 receptor expression and exacerbates tubulointerstitial fibrosis in mice with unilateral ureteral obstruction. LB044)

A review paper was published on this topic in Clinical Science (Angiotensin-(1-7) in kidney disease: A review of the controversies. Zimmerman, D and Burns, KD. Clin Sci (2012) 123, 333-346)

1.0 Introduction

1.1 The Renin Angiotensin System

The renin angiotensin system (RAS) is an extensively studied hormonal system that includes endocrine, paracrine, and autocrine signalling pathways (Kumar et al., 2012). Beginning with the discovery of renin in 1898 as a substance in renal extracts with pressor effects, the RAS has expanded to include multiple receptors, enzymes and bioactive peptides (Basso et al., 2001; Kumar et al., 2012). The enzymatic cascade of the RAS begins with the conversion of angiotensinogen (AGT) to angiotensin (Ang) I by renin and subsequently, Ang I into Ang II by angiotensin converting enzyme (ACE) (Figure 1). Once generated, Ang II can bind to two different G-protein coupled receptors (GPCRs), Ang II type 1 (AT1) or type 2 (AT2) receptors (Horiuchi et al., 2012).

Within the kidney, AT1 receptor mRNA has been detected in all tubular nephron segments, glomerular podocytes and mesangial cells, and vascular smooth muscle cells throughout the renal vasculature including the afferent and efferent arterioles (Carey et al., 2003; Miyata et al., 1999). AT2 receptor expression is high in the fetal kidney but rapidly decreases after birth. mRNA for the AT2 receptor has been found in proximal tubular cells, mesangial cells, the afferent arteriole and interstitial cells (Carey et al., 2003).

While the actions of the octapeptide Ang II have been well characterized, accumulating evidence suggests that the heptapeptide, Angiotensin-(1-7) [Ang-(1-7)] exerts important biological effects. Ang-(1-7) can be generated either directly from Ang II or Ang I, or indirectly from Ang I. The homologue of ACE, angiotensin converting

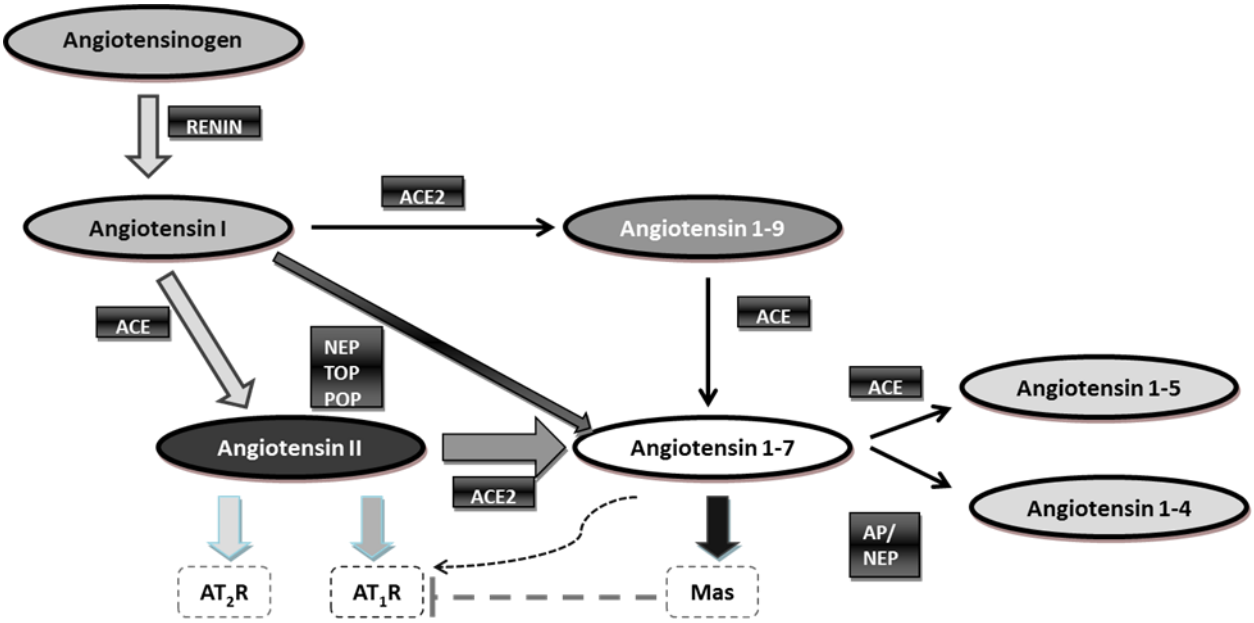

Figure 1: Pathways for the formation and degradation of Ang-(1-7). Pathways for the formation and degradation of Ang-(1-7) in kidney. (i) ACE2-dependent degradation of Ang II or ACE2-mediated cleavage of Ang I which can be converted to Ang-(1-7) by ACE. (ii) prolyl oligopeptidase (POP)-, neprilysin (NEP)-, or thimet oligopeptidase (TOP)-mediated degradation of Ang I. Ang-(1-7) is metabolised by either ACE to Ang-(1-5) or aminopeptidase (AP) or neprilysin to Ang-(1-4). Ang-(1-7) binds to the G-protein coupled receptor, Mas. At high concentrations, Ang-(1-7) may bind to and activate the AT1 receptor (as indicated by the dotted arrow). The Mas receptor is a physiological antagonist of the AT1 receptor. Adapted from (Zimmerman et al., 2012).

Abbreviations

ACE: angiotensin converting enzyme

NEP: neprilysin

TOP: thimet oligopeptidase

POP: prolyl oligopeptidase

AP: aminopeptidase

enzyme 2 (ACE2), is responsible for direct conversion of Ang II to Ang-(1-7) via cleavage of the Pro^{7}-Phe^{8} bond of Ang II. Ang-(1-7) can be directly generated from Ang I via several tissue endopeptidases including, prolyl oligopeptidase, neutral endopeptidase, or oligopeptidase. Ang-(1-7) is formed indirectly from Ang I through generation of Ang-(1-9) by ACE2 and subsequent degradation by ACE to form Ang-(1-7) (Ferrario, 2011). Ang-(1-7) has been shown to have a half-life of approximately 10 seconds in rats (Yamada et al., 1998) but has also been shown to accumulate in the plasma over time when administered subcutaneously (Mordwinkin et al.). Ang-(1-7) can be degraded to form either Ang-(1-5) or Ang-(1-4) by ACE or neprilysin, respectively (Chappell et al., 1998). No physiological role has yet been elucidated for either Ang-(1-5) or Ang-(1-4).

1.2 Angiotensin-(1-7) Signalling in the Kidney

Ang-(1-7) is regarded as an anti-hypertensive and anti-hypertrophic peptide that generally counteracts the effects of Ang II. Indeed, treatment of hypertensive subjects with ACE inhibitors has been shown to elevate circulating Ang-(1-7) levels suggesting Ang-(1-7) may play a role in ACE-dependent systolic blood pressure (SBP) reduction (Ferrario et al., 1991). In agreement with this, Iyer et al (Iyer et al., 1998) found elevated plasma Ang-(1-7) levels in the spontaneously hypertensive rat (SHR) treated with an ACE inhibitor and an Angiotensin Receptor Blocker (ARB). Administration of an antibody directed against Ang-(1-7) reversed the effects of ACE inhibitor and ARB treatment in the SHR providing strong evidence for a role of Ang-(1-7) in the

maintenance of SBP (Iyer et al., 1998). The anti-hypertensive effects of Ang-(1-7) have been linked to nitric oxide (NO) production and vasodilatation. Although studies have indicated that Ang-(1-7) has cardioprotective effects in both diabetic (Benter et al., 2007; Singh et al., 2011) and non-diabetic induced cardiac injury (Grobe et al., 2007; Loot et al., 2002), the effects of Ang-(1-7) within the kidney are incompletely understood.

In vivo detection of Ang-(1-7) was first reported in rat brain, adrenal, and plasma in 1989 (Chappell et al., 1989). Under physiological conditions, Ang-(1-7) is present in the plasma and kidney in picomolar concentrations, similar to Ang II (Pendergrass et al., 2008). Furthermore, Ang-(1-7) has been found in the urine in substantial amounts. In fact, urinary Ang-(1-7) is decreased in patients with untreated hypertension compared to healthy controls (Ferrario et al., 1998), providing initial evidence for a physiological role of Ang-(1-7) in human blood pressure (BP) regulation.

Ang-(1-7) has been identified as the endogenous ligand for the Mas receptor (Santos et al., 2003), another GPCR of the RAS. In mice lacking the Mas receptor, radioligand binding of Ang-(1-7) is abolished (Santos et al., 2003). The Mas receptor has been found in several tissues, including the kidney, heart, vasculature, liver, spleen, testis, and lung (Alenina et al., 2008). Within the kidney, the Mas receptor has been localized to afferent arterioles, proximal tubules, collecting ducts, the thick ascending limb of Henle, and the glomeruli of certain species (Gwathmey et al., 2010; Ren et al., 2002; Velkoska, Dean, Burchill et al., 2010). The Mas receptor may act as a physiological antagonist of the AT1 receptor *in vitro* through the formation of a hetero-oligomeric complex which attenuates Ang II/AT1 receptor signalling (Kostenis et al., 2005). The actions of Ang-(1-7) on the Mas receptor can be prevented by the Mas

receptor antagonist, A779 through displacement of the peptide from the receptor, however the exact mechanism of action of A779 is unknown (Gironacci et al.; Santos et al., 2003). Several Mas-related genes (mrgs) have been identified which code for GPCRs. At present, the binding affinity of Ang-(1-7) for these receptors is unknown. (Dong et al., 2001).

Ang-(1-7) signalling within the kidney has proven complex and appears to be species-, nephron-segment- or even cell-specific. Ang-(1-7) dilates isolated preconstricted afferent arterioles from rabbits, an effect that can be blocked by the Ang-(1-7) antagonist, A779 (Ren et al., 2002). This vasodilatory effect appears to be mediated via release of nitric oxide (NO) (Gwathmey et al., 2010). In proximal straight tubules isolated from rats, Ang-(1-7) has a biphasic effect on fluid absorption, with high concentrations (10^{-8} M) decreasing transport and low concentrations (10^{-12} M) stimulating transport, via binding to AT1 receptors as shown by blocking these effects with an angiotensin receptor blocker (ARB) (Garcia et al., 1994). In isolated pig proximal tubular cells, Ang-(1-7) reverses the stimulatory effect of Ang II on basolateral Na-ATPase activity and net sodium reabsorption via an A779-sensitive receptor (Lara et al., 2002). These *in vitro* results indicate the potential for complex interactions amongst angiotensin peptides and their receptors in the proximal tubule, which could ultimately lead to activation of common downstream pathways.

Within the proximal tubule, increasing evidence suggests Ang-(1-7) inhibits the growth stimulatory effects of Ang II. In rat proximal tubular cells, Ang-(1-7) attenuates Ang II stimulated phosphorylation of mitogen activated protein kinases (MAPKs), including p38, ERK1/2 (extra-cellular related kinase), and JNK (c-Jun N-terminal

kinase). The inhibitory effect of Ang-(1-7) is blocked by pre-treatment with A779 (Su et al., 2006). In LLC-PK_1 cells, a pig proximal tubular cell line, Ang-(1-7) inhibits glucose induced p38 MAPK phosphorylation. This effect was attributed to increased activity of SHP-1 (Src homology region 2 domain-containing phosphatase-1), a protein tyrosine phosphatase. Ang-(1-7) also attenuates glucose-induced TGF-β production but has no effect on increased fibronectin or collagen production in these cells (Gava et al., 2009). These data indicate that Ang-(1-7) inhibits both Ang II and glucose-induced MAPK phosphorylation in proximal tubular cells. In addition, the inhibition of glucose-induced TGF-β indicates Ang-(1-7) may be protective in a diabetic environment. However, in the absence of RAS activation or high glucose, high concentrations (10^{-5} M) of Ang-(1-7) stimulate the expression of TGF-β and connective tissue growth factor (CTGF) as well as markers of epithelial-to-mesenchymal transition (EMT) in rat kidney epithelial cells (NRK). These effects are blocked by pre-treatment with A779 (Burns et al., 2009). However, in the presence of high glucose, high concentrations of Ang-(1-7) (10^{-5} M) prevent EMT and TGF-β production in NRK cells (Zhou et al., 2012). Accordingly, the protective effects of Ang-(1-7) in the proximal tubule may be confined to states of RAS activation or a high glucose environment.

The complex signalling pathways of Ang-(1-7) are not confined to proximal tubular cells. Within mesangial cells, the variable responses to Ang-(1-7) may be the result of different culture conditions or species. For example, in human mesangial cells, incubation with Ang-(1-7) stimulates MAPK phosphorylation and arachidonic acid release, an effect blocked by A779. Furthermore, Ang-(1-7) has no effect on Ang II- or glucose-induced p38 MAPK phosphorylation in these cells (Zimpelmann et al., 2009).

Similarly, in rat mesangial cells, Ang-(1-7) stimulates ERK1/2 MAPK phosphorylation (G. C. Liu et al., 2012). In contrast, in primary cultures of rat mesangial cells, Ang-(1-7) attenuates high glucose-induced nicotinamide adenine dinucleotide phosphate (NADPH) oxidase activation (Oudit et al., 2010). In primary cultures of mouse mesangial cells, Ang-(1-7) inhibits Ang II-induced MAPK phosphorylation, and expression of NADPH oxidase subunits (Moon et al., 2011).

In summary, the effects of Ang-(1-7) on signalling *in vitro* are complex and appear to be cell specific and species specific. This complexity may underlie the contradictory data obtained *in vivo* on the role of Ang-(1-7) in various forms of kidney disease.

1.3 Chronic Kidney Disease

It is estimated that approximately 2 million Canadian have chronic kidney disease (CKD). CKD consists of kidney damage and/or decreased kidney function that persists for at least 3 months. More specifically, in humans, CKD is defined by a glomerular filtration rate (GFR) less than 60 mL/min/1.73 m^2 and/or the presence of albuminuria, hematuria, or renal damage as indicated by radiologic imaging. CKD is divided into 5 stages based on severity and defined by GFR, with the most severe, or Stage 5 CKD, being defined as a GFR less than 15 mL/min/1.73 $m^{2,}$ a condition that requires kidney replacement therapy with dialysis or transplantation to sustain life (Fink et al., 2012).

The decline in renal function seen in CKD is associated with progressive renal tubulointerstitial fibrosis, tubular loss through apoptosis, and the loss of peritubular

capillaries (Eddy, 2005). Tubulointerstitial fibrosis is the result of excess synthesis and deposition of extracellular matrix proteins, including collagens and fibronectin, by myofibroblasts, or activated fibroblasts (Fragiadaki et al., 2011). An activated RAS has been implicated in the activation of myofibroblasts and the progression of renal fibrosis (Meran et al., 2011). Accordingly, markers of renal injury including collagen I, III, and IV, fibronectin and α-SMA expression, macrophage infiltration, and urinary albumin excretion were all elevated in rats that received Ang II (s.c. osmotic minipumps) (Z. Liu, X. R. Huang, & H. Y. Lan, 2012).

1.4 Treatment of Chronic Kidney Disease

The development of treatments that block the actions of the RAS has led to major advances in delaying the progression of CKD. Pharmacological agents that inhibit ACE (ACE inhibitors) or block the AT1 receptor [Angiotensin Receptor Blockers (ARBs)] interfere with the production or actions of Ang II. ACE inhibitors and ARBs have proven effective in delaying the progression of both diabetic and non-diabetic CKD in humans (Jafar et al., 2001; Lewis et al., 1993; Turner et al., 2012). In adriamycin-induced nephropathy in mice, treatment with an ACE inhibitor attenuated proteinuria, renal TGF-β expression and MAPK activation compared to untreated mice. In rats, treatment with the ARB Losartan has been shown to reduce tubular injury and TGF-β expression, proteinuria and glomerulosclerosis in models of diabetic and non-diabetic CKD (Fraune et al., 2012; Huang et al., 2011; Manni et al., 2012). Despite the successes achieved with ACE inhibitors and ARBs, these agents do not completely prevent the progression

of CKD, either alone or when used together, suggesting there may be alternative pathways responsible for the progression of CKD (Remuzzi et al., 2002).

1.5 Angiotensin-(1-7) in Chronic Kidney Disease

Presently, there is little data available on the role of Ang-(1-7) in CKD. Studies in humans have focused on descriptive data about the levels of either Ang-(1-7) or ACE and ACE2. In children with hypertension and CKD plasma levels of Ang-(1-7) are significantly elevated compared to control subjects (Simoes e Silva et al., 2006). Interestingly, children with CKD who were normotensive did not have elevated plasma Ang-(1-7) suggesting a connection between hypertension and the generation of Ang-(1-7). In renal biopsies from patients with IgA nephropathy, glomerular and tubulointerstitial staining for ACE2 was significantly reduced compared to control subjects while glomerular ACE was significantly increased (Mizuiri et al., 2011). An increase in the intrarenal ACE/ACE2 ratio would favour the generation of Ang II and the degradation of Ang-(1-7), potentially promoting nephron loss in IgA nephropathy. However the role of Ang-(1-7) remains unclear given that elevated Ang II alone could be responsible for these effects.

Despite increasing evidence that Ang-(1-7) attenuates pro-fibrotic signalling and EMT *in vitro* the role of Ang-(1-7) in experimental CKD remains unclear. Indeed, studies examining the effects of exogenous Ang-(1-7) in experimental CKD have generated data that are difficult to reconcile. Treatment of experimental glomerulonephritis, induced by anti-Thy-1 antibody, in male rats with Ang-(1-7) (24 μg/kg/hr) for 5 days

resulted in a reduction in proteinuria, glomerulosclerosis, inflammatory cell infiltration, and glomerular mRNA for fibronectin and TGF-β (Zhang et al., 2010). These data suggest a protective role for Ang-(1-7) in experimental glomerulonephritis. However, in male mice with adriamycin-induced glomerular injury treatment with Ang-(1-7) (24 μg/kg/hr) had no effect on systolic blood pressure (SBP) or established proteinuria, despite elevated plasma Ang-(1-7) levels (van der Wouden et al., 2005). Whether these contrasting results of Ang-(1-7) can be explained by differences in the timing of treatment initiation or the state of RAS activation requires additional investigation.

Delivery of exogenous Ang-(1-7) in the 5/6 nephrectomy (5/6 Nx) model of experimental CKD has been associated with beneficial effects. In male C57Bl/6 mice subject to 5/6 Nx and treated with Ang-(1-7) (12.5 μg/kg/hr) for 12 weeks, elevations in plasma urea and creatinine were attenuated compared to untreated mice or mice that received the antihypertensive agent, hydralazine. In addition, cardiac function was preserved in mice that received Ang-(1-7) compared to mice that received hydralazine (Y. Li et al., 2009). Importantly, Ang-(1-7) had the same SBP lowering effect as hydralazine, suggesting the beneficial effects were not due a reduction in SBP alone (Y. Li et al., 2009). In a separate study, treatment of male 5/6 Nx FVB/N mice with Ang-(1-7) (24 μg/kg/hr) for only 4 weeks was associated with a significant increase in both renal and plasma Ang-(1-7) levels but had no effect on glomerular filtration rate (GFR) and only caused a non-significant reduction in urinary albumin excretion. Ang-(1-7) infusion was associated with an increase in relative mesangial area (Dilauro et al., 2010), indicating Ang-(1-7) may stimulate pro-fibrotic pathways in mesangial cells; an effect seen *in vitro* in human mesangial cells (Zimpelmann et al., 2009). In male rats subject to

5/6 Nx and treatment with Ang-(1-7) (24 μg/kg/hr) for 10 days a surprising increase in SBP, proteinuria, and plasma urea and creatinine levels was seen compared to vehicle treated rats (Velkoska, Dean, Griggs et al., 2010). Plasma levels of Ang-(1-7) were unchanged in this study despite delivery of Ang-(1-7), an effect attributed to increased cardiac ACE activity. Thus, although the effects of Ang-(1-7) in the 5/6 Nx model of CKD are unclear, data from these studies suggest that both dose and duration of treatment play an important role in determining the outcome.

1.6 Unilateral Ureteral Obstruction as a Model of Progressive Renal Fibrosis

Originally developed in the rabbit, the unilateral ureteral obstruction (UUO) model has been used to study the development of progressive renal fibrosis (Chevalier et al., 2009), often considered the final common pathway in CKD regardless of etiology (Meran et al., 2011). The model involves ligation of one ureter causing hydronephrosis of the obstructed kidney and subsequent tubular cell atrophy, interstitial inflammation and fibrosis (Klahr et al., 2002). There are three major pathways involved in the progression of renal fibrosis in the UUO model: 1) interstitial macrophage infiltration that leads to tubular apoptosis and fibroblast proliferation and activation; 2) tubular cell death by apoptosis leading to tubular atrophy; 3) phenotypic transition of renal epithelial cells to myofibroblasts (Chevalier et al., 2009). Several factors are increased in the obstructed kidney and play major roles in the development and progression of renal injury including Ang II and TGF-β, chemoattractants such as monocyte chemoattractant protein-1, various adhesion proteins, and collagens I, III, and IV (Klahr et al., 2002).

Ang II has been identified as a major mediator in the progression of renal fibrosis in the UUO model. Fern et al (1999) attributed 50-60% of the fibrosis seen in UUO to expression of the angiotensinogen gene. Furthermore, studies using ACE inhibitors or AT1 receptor knock out (KO) mice indicate that at least 50% of the resulting fibrosis in UUO is due to the actions of Ang II (Guo et al., 2001).

There are several advantages to the UUO model including that mice remain relatively healthy and do not develop uraemia due to the functional unobstructed kidney. Furthermore, the unobstructed kidney can serve as a control avoiding the need for sham operated animals. No exogenous toxin is needed to induce renal injury and as such the renal effects seen are not complicated by concerns about toxin effects within the kidney (Chevalier et al., 2009; Dendooven et al., 2011). Injury induced by UUO in C57Bl6/J mice has been shown to be irreversible after as a little as three days despite reversal of obstruction, indicating the UUO model more accurately mimics the pathogenesis of CKD rather than acute kidney injury, which is generally considered to be reversible.

1.7 The Role of Ang-(1-7) in Unilateral Ureteral Obstruction

Studies using the ACE2 KO mouse in UUO have provided some information about the potential role of Ang-(1-7) in renal fibrosis. As noted earlier, ACE2 is a membrane bound carboxypeptidase that preferentially cleaves carboxy-terminal amino acids. As the only known active homologue of ACE within the human genome, ACE2 plays an important role in counterbalancing the actions of ACE by degradation of Ang II

to Ang-(1-7) (Santos et al., 2008). ACE2 has been localized within the kidney specifically to tubular epithelial cells, renal vascular cells and the glomeruli (N. Li et al., 2005; Ye et al., 2006). Accumulating evidence suggests ACE2 has an important role in the development of diabetic kidney disease. In experimental diabetes, ACE2 inhibition or gene deletion exacerbates the progression of renal injury (Shiota et al., 2010; Soler et al., 2007; Wong et al., 2007). Furthermore, in the 5/6 Nx model of early chronic kidney disease, ACE2 inhibition is associated with a significant increase in urinary albumin excretion (Dilauro et al., 2010). These studies clearly indicate a protective role for ACE2 in the progression of diabetic and non-diabetic renal injury. However, the role of ACE2 in the progression of renal fibrosis in the UUO model has only recently been evaluated.

To examine the role of ACE2 in UUO, Liu et al (2012) performed UUO in ACE2 KO mice for 3 or 7 days. Obstructed kidneys from ACE2 KO mice showed enhanced renal injury compared to wild type mice as evidenced by increased extracellular matrix deposition, tubular atrophy, and collagen I and α-SMA expression. Furthermore, ACE2 KO led to greater inflammatory infiltration in obstructed kidneys compared to wild type mice. Enhanced renal injury was attributed to increased Ang II signalling via ERK1/2 MAPK, TGF-β, and SMAD2/3 in obstructed kidneys from ACE2 KO mice. Deletion of ACE2 was associated with an increase in Ang II and a decrease in Ang-(1-7) levels in obstructed kidneys compared to wild type mice (Z. Liu, X. R. Huang, H. Y. Chen et al., 2012). Thus, enhanced Ang II signalling could be attributed to either increased Ang II levels or a decline in counter-regulatory signalling via Ang-(1-7). While this study

suggests an important role for ACE2 in the progression of renal injury in the UUO model, the contributions of Ang-(1-7) remain unclear.

1.8 Renal Phenotype of Mas Receptor Knock Out Mice

Mice lacking the Mas receptor (Mas KO) have provided information on the role of endogenous Ang-(1-7) in renal structure and function. Mas KO mice on the C57Bl/6 background have normal BP, but reduced urine volume and fractional sodium excretion compared to wild type mice. These data suggest a loss of the natriuretic response to Ang-(1-7) within the nephron. In addition, Mas KO mice have elevated GFR, proteinuria, elevated renal TGF-β mRNA and extracellular matrix proteins including collagen and fibronectin. These findings suggest the Mas receptor plays a role in mediating anti-fibrotic pathways in the kidney. However, Mas KO mice had elevated renal AT1 receptor mRNA levels and thus the contribution of AT1 receptor signaling needs further exploration (Pinheiro et al., 2009).

1.9 The Effect of Mas Knockout in Unilateral Ureteral Obstruction

Esteban et al (2009) examined the role of the Mas receptor in the progression in renal fibrosis using mice lacking the Mas receptor (Mas KO). Mas KO mice were subject to UUO for 2, 5 or 7 days. After two days, obstructed kidneys from wild type mice showed mild tubular damage and inflammatory infiltration, whereas obstructed kidneys from Mas KO mice showed no tubular damage or inflammatory infiltration. By seven

days of UUO, wild type mice showed pronounced fibrosis and inflammatory infiltration in obstructed kidneys when compared to obstructed kidneys from Mas KO mice. Furthermore, wild type mice showed a greater increase the ratio of pro-apoptotic Bax versus anti-apoptosis Bcl-xL in obstructed kidneys compared to Mas KO. These unexpected data suggest deletion of the Mas gene attenuates the progression of renal injury in UUO.

To further assess the role of Ang-(1-7)/Mas receptor signalling in the UUO model, Esteban et al (2009) treated wild type mice with Ang-(1-7) (25 μg/kg/hr) and subjected them to UUO for 5 days. Treatment with Ang-(1-7) caused a greater increase in matrix deposition and inflammation in obstructed kidneys compared to obstructed kidneys of mice that received vehicle. In addition, treatment with Ang-(1-7) was associated with activation of nuclear factor-kappa B (NF-kB), an important pro-inflammatory transcription factor, in obstructed kidneys compared to vehicle treated mice suggesting a pro-inflammatory role for Ang-(1-7) in the UUO model.

To examine whether the pro-inflammatory effects of Ang-(1-7) infusion were dependent on existing renal injury, Ang-(1-7) (65 μg/kg/hr) was infused into healthy wild type mice for 5 days. Infusion of Ang-(1-7) was associated with an increase in renal macrophage infiltration that was not seen in mice that received A779 or in Mas KO mice. Furthermore, the inflammatory response remained when Ang-(1-7) was infused into mice that lacked AT1 and AT2 receptors, suggesting cross-reactivity with Ang II receptors is not responsible for Ang-(1-7)-stimulated renal injury (Esteban et al., 2009).

These data suggest a pro-inflammatory role for Ang-(1-7) and the Mas receptor in the UUO model. These results are difficult to explain given the protective effects of Ang-(1-7) seen in other models of kidney injury. However it is possible that the doses delivered in the study result in high intra-renal concentrations of Ang-(1-7) which may activate pro-fibrotic and pro-inflammatory responses via the Mas that require further clarification.

1.10 Summary and Rationale

In summary, CKD is a progressive disease involving extracellular matrix deposition and fibrosis ultimately leading to loss of renal function. Ang II plays a major role in the pathophysiology of CKD and while pharmacological inhibitors of either Ang II production or signalling have proven effective in delaying CKD progression, there may be alternative pathways, including Ang-(1-7)/Mas signalling, that may provide another target for treatment. However, the effects of Ang-(1-7) whether *in vitro* or in experimental CKD remain incompletely understood. While several studies indicate a protective role for Ang-(1-7) several others suggest a potential pro-fibrotic or pro-inflammatory role for the heptapeptide. These contradictory effects of Ang-(1-7) may be the result of dose, duration, experimental model, or strain specific responses to Ang-(1-7). Accordingly, we sought to determine the effects of Ang-(1-7) in the UUO model of CKD using both Ang-(1-7) antagonism and Ang-(1-7) infusion. Three separate doses of Ang-(1-7) were chosen to evaluate whether pro-fibrotic and pro-inflammatory effects seen in this model upon Ang-(1-7) administration are related to dose. Further

understanding of the role of Ang-(1-7) in CKD may elucidate the reasons behind the controversy present in the literature and provide novel therapeutic targets in human CKD.

1.11 Objectives

The major objective of this study was to evaluate the effects of Ang-(1-7) in a mouse model of renal fibrosis, unilateral ureteral obstruction (UUO).

Several specific objectives for this study were:

1. To determine the effect of Ang-(1-7) antagonism, using A779, on the progression of tubulointerstitial injury in the UUO model.

2. To determine the dose dependent effects of exogenous Ang-(1-7) on the progression of tubulointerstitial injury in the UUO model. Three doses of Ang-(1-7) were used: 6 µg/kg/hr, 24 µg/kg/hr, 62 µg/kg/hr.

3. To determine the effect of co-administration of A779 and Ang-(1-7) on the progression of tubulointerstitial injury in the UUO model.

4. To determine the effects of A779 on signalling in primary cultures of mouse proximal tubular cells.

1.12 Hypothesis

The main hypothesis of this study was that endogenous Ang-(1-7) and delivery of low dose exogenous Ang-(1-7) would ameliorate renal injury in UUO. On the other hand, it was hypothesized that delivery of exogenous high dose Ang-(1-7) would exacerbate renal injury associated with UUO.

Specific hypotheses for this study were:

1. Angiotensin-(1-7) antagonism, using A779, was predicted to exacerbate renal injury caused by UUO.

2. Exogenous Angiotensin-(1-7) was hypothesized to ameliorate renal injury associated with UUO at low (6 µg/kg/hr) and possibly moderate (24 µg/kg/hr) while high (62 µg/kg/hr) dose Ang-(1-7) would exacerbate renal injury.

3. Co-administration of A779 with Ang-(1-7) was hypothesized to reduce renal injury associated with UUO by blocking deleterious Ang-(1-7)/Mas mediated signalling pathways stimulated by high intra-renal levels of Ang-(1-7).

4. Administration of A779 to primary cultures of mouse proximal tubular cells was hypothesized to have no effect on signalling in these cells.

2.0 Materials and Methods

2.1 Experimental Protocol

2.1.1 General

Male C57Bl/6 mice, at 10 weeks of age, were obtained from Charles River Laboratories (Montreal, QC, Canada). Mice were housed in the Animal Care Facility at the University of Ottawa with free access to food and water. All experimental protocols were approved by the University of Ottawa Animal Care and Use Committee and performed according to the recommendations of the Canadian Council for Animal Care. At 12 weeks of age, mice were randomly divided into the groups outlined below. The project consisted of a preliminary study followed by three studies with a specific set of objectives. All mice were subject to UUO for 10 days. All drugs were delivered by subcutaneously implanted osmotic minipumps (Alzet Model 1002, Alza Corp., Palo Alto, CA, USA). Vehicle treated mice received Alzet minipumps containing sterile saline. As Alzet minipumps have a delay of approximately 2 hrs before peptides are released, pumps were placed in sterile saline for 2 hrs prior to implantation (Esteban et al., 2009).

2.1.2 Unilateral Ureteral Obstruction Procedure

All mice were subjected to UUO surgery, as previously described (Esteban et al., 2009; J. Ma et al., 1998). Unobstructed kidneys served as control kidneys. Surgery was performed under halothane anaesthesia. Prior to surgery, mice received 2-3 mLs of sterile saline s.c. The UUO surgery was performed by making an incision approximately

1 cm lateral of the midline towards the left flank of the mouse. The skeletal muscle was cut and retracted to expose the left kidney. The left ureter was located and dissected free of any connective tissue before two 6-0 silk ligatures were tied around the ureter - the upper ligature just below the left pole of the kidney and the lower ligature approximately 0.5 cm distal to the lower pole down the ureter. The ureter was divided between the ligatures. The muscle incision was sutured and the skin incision was closed with wound clips. Immediately upon completion of the UUO surgery Alzet osmotic minipumps were implanted for s.c. drug delivery. Implant sites were sealed with wound clips. Mice received saline or buprenorphine post-operatively at the discretion of University of Ottawa Animal Care for fluid maintenance and pain management, respectively. Wound clips were removed 7 days post-surgery. For all experiments, animals were sacrificed 10 days after UUO, except in initial time point studies which included a 7 and 10 day duration.

Preliminary studies were conducted to determine the optimal time point for this study and the effect of the ARB Losartan in the UUO model.

2.1.2 (a) Preliminary Study – Time Point Determination

1. UUO for 7 or 10 days (n = 3 for each time point)

2.1.2 (b) Effect of Losartan in UUO

1. Vehicle treated mice (n = 8)

2. Losartan treated mice (25 mg/kg/day) (n = 8)

2.1.2 (c) Part 1: The effect of Angiotensin-(1-7) antagonism, using A779, in UUO

1. Vehicle treated mice (n = 12)
2. A779 treated mice (31 µg/kg/hr) (n = 12)

2.1.2 (d) Part 2: Dose-dependent effect of exogenous Angiotensin-(1-7) in UUO

The doses used in this study were based on doses used throughout the literature (Benter et al., 2007; Benter et al., 2008; Esteban et al., 2009) and advice received from Dr. Robson Santos.

1. Vehicle treated mice (n = 6)
2. Ang-(1-7) treated mice (6 µg/kg/hr) (n = 6)
3. Ang-(1-7) treated mice (24 µg/kg/hr) (n = 6)
4. Ang-(1-7) treated mice (62 µg/kg/hr) (n = 6)

2.1.2 (e) Part 3: Effect of co-administration of A779 and Angiotensin-(1-7) UUO

In Part 3 of this study, the dose of A779 was increased to be in excess of the dose of Ang-(1-7) given.

1. Vehicle treated mice (n = 6)

2. A779 treated mice (83 µg/kg/hr) (n = 6)

3. Ang-(1-7) treated mice (62 µg/kg/hr) (n = 6)

4. Combination A779 and Ang-(1-7) treated mice (62 µg/kg/hr and 83 µg/kg/hr, respectively) (n = 6)

2.2 Blood Pressure Measurement

Systolic blood pressure (SBP) was monitored by tail cuff plethysmography (BP-2000, Visitech Systems, Apex, NC, USA) as previously described (Nadarajah et al.). Mice were trained for five consecutive days at 11 weeks of age. Experimental measures were taken at two time points: baseline measures were taken prior to surgery at 12 weeks of age and final measures were taken prior to sacrifice. Values for SBP are presented as the average of 8-10 measures per mouse.

2.3 Tissue Preparation

Mice were anaesthetized by isoflurane and euthanized by cardiac puncture 10 days post UUO surgery. Mice were perfused through the left ventricle with 10 mL ice cold phosphate buffered saline (PBS) before collection of tissue. The unobstructed and obstructed kidneys were processed and stored as follows: each kidney was quickly removed, weighed and bisected longitudinally with one half for histological analysis and the other half for immunoblotting, RNA isolation, and NADPH oxidase activity analysis. Tissue for histological analysis was fixed in 4% formalin. After the medulla was

removed, renal cortical tissue was snap frozen in liquid nitrogen and stored at -80°C for immunoblot analysis of fibronectin, α-SMA, TGF-β, and AT1 and AT2 receptors.

2.4 Plasma Analysis and Hematocrit Measurements

Blood samples for plasma analysis were collected by cardiac puncture using a heparinized syringe. Blood was transferred to 1.5 mL tubes containing an ice cold solution of protease inhibitor cocktail (0.01 mM p-hydroxy-mercury benzoate, 1.5 mM o-phenanthroline, 0.01 mM phenylmethylsulfonyl fluoride [PMSF], 0.05 mM pepstatin A, and 10 mM ethylenediaminetetraacetic acid [EDTA]) and centrifuged at 3000 x g for 10 min at 4°C. Plasma was stored at -80°C. Plasma electrolytes (Na^+, K^+, Cl^-, Ca^{2+}, PO_4^{3-}, HCO_3^-, Mg^{2+}), urea, creatinine, glucose, triglycerides, cholesterol, and albumin were analysed by Idexx Laboratories (Markham, ON, Canada).

A small volume (<20 µL) of blood was collected in heparinized micro-hematocrit capillary tubes (Baxter, Deerfield, IL, USA) for hematocrit measurements. Capillary tubes were spun at 2000 x g for 5 min at room temperature and hematocrit measurements were performed using a micro-hematocrit capillary tube reader (Critocaps, Oxford Lab., Baxter, Deerfield, IL, USA).

2.5 Histochemistry

At sacrifice, sections of mouse kidney were fixed in 4% formalin, dehydrated, and embedded in paraffin. Tissue sections were cut in 5 μm sections and stained with periodic acid Schiff. Kidney sections were analyzed in a blinded fashion for tubulointerstitial injury, macrophage infiltration, and apoptosis. Tubulointerstitial injury was assessed using a semi-quantitative scoring scale (Mizuno et al., 2001): 0: normal kidney, 1: minimal fibrosis (<25%), mild fibrosis (25-50%), moderate fibrosis (50-75%), 4: severe fibrosis (>75%). Tubulointerstitial injury was assessed by taking 5 images per kidney at 40X and grading them as described above. Images were analyzed without knowledge of treatment groups. Macrophage infiltration was assessed by anti-F4/80 staining. Sections were deparaffinized in xylene and rehydrated with 100% ethanol before being treated with Proteinase K for 25 min at 37°C and washing with 1X PBS. Sections were blocked with 10% donkey serum in 1% BSA in PBS for 1 hr before incubation with 1:200 anti - F4/80 antigen rat monoclonal anti-mouse antibody (eBioscience, San Diego, CA, USA) for 12-18 hrs at 4°C. Sections were rinsed with PBS before endogenous peroxidase activity was blocked by incubating the slides with 0.3% H_2O_2 for 30 min at room temperature. Secondary biotinylated donkey anti-rat IgG (1:200) was applied for 1 hr at room temperature following by streptavidin-conjugated horseradish peroxidase (Vector Laboratories, Burlingame, CA, USA) for 30 min and consequent DAB substrate development. Five images were taken per section at 40X magnification and a computer software program was used to analyze positive staining area. Images were analyzed without knowledge of treatment groups. Results are expressed as percent positive F4/80 staining. Apoptosis in renal cortical and medullary

regions was assessed using the terminal deoxynucleotidyl transferase dUTP nick end labeling (TUNEL) Apoptosis Detection Kit (Genscript, Piscataway, NJ, USA) according to manufacturer instructions. Section analysis was performed without knowledge of treatment groups by taking 5 images at 20X magnification per renal section. Each section was examined for TUNEL positive nuclei. Results are expressed as the number of TUNEL positive nuclei per field. DNAse treated sections and intestinal sections were used as positive controls for TUNEL positive nuclei.

2.6 Immunoblotting

2.6.1 General Protocol

Renal cortical tissue was homogenized using a COE CapMixer desktop homogenizer (GC America, Alsip, IL, USA). Lysis buffer (1X PBS, 1% tert-Octylphenoxy poly(oxyethylene)ethanol (IGEPAL), 0.5% sodium deoxycholate, 0.1% sodium dodecyl sulfate [SDS], 50 mM Tris-HCl, 2.0 mM Na_3PO_4, 1.0 mM PMSF, 1 µg/mL leupeptin, 100 µg/mL aprotonin, 100 µg/mL pepstatin) was added to homogenized tissue and samples were centrifuged at 13 000 g for 5 min. Supernatant was collected and stored at -80°C for determination of protein concentration and immunoblotting. Protein concentration was measured by BioRad D_C Protein Assay (BioRad, Mississauga, Ontario, Canada). Samples were prepared with equal amounts of protein lysate (20 µg) and 6X loading buffer (7.0% 4X Tris-HCl/SDS, 3.0% mL glycerol, 0.1 g/mL SDS, 6.0% β-mercaptoethanol, 0.12 mg/mL bromophenol blue) with distilled water to a total volume of 36 µL for loading. Samples were boiled for 5 min prior to loading on 7.5% to 15% SDS-polyacrylamide gels (1.5M Tris-HCl pH 8.8, 40% acrylamide/Bis 37.5:1, 10% SDS,

10% ammonium persulphate [APS], 0.05% tetramethylethylenediamine [TEMED] for 1 gel), chosen based on molecular weight of proteins, with a 4% stacking gel (1.5M Tris-HCl ph 8.8, 40% acrylamide/Bis 37.5:1, 10% SDS, 10%APS, 0.1% TEMED) and transferred to nitrocellulose membranes (BioRad). Membranes were washed in Tris-buffered saline (pH 7.6) containing 0.1% Tween (TBS-T) prior to blocking with 5% skim milk in TBS-T for 1 hr at room temperature. Membranes were incubated with primary antibody for 12-18 hrs at 4°C. After incubation, membranes were washed 4 times for 5 mins with TBS-T prior to incubation with their respective secondary antibodies for 1 hr at room temperature and washed 4 times for 5 mins with TBS-T. A list of primary and secondary antibodies and their concentrations is depicted in Appendix 1. Proteins were detected by enhanced chemiluminescence (ECL; GE Health Care Bio-Sciences, Baie d-Urfe, Quebec, Canada). To control for protein loading, membranes were stripped and reprobed with antibody to GAPDH. Immunoblot signals were quantified by densitometry and corrected for total protein levels using image-analysis software (Scion Image, Scion Corporation, Houston, TX, USA).

2.6.2 Determination of AT1 Receptor Expression in Renal Cortical Tissue

To determine the specificity of antibodies developed against the AT1 receptor, mouse $AT1_{a/b}$ knock out renal and heart tissues were obtained from the laboratory of Dr. Thomas M. Coffman (Duke University Medical Centre, Durham, NC, USA). KO renal and cardiac tissues were homogenized as described above and run on 10% SDS-PAGE gels along with protein lysates from wild type unobstructed and obstructed kidney

cortices from vehicle treated mice. Three antibodies from Santa Cruz (sc-579, sc-31181, sc-1173) (Santa Cruz, CA, USA), Sigma Aldrich (SAB3500209) (Oakville, ON, Canada) and Almone Labs (AAR-011) (Jerusalem, Israel) were tested to determine their specificity to the AT1 receptor.

2.7 Measurement of NAPDH Oxidase Activity

The lucigenin chemiluminescence assay was used to determine NAPDH oxidase activity in tissue and cell homogenates (Yogi et al., 2008). Tissues were homogenized in lysis buffer (20 mM KH_2PO_4, 1 mM ethylene glycol tetraacetic acid [EGTA] with 1 µg/mL aprotinin, 1 µg/mL leupeptin, 1 µg/mL pepstatin and 1 mM PMSF) using glass homogenizers and kept on ice. After stimulation, cells were washed with ice cold PBS and scraped in assay phosphate buffer (50 mmol/L KH_2PO_4, 1 mmol/L EGTA, 150 mmol/L sucrose, pH 7.4) and transferred to 1.5 mL tubes. Protein concentration was determined using the BioRad D_C Protein Assay and 20 ug of protein was used in the assay for both tissue and cell samples. The reaction was initiated by addition of NAPDH (0.1 mM) to the suspension (250 µL final volume) containing prepared sample (50 µL), lucigenin (5 µM), and assay phosphate buffer. Luminescence was measured using a luminometer (Lumistar Galaxy, BMG Technologies [Allmendgruen, Germany]) every 1.8 sec for 3 min. Buffer blank not containing experimental sample was subtracted from each reading.

2.8 RT-PCR for AT1, AT2 and Mas Receptors

RNA was isolated from renal cortical tissue using a commercial kit (RNeasy, Qiagen Inc., Toronto, ON, Canada) and treated with DNAse (Invitrogen Canada Inc., Burlington, ON, Canada) to remove any remaining genomic DNA. RNA samples were reverse transcribed and subjected to real-time PCR, using a one-step master mix (TaqMan Gene Expressions Assays, Applied Biosystems Inc., Foster City, CA, USA) that contained primers for mouse AT1 (Applied Biosystems Inc., Catalogue no: Mm00616371_m1), AT2 (Applied Biosystems Inc., Catalogue no: Mm01341373_m1), or Mas (Applied Biosystems Inc., Catalogue no: Mm00434823_s1) receptors. PCR was performed with an ABI 7000 Sequence Detection System (Applied Biosystems Inc.) with an initial denaturing step at 95°C, followed by 40 cycles of amplification, with denaturing for 15 sec at 95°C and annealing/extension for 1 min at 60°C. PCR was also performed with primers for mouse GAPDH (Applied Biosystems Inc., catalogue no. 4352339E) as an internal control. mRNA was quantified by comparing the cycle numbers required for the fluorescence of PCR products to reach threshold (Nadarajah et al., 2012). All experiments included controls where reverse transcriptase was not added to the reaction mix.

2.9 Cell Culture

Cell culture experiments were conducted in MCT cells, an SV-40 transformed mouse cortical tubular epithelial cell line, and primary cultures of proximal tubular cells from male C57Bl/6J mice. The MCT cells were obtained from Dr. R.L. Hebert's laboratory

(University of Ottawa, Ottawa, ON, Canada). MCT cells were cultured in Dulbecco's modified Eagle medium nutrient mixture – Ham's F12 (DMEM/F-12), supplemented with 1% L-glutamine, 10% fetal bovine serum (FBS), penicillin (100 U/mL) and streptomycin (100 µg/mL) and maintained between passages 11 and 17. Cells were maintained at 37°C in a humidified environment of 5% CO_2/room air. Experiments were performed on cells that reached approximately 75% confluence that had been growth arrested by removal of FBS from the culture medium for 16 to 24 hrs.

Primary cultures of mouse proximal tubular cells were prepared using a method for the isolation of rat proximal tubules by Vinay et al. (Vinay et al., 1981). In brief, both kidneys were removed from anaesthetized C57Bl/6J mice, and the cortices minced in Buffer A (105 mM NaCl, 24 mM $NaHCO_3$, 5 mM KCl, 1.5 mM $CaCl_2$, 1.0 mM $MgSO_4$, 2.0 mM Na_2HPO_4, 5.0 mM D-glucose, 1.0 mM alanine, 4.0 mM Na-lactate, 10.0 mM N-2-hydroxyethylpiperazine-N-2-ethanesulphonic acid (HEPES) (pH 7.4), 0.2% BSA, 0.03% collagenase (Type IV, Sigma Adrich), and 0.01% trypsin inhibitor (Sigma Aldrich). The suspension was bubbled for with 5% CO_2 and 95% O_2 for 30 min in a 37°C water bath. After digestion, the suspension was strained through a 250 µm brass sieve and centrifuged for 1 min at 100 x g to obtain a pellet. The pellet was resuspended in Buffer A (without collagenase or tryspin inhibitor) and centrifuged for 1 min at 100 x g to obtain a second pellet. The pellet was resuspended, without shaking, in a 4°C 42% Percoll (Sigma Aldrich)/68% Buffer A gradient and centrifuged for 30 min at 26000 x g at 4°C. The tissue suspension separated into 4 distinct layers, with the F4 layer containing proximal tubular segments. This layer was carefully removed and washed by suspending in culture medium and centrifuging at 100 X g for 1 min to obtain a pellet.

This pellet was resuspended in culture medium and seeded onto culture dishes. Cells were initially grown in a defined medium – DMEM/F-12, insulin (5 mg/mL), transferrin (5 mg/mL), selenium (5ng/mL), hydrocortisone (50 nM), and 3, 3, 5 – triiodo-L-thyronine (2.5 nM), supplemented with fetal bovine serum (10%), penicillin (100 U/mL), and streptomycin (100 mg/mL). After 24 hrs, cells were incubated in defined medium without FBS. Cells were maintained at 37°C in a humidified environment of 5% CO2/room air. Experiments were performed on cells that reached approximately 75% confluence and had been growth arrested by incubation in DMEM/F-12 for 24 hrs. This procedure yields a preparation that consists of approximately 97% proximal tubules (by microscopy) (Su et al., 2006).

Cells to be used for immunoblotting were lysed in a buffer containing 62.5 mM Tris-HCl (pH 6.8), 2% w/v SDS, 10% glycerol, 50 mM DTT, and 0.1% w/v bromophenol blue. Lysates were sonicated for 5 sec, and boiled 5 min, followed by centrifugation for 5 min at 12 000 x g to remove insoluble debris. Samples were stored at -20°C until loading on a SDS-PAGE for analysis of p38 and ERK1/2 MAPK phosphorylation.

To determine if A779 was stimulating pro-growth or pro-differentiation pathways, primary cultures of mouse proximal tubular cells were incubated with 10^{-5} M A779 for 15 min. In addition, cells were incubated with 10^{-7} M Ang-(1-7), 10^{-6} M Ang II, 10^{-5} M phorbol 12-myristate 13-acetate (PMA). In some experiments cells were pre-incubated with Ang-(1-7) for 15 min prior to stimulation with Ang II. Cell lysates were run on 10% SDS-polyacrylamide gels which were transferred to nitrocellulose membranes and probed for phosphorylated p38 and ERK MAPKs. To control for protein loading,

membranes were stripped and reprobed using antibodies directed towards total p38 and ERK. Immunoblots were analyzed as described above.

2.10 Statistical Analyses

Data were analyzed using GraphPad Prism (GraphPad Software version 4.03, San Diego, CA, USA). All values are reported as means ± standard error of the mean (SEM). Statistical comparisons were made using one-way analysis of variance (ANOVA) followed by Bonferroni's post-hoc test when multiple groups were compared or student's *t* test where two groups were compared. P values less than 0.05 were considered significant.

3.0 Results

3.1 Establishing the UUO Model

3.1.1 Time Course

The time course of studies in UUO in mouse vary from as short as one day (Xiong et al., 2012) to more than 14 days (Babelova et al., 2012; Eddy et al., 2012). To determine the optimal time course for UUO in our laboratory, female FVB/N mice were subject to UUO for 7 or 10 days. Female FVB/N mice were chosen for this part of the study due to availability. Renal cortical fibronectin expression was assessed by immunoblot to evaluate the degree of injury at these time points (Figure 27, Appendix 2). Fibronectin expression in obstructed renal cortices from mice that underwent UUO for 7 days was not significantly increased compared to unobstructed kidneys. Ten days of UUO caused a significant increase in renal cortical fibronectin expression compared to unobstructed kidneys. Based on these data, a 10 day time point was chosen for all subsequent studies. 12 week old male C57Bl/6 mice were used in all studies. This strain of mouse was chosen to replicate the methods used by Esteban et al (Esteban et al., 2009). The mortality rate for all portions of this study was 0%.

3.1.2 ARB treatment and UUO

Previous studies have shown ARB treatment to ameliorate the renal injury associated with UUO (Han et al., 2010; Higashi et al., 2010; Sugiyama et al., 2005). Thus this experiment was conducted to evaluate the effects of Losartan treatment in UUO. Male C57Bl/6 mice underwent UUO for 10 days and were treated with vehicle or

Losartan (25 mg/kg/day); SBP and markers of renal injury were evaluated. At baseline no differences were seen in SBP and body weight between groups (Table 9-10, Appendix 2). After 10 days of UUO, SBP remained unchanged. In addition, body weight, unobstructed or obstructed kidney weight and heart weight to body weight ratios were not different between mice that received vehicle or Losartan.

To assess renal injury, immunoblotting was performed for fibronectin, TGF-β, and α-SMA (Appendix 2 for Supplementary Data). Renal cortical fibronectin was significantly elevated in obstructed kidneys from mice that received vehicle ($p < 0.001$) or Losartan ($p < 0.01$) compared to unobstructed kidneys (Figure 28, Appendix 2). Treatment with Losartan was associated with a reduction in renal cortical fibronectin expression in obstructed kidneys compared to obstructed kidneys from vehicle treated mice; however, this decrease did not reach statistical significance. Obstruction in vehicle treated mice led to a significant increase in renal cortical TGF-β expression compared to unobstructed kidneys ($p < 0.001$) (Figure 29, Appendix 2). TGF-β expression was not significantly elevated in obstructed renal cortices of mice that received Losartan compared to unobstructed renal cortices. Furthermore, treatment with Losartan caused a significant reduction ($p < 0.001$) in renal cortical TGF-β expression in obstructed kidneys compared to obstructed kidneys from mice that received vehicle. UUO caused a significant increase ($p < 0.001$) in renal cortical α-SMA expression in obstructed kidneys compared to unobstructed kidneys (Figure 30, Appendix 2). Renal cortical α-SMA expression was unaffected by treatment with Losartan.

Thus, treatment with Losartan partially attenuated renal fibronectin while significantly reducing TGF-β expression, suggesting alternative, non-AT1 receptor mediated pathways for the production of fibronectin and α-SMA.

3.2 Part 1: Effect of Angiotensin-(1-7) antagonism, via A779, in UUO

3.2.1 Whole Animal Data

To determine the role of endogenous Ang-(1-7) in UUO, 12 mice were treated with A779 (31 µg/kg/hr), the Ang-(1-7) antagonist. At baseline, SBP was not different between mice that received vehicle or A779 (Table 1). UUO did not affect SBP or body weight. Treatment with A779 had no effect on SBP, body weight, unobstructed and obstructed kidney weight to body weight ratios, heart weight to body weight ratios, or any plasma characteristics (Tables 1-3).

3.2.2 Effect of the Angiotensin-(1-7) antagonist, A779 on renal cortical fibronectin, TGF-β, and α-SMA expression

UUO caused a significant increase ($p < 0.001$) in renal cortical fibronectin expression compared to unobstructed kidneys (Figure 2). A779 treatment caused a further significant increase ($p < 0.001$) in fibronectin expression in obstructed renal cortices. In addition, a small increase in renal fibronectin expression was seen in unobstructed kidneys from mice that received A779, but this did not reach statistical significance.

Table 1: Effect of A779 on SBP in UUO

	Vehicle		**A779**	
	Baseline	UUO	Baseline	UUO
SBP (mmHg)	101.7±3.6	114.1±5.3	108.6±5.0	108.6±7.3

Abbreviations

SBP: systolic blood pressure

UUO: unilateral ureteral obstruction

Data are means ± SEM. (n = 12)

p = n.s. for all group comparisons

Table 2: Effect of A779 on body and organ weights in UUO

	Vehicle	**A779**
	10 Days Post UUO	
Body Weight (g)	(26.4±0.3) 27.4±0.3	(27.1±0.1) 27.8±0.1
UKW/BW (mg/g)	9.6±0.6	9.8±0.4
OKW/BW (mg/g)	8.1±0.4	8.2±0.4
HW/BW (mg/g)	8.6±0.5	8.8±0.5

Baseline body weight indicated in parenthesis.

Abbreviations

UUO: unilateral ureteral obstruction

BW: body weight

UKW: unobstructed kidney weight

OKW: obstructed kidney weight

HW: heart weight

Data are means ± SEM. (n = 12)

p = n.s. for all group comparisons

Table 3: Effect of A779 on plasma characteristics in UUO

	Vehicle	**A779**
	10 Days Post UUO	
Hematocrit (%)	41.9±1.2	41.7±1.1
Na^+	146.2±1.0	147.3±0.4
K^+	4.9±0.2	4.2±0.1
Ca^{2+}	2.3±0.1	2.4±0.1
PO_4^{3-}	2.1±0.2	2.3±0.2
HCO_3-	23.5±0.7	22.0±1.5
Mg^{2+}	0.9±0.1	1.0±0.1
Glucose	14.8±1.0	12.8±1.1
Cholesterol	2.4±0.23	2.6±0.2
Triglycerides	0.7±0.2	0.9±0.1
Albumin (g/L)	22.7±3.7	27.7±1.0
Urea (g/dL)	9.4±1.1	8.7±0.4
Creatinine (μM)	12.2±1.1	10.8±0.9

Values are in mM unless otherwise indicated.

Abbreviations

UUO: unilateral ureteral obstruction

Data are means ± SEM. (n = 6)

p = n.s. for all group comparisons

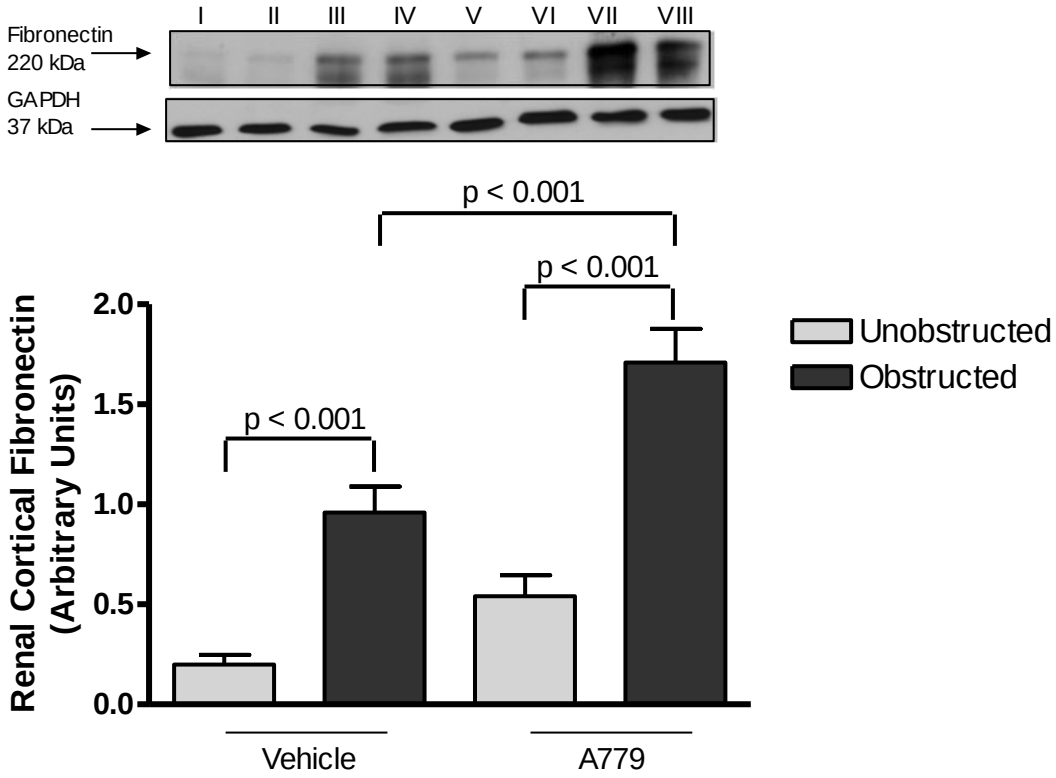

Figure 2: Effect of A779 on renal cortical fibronectin expression in UUO. Fibronectin expression in unobstructed and obstructed kidney cortex from male C57Bl/6 mice that underwent UUO for 10 days and received either vehicle or A779 (31 µg/kg/hr). Representative immunoblot depicted above. Lane I, II: unobstructed, vehicle; Lane III, IV: obstructed, vehicle; Lane V, VI: unobstructed, A779; Lane VII, VIII: obstructed, A779. Data are means ± SEM (n = 12).

Similarly, TGF-β expression was significantly increased ($p < 0.01$) in obstructed kidneys compared to unobstructed kidneys from vehicle treated mice (Figure 3). Treatment with A779 resulted in a further increase ($p < 0.01$) in TGF-β expression in obstructed kidneys. TGF-β expression was unaffected by A779 treatment in unobstructed kidneys. Immunoblotting for TGF-β revealed two bands, one at 12.5 kDa and one at 25 kDa, the latter representing the dimer form of TGF-β.

Renal cortical α-SMA expression was significantly elevated ($p < 0.001$) in obstructed kidneys from mice that received vehicle compared to unobstructed kidneys (Figure 4). α-SMA was further significantly increased ($p < 0.05$) in obstructed renal cortices from mice that received A779. A non-significant increase in α-SMA expression was noted in unobstructed renal cortices from mice that received A779.

3.2.3 Effect of Ang-(1-7) antagonism on renal cortical NADPH oxidase activity

To assess whether ROS generation was involved in A779 mediated renal injury, renal cortical NAPDH oxidase activity was measured using the lucigenin assay. Renal NAPDH oxidase activity was not significantly elevated in obstructed kidneys from vehicle treated mice (Figure 5). Treatment with A779 led to a significant increase ($p < 0.01$) in renal cortical NADPH oxidase activity in obstructed kidneys compared to unobstructed kidneys. In addition, A779 treatment caused a significant increase ($p < 0.01$) in renal cortical NAPDH oxidase activity compared to obstructed kidneys from vehicle treated mice.

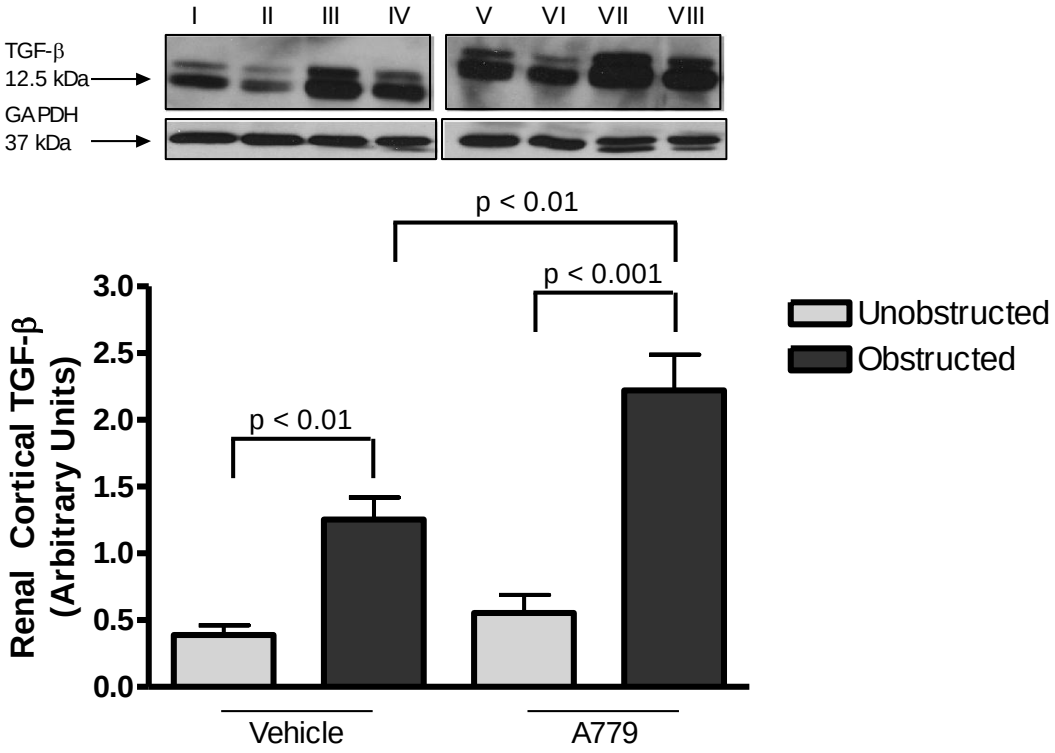

Figure 3: Effect of A779 on renal cortical TGF-β expression in UUO. TGF-β expression in unobstructed and obstructed kidney cortex from male C57Bl/6 mice that underwent UUO for 10 days and received either vehicle or A779 (31 µg/kg/hr). Representative immunoblot depicted above. Lane I, II: unobstructed, vehicle; Lane III, IV: obstructed, vehicle; Lane V, VI: unobstructed, A779; Lane VII, VIII: obstructed, A779. Data are means ± SEM (n = 12).

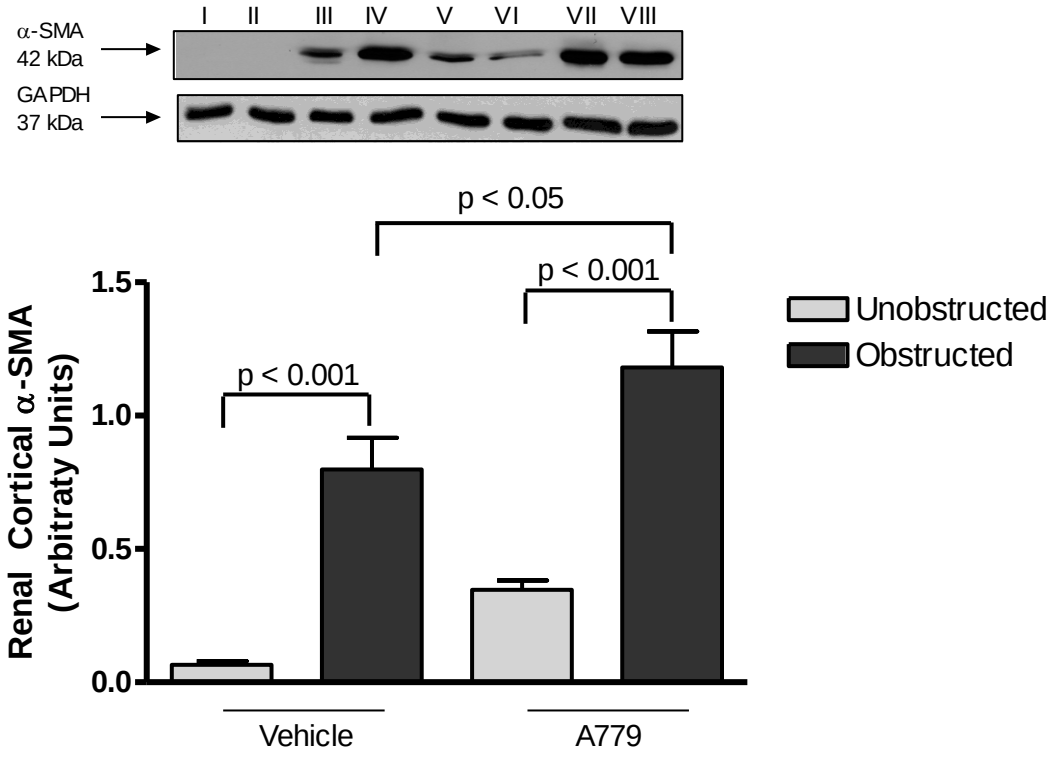

Figure 4: Effect of A779 on renal cortical α-SMA expression in UUO. α-SMA expression in unobstructed and obstructed kidney cortex from male C57Bl/6 mice that underwent UUO for 10 days and received either vehicle or A779 (31 µg/kg/hr). Representative immunoblot depicted above. Lane I, II: unobstructed, vehicle; Lane III, IV: obstructed, vehicle; Lane V, VI: unobstructed, A779; Lane VII, VIII: obstructed, A779. Data are means ± SEM (n = 12).

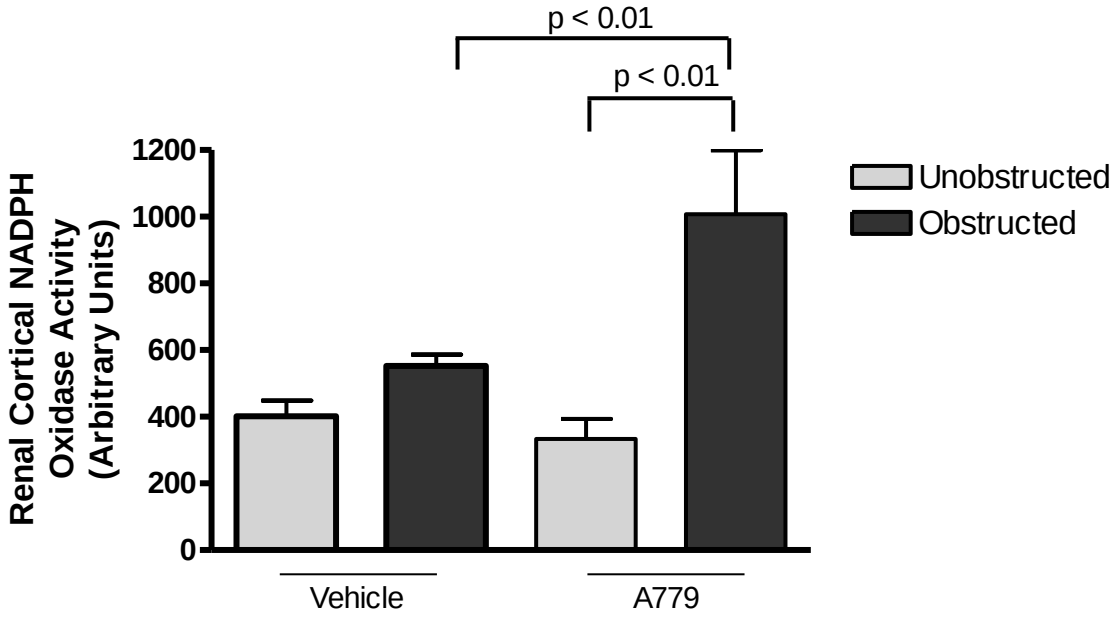

Figure 5: Effect of A779 on renal cortical NADPH oxidase activity in UUO. Renal cortical NADPH oxidase activity in unobstructed and obstructed kidneys from male C57Bl/6 mice that underwent UUO for 10 days and received vehicle or 31 g/kg/hr A779 via subcutaneous osmotic minipump. Data are means ± SEM (n = 6).

3.2.4 Effect of Angiotensin-(1-7) antagonism on tubulointerstitial fibrosis, inflammation, and apoptosis

Scores for tubulointerstitial fibrosis in unobstructed kidneys after 10 days UUO were zero (data not shown). UUO was associated with a significant increase ($p < 0.001$) in tubulointerstitial fibrosis scores compared to unobstructed kidneys (Figure 6). Treatment with A779 caused a further significant increase ($p < 0.001$) in tubulointerstitial fibrosis scores in obstructed kidneys compared to obstructed kidneys from vehicle treated mice.

Macrophage infiltration, as assessed by anti-F4/80 staining, was significantly increased ($p < 0.001$) in obstructed kidneys from vehicle treated mice compared to unobstructed kidneys (see Figure 7). Similarly, obstructed kidneys from mice treated with A779 showed significantly greater ($p < 0.001$) anti-F4/80 staining when compared to unobstructed kidneys from mice that received A779. However, no additional macrophage infiltration was seen in obstructed kidneys from mice that received A779 compared to obstructed kidneys from vehicle treated mice.

Unobstructed kidneys from vehicle treated mice showed no apoptotic nuclei (data not shown). Apoptosis was significantly increased ($p < 0.001$) in obstructed kidneys from vehicle treated mice compared to unobstructed kidneys (Figure 8). Treatment with A779 caused a further significant increase ($p < 0.001$) in apoptosis in obstructed kidneys compared to obstructed kidneys from vehicle treated mice (see Figure #). Apoptosis in unobstructed kidneys was not affected by A779 treatment.

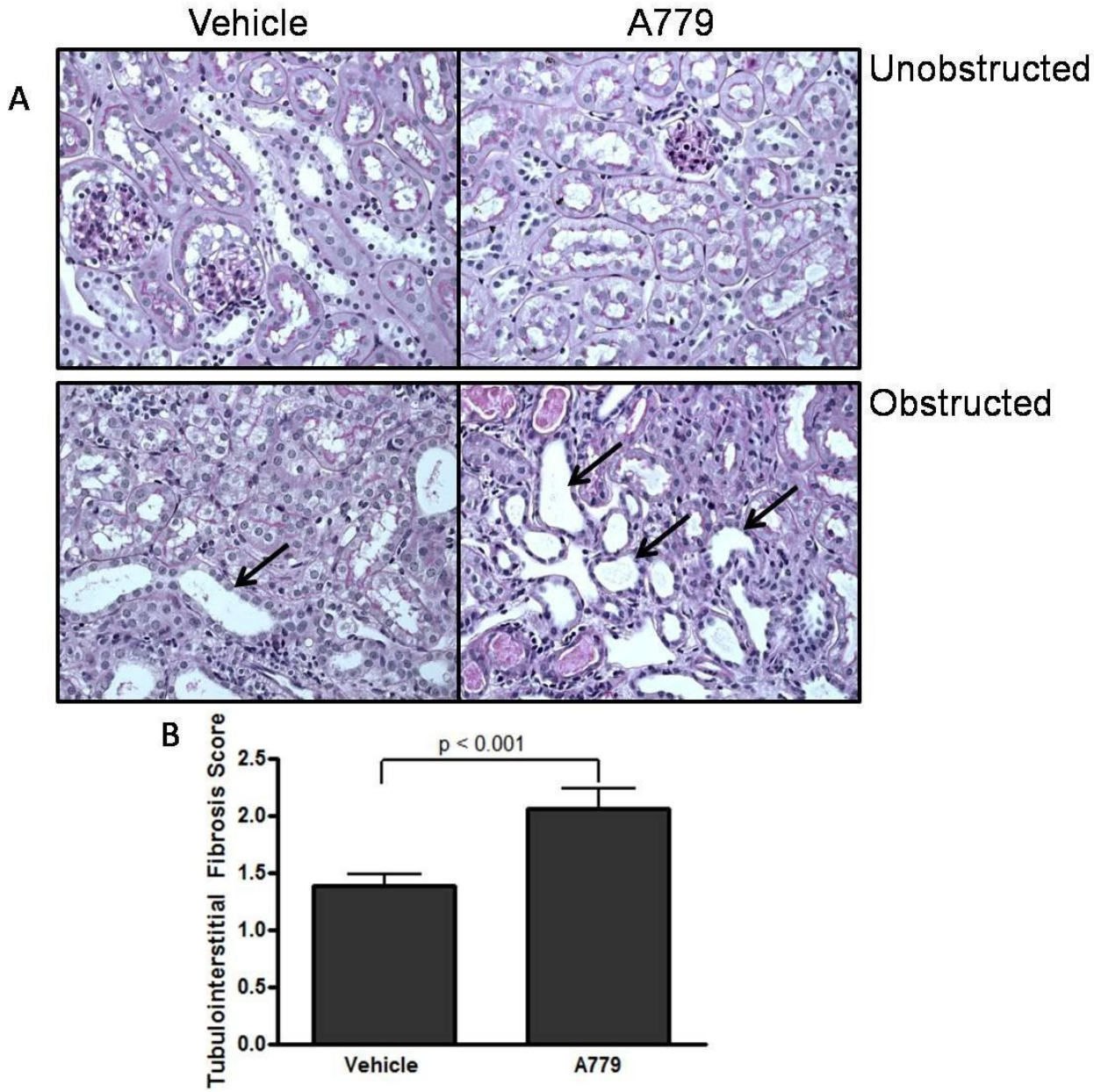

Figure 6: Effect of A779 on tubulointerstitial fibrosis scores in UUO. (A) Periodic Acid Schiff staining of paraffin embedded sections from renal sections of male C57Bl/6 mice that underwent UUO and treatment with vehicle or A779 (31 µg/kg/hr). Arrows indicate areas of tubular dilatation and atrophy. (B) Tubulointerstitial fibrosis scores from PAS stained sections of obstructed kidneys from male C57Bl/6 mice after 10 days of UUO and treatment with or without A779. Values are means ± SE (n = 6). Sections were evaluated blindly.

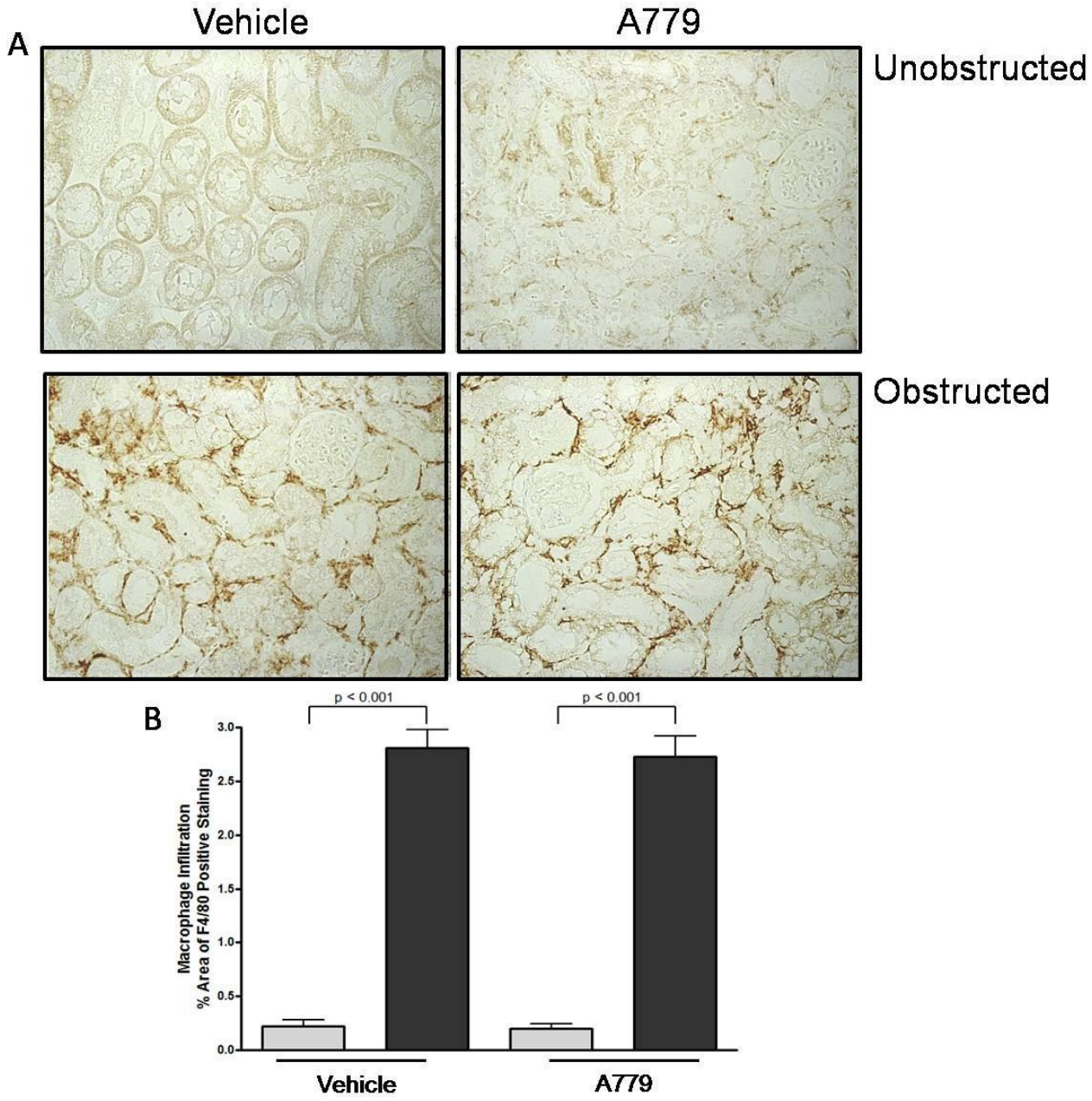

Figure 7: Effect of A779 on macrophage infiltration in UUO. (A) Anti-F4/80 staining of paraffin embedded renal sections of mice that underwent UUO for 10 days and received vehicle or A779 (31 µg/kg/hr). (B) Quantification of F4/80 positive area from obstructed and unobstructed kidneys. Values are means ± SE (n = 6). Sections were evaluated blindly.

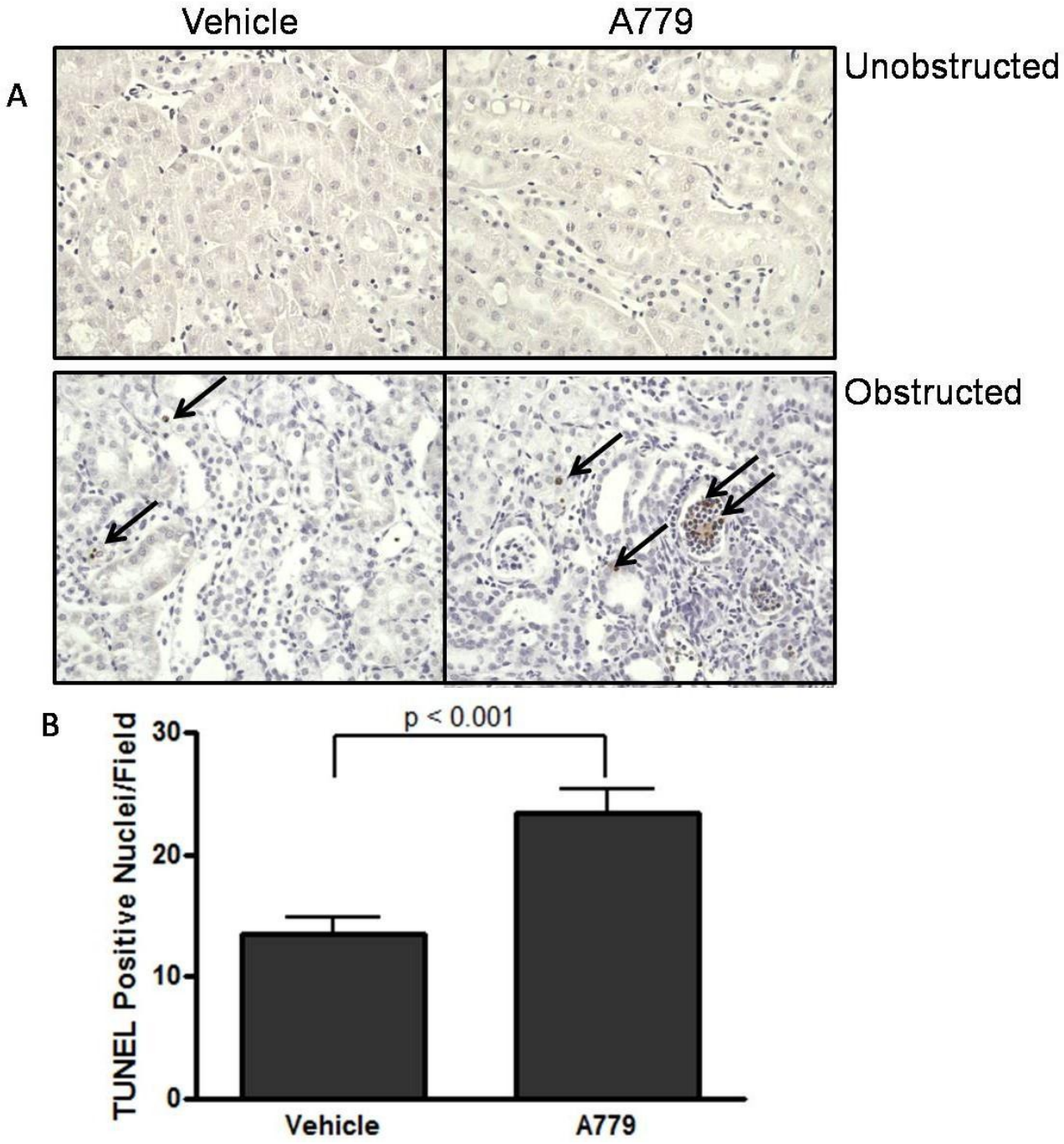

Figure 8: Effect of A779 on apoptosis in UUO. (A) TUNEL staining of renal cortices from male C57Bl/6 mice that underwent UUO for 10 days and treatment with vehicle or A779 (31 µg/kg/hr). Arrows indicate apoptotic cells. (B) Quantification of apoptotic nuclei, as assessed by TUNEL assay, in obstructed kidneys. Values are means ± SE (n = 6). Sections were evaluated blindly.

3.3 Part 2: Effect of exogenous Angiotensin-(1-7) in UUO

3.3.1 Whole animal data

To evaluate the effects of exogenous Ang-(1-7) in UUO male C57Bl/6 mice underwent UUO for 10 days and received vehicle or 6, 24, or 62 µg/kg/hr Ang-(1-7) (s.c. osmotic minipump).

At baseline, SBP and body weights were not different between groups (Tables 11-12, Appendix 2). Treatment at any dose of Ang-(1-7) did not affect SBP, body weight, unobstructed and obstructed kidney and heart weight to body weight ratios, or any plasma characteristics examined (Tables 11-13, Appendix 2) compared to mice that received vehicle.

3.3.2 Effect of exogenous Ang-(1-7) on renal cortical fibronectin, TGF-β and α-SMA expression after 10 days of UUO

UUO was associated with an increase in renal cortical fibronectin expression in obstructed kidneys of mice that received vehicle compared to unobstructed kidneys (Figure 9). Similarly, all doses of Ang-(1-7) were associated with a significant increase ($p < 0.05$ to $p < 0.001$) in fibronectin expression in obstructed kidneys compared to unobstructed kidneys. Treatment with Ang-(1-7) caused a further significant increase ($p < 0.01$ to $p < 0.001$) in fibronectin expression in obstructed renal cortices compared to obstructed kidneys from vehicle treated mice. In addition, all doses of Ang-(1-7) led to a slight increase in fibronectin expression in unobstructed kidneys, although this did not reach statistical significance compared to unobstructed kidneys from vehicle treated mice.

Renal cortical TGF- β expression was increased with obstruction in vehicle treated mice (Figure 10). TGF-β was significantly elevated ($p < 0.01$) in obstructed kidneys from mice that received 6 or 24 µg/kg/hr Ang-(1-7) compared to unobstructed kidneys. In addition, treatment with 24 µg/kg/hr Ang-(1-7) caused a further significant increase ($p < 0.001$) in renal cortical TGF-β expression in obstructed renal cortices compared to obstructed kidneys from mice that received vehicle. A small increase in TGF-β was noted in unobstructed kidneys from mice that received 24 µg/kg/hr Ang-(1-7) compared to mice that received vehicle, but this did not reach statistical significance. In contrast, treatment with 62 µg/kg/hr Ang-(1-7) had no effect on renal cortical TGF-β expression in unobstructed or obstructed kidneys compared to mice that received vehicle.

UUO caused a significant increase ($p < 0.05$) in α-SMA expression compared to unobstructed renal cortices (Figure 11). Treatment at any dose of Ang-(1-7) was associated with a significant increase ($p < 0.001$) in α-SMA in obstructed renal cortices compared to unobstructed kidneys. Exogenous Ang-(1-7) caused a dose dependent increase in renal cortical α-SMA expression in obstructed kidneys that reached significance at 62 µg/kg/hr Ang-(1-7) ($p < 0.001$), compared to obstructed kidneys from mice that received vehicle. α-SMA expression was not affected in unobstructed kidneys at any dose of Ang-(1-7).

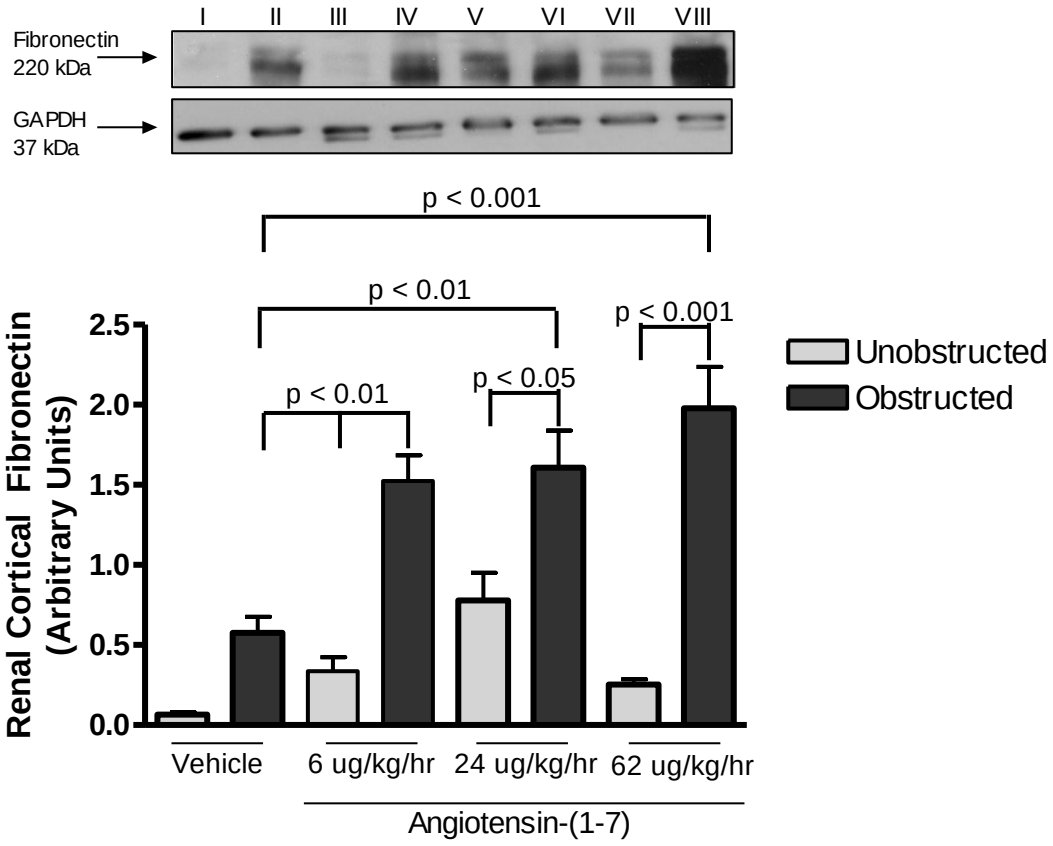

Figure 9: Effect of exogenous Angiotensin-(1-7) on renal cortical fibronectin expression in UUO. Fibronectin expression in unobstructed and obstructed kidney cortex from male C57Bl/6 mice that underwent UUO for 10 days and received vehicle or Ang-(1-7) (6, 24, or 62 µg/kg/hr). Representative immunoblot depicted above. Lane I: unobstructed, vehicle; Lane II: obstructed, vehicle; Lane III: unobstructed 6 µg/kg/hr Ang-(1-7); Lane IV: obstructed 6 µg/kg/hr Ang-(1-7); Lane V: unobstructed 24 µg/kg/hr Ang-(1-7); Lane VI: obstructed 24 µg/kg/hr Ang-(1-7); Lane VII: unobstructed 62 µg/kg/hr Ang-(1-7); Lane VIII: obstructed 62 µg/kg/hr Ang-(1-7). Data are means ± SEM (n = 6).

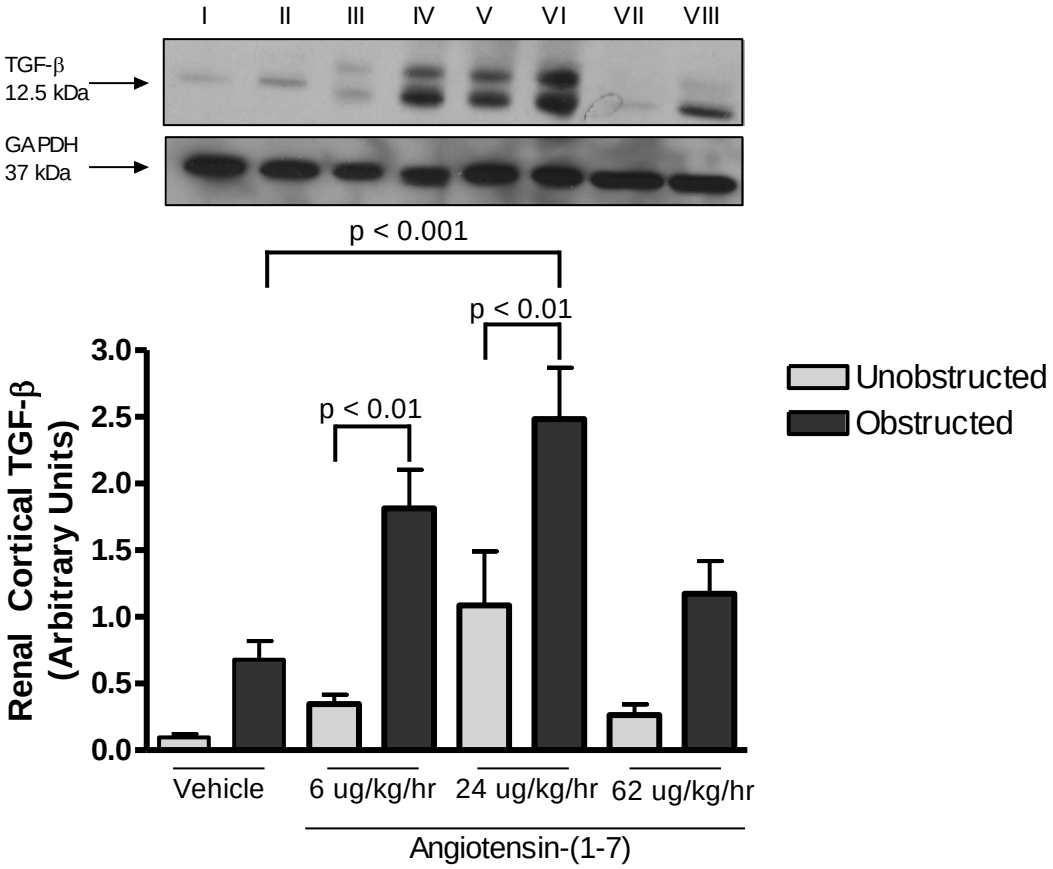

Figure 10: Effect of exogenous Angiotensin-(1-7) on renal cortical TGF-β expression. TGF-β expression in unobstructed and obstructed kidney cortex from male C57Bl/6 mice that underwent UUO for 10 days and received vehicle or Ang-(1-7) (6, 24, or 62 µg/kg/hr). Representative immunoblot depicted above. Lane I: unobstructed, vehicle; Lane II: obstructed, vehicle; Lane III: unobstructed 6 µg/kg/hr Ang-(1-7); Lane IV: obstructed 6 µg/kg/hr Ang-(1-7); Lane V: unobstructed 24 µg/kg/hr Ang-(1-7); Lane VI: obstructed 24 µg/kg/hr Ang-(1-7); Lane VII: unobstructed 62 µg/kg/hr Ang-(1-7); Lane VIII: obstructed 62 µg/kg/hr Ang-(1-7). Data are means ± SEM (n = 6).

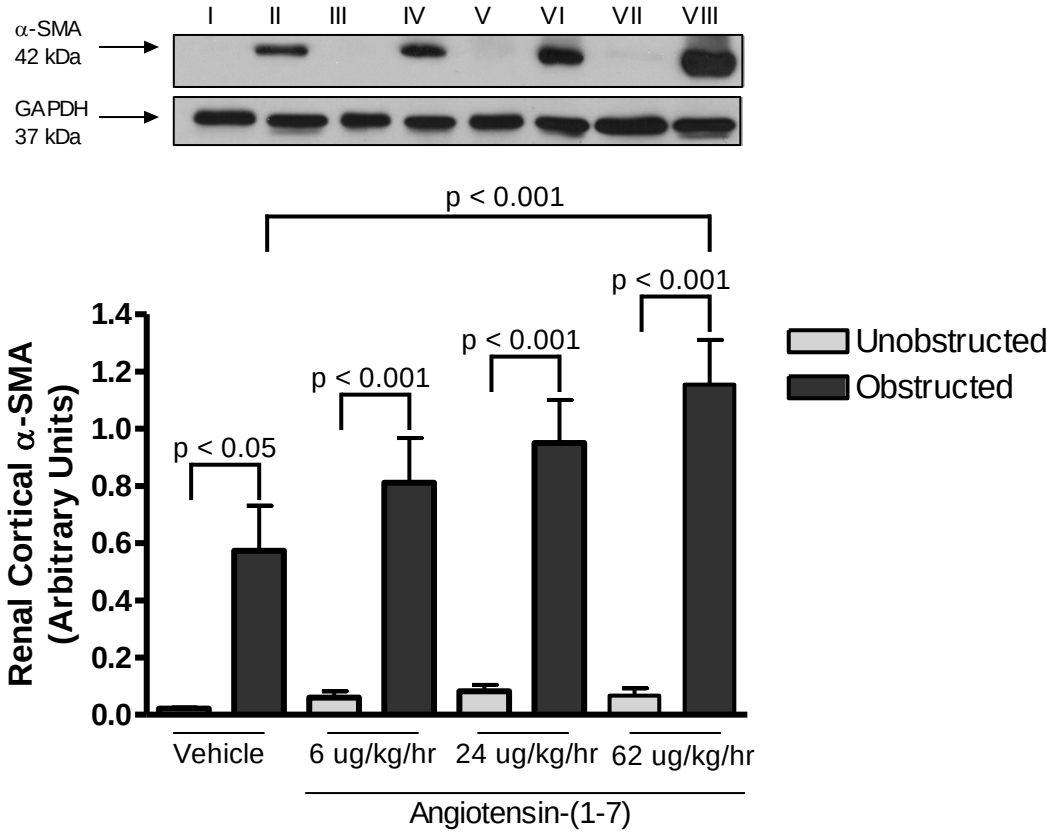

Figure 11: Effect of exogenous Angiotensin-(1-7) on renal cortical α-SMA expression in UUO. α-SMA expression unobstructed and obstructed kidney cortex from male C57Bl/6 mice that underwent UUO for 10 days and received vehicle or Ang-(1-7) (6, 24, or 62 µg/kg/hr). Representative immunoblot depicted above. Lane I: unobstructed, vehicle; Lane II: obstructed, vehicle; Lane III: unobstructed 6 µg/kg/hr Ang-(1-7); Lane IV: obstructed 6 µg/kg/hr Ang-(1-7); Lane V: unobstructed 24 µg/kg/hr Ang-(1-7); Lane VI: obstructed 24 µg/kg/hr Ang-(1-7); Lane VII: unobstructed 62 µg/kg/hr Ang-(1-7); Lane VIII: obstructed 62 µg/kg/hr Ang-(1-7).Data are means ± SEM (n = 6).

3.3.3 Effect of exogenous Ang-(1-7) on renal cortical NADPH oxidase activity

Based on the above results which suggest that all doses of Ang-(1-7) enhance renal injury in the UUO model we sought to determine whether NAPDH oxidase activation played a role. NADPH oxidase activity was assessed on homogenized renal cortices using the lucigenin assay.

NADPH oxidase activity was not significantly affected by obstruction in vehicle treated mice (Figure 12). Ang-(1-7) administration was associated with a significant increase ($p < 0.01$ to $p < 0.001$) in renal cortical NADPH oxidase activity in obstructed kidneys compared to obstructed kidneys from vehicle treated mice. In addition, renal cortical NADPH oxidase activity was significantly elevated ($p < 0.05$ to $p < 0.01$) in unobstructed kidneys from mice that received 24 µg/kg/hr or 62 µg/kg/hr Ang-(1-7) compared to unobstructed kidneys from vehicle treated mice.

3.3.4 Effect of exogenous Ang-(1-7) on tubulointerstitial fibrosis, inflammation, and apoptosis

Tubulointerstitial fibrosis scores for unobstructed kidneys from all groups were zero (data not shown). Obstruction was associated with a significant increase ($p < 0.001$) in tubulointerstitial fibrosis scores compared to unobstructed kidneys (Figure 13). Treatment with Ang-(1-7) caused a significant increase ($p < 0.001$) in tubulointerstitial fibrosis scores in obstructed kidneys compared to unobstructed kidneys. Exogenous administration of Ang-(1-7) caused an increase in tubulointerstitial fibrosis scores in obstructed kidneys that reached significance at high dose Ang-(1-7) (62 µg/kg/hr) ($p < 0.05$) compared to obstructed kidneys from vehicle treated mice.

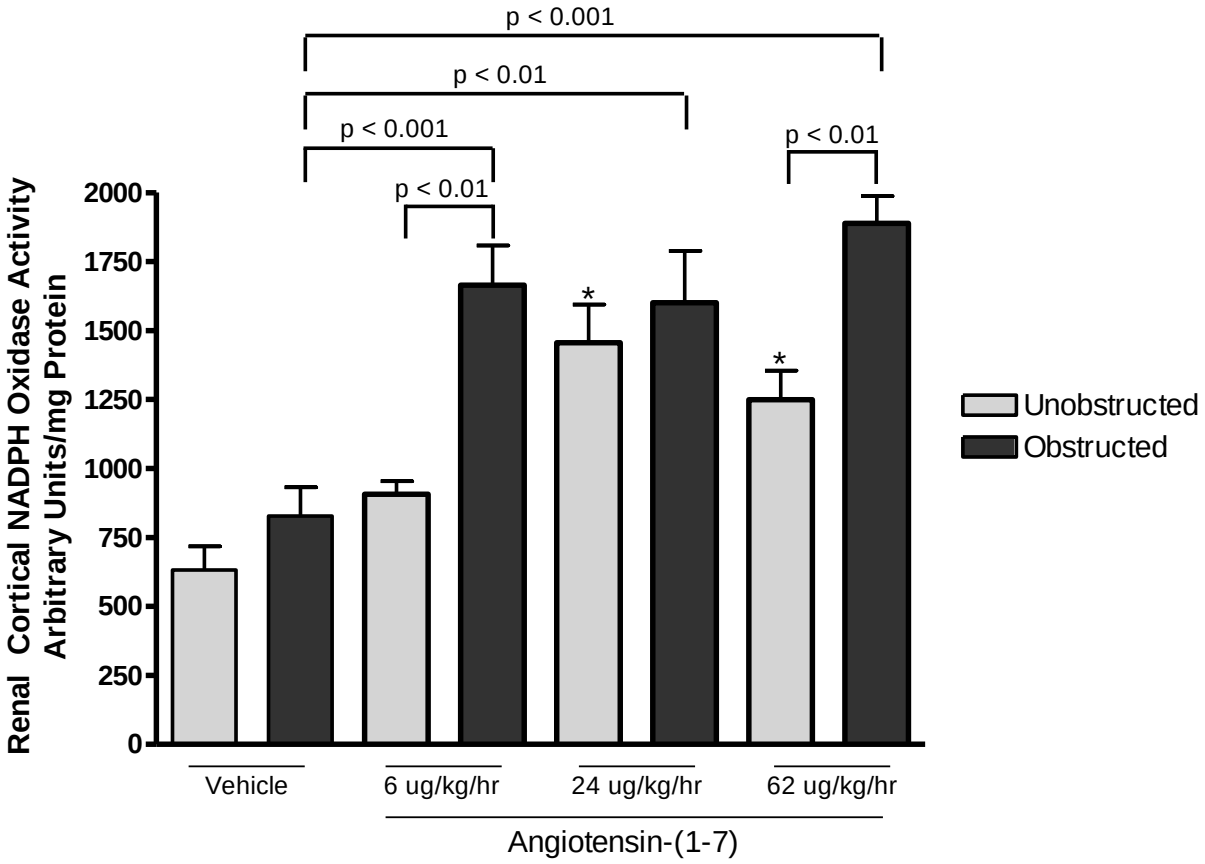

Figure 12: Effect of exogenous Angiotensin-(1-7) on renal cortical NAPDH oxidase activity in UUO. Renal cortical NAPDH oxidase activity as assessed by lucigenin assay in unobstructed and obstructed kidneys from mice that received vehicle or one of three doses of Ang-(1-7) via subcutaneous osmotic minipump. Data are means ± SEM (n = 6). * $p < 0.05$ vs. vehicle unobstructed kidney.

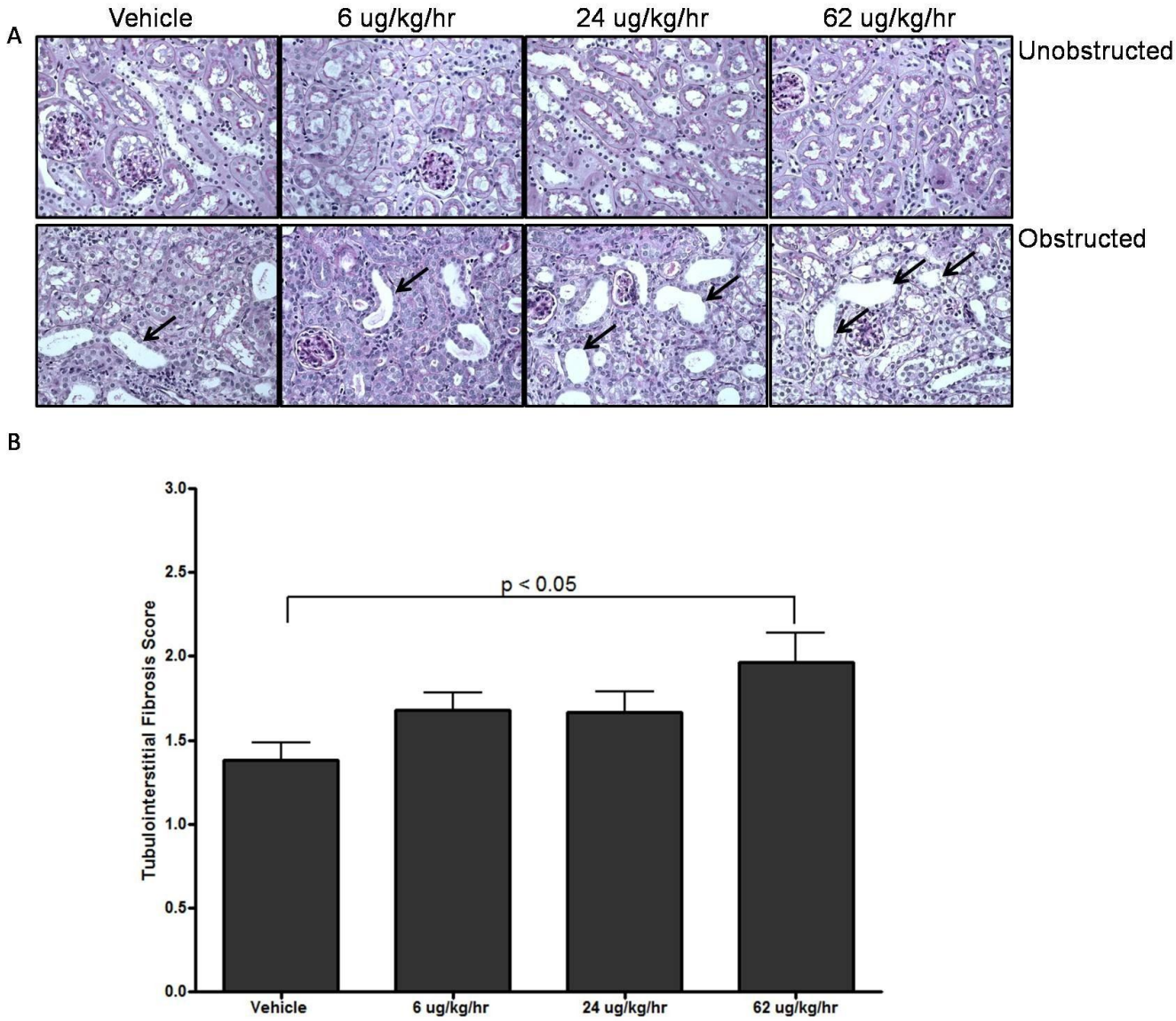

Figure 13: Effect of exogenous Angiotensin-(1-7) on tubulointerstitial fibrosis scores in UUO. (A) Periodic Acid Schiff staining of paraffin embedded sections from renal sections of male C57Bl/6 mice that underwent UUO and treatment with vehicle or Ang-(1-7) (6, 24, or 62 µg/kg/hr). Arrows indicate areas of tubular dilatation and atrophy. (B) Tubulointerstitial fibrosis scores from PAS stained sections of obstructed kidneys. Values are means ± SEM (n = 6). Sections were evaluated blindly.

UUO caused an increase in macrophage filtration compared to unobstructed kidneys (Figure 14). Treatment with Ang-(1-7) caused a significant increase ($p < 0.001$) in macrophage infiltration in obstructed kidneys compared to unobstructed kidneys. Exogenous administration of Ang-(1-7) caused a further significant increase ($p < 0.001$) in anti-F4/80 staining in obstructed kidneys compared to obstructed kidneys from vehicle treated mice. Inflammation was unaffected in unobstructed kidneys.

No apoptosis was detected in unobstructed kidneys (data not shown). Apoptosis was significantly increased ($p < 0.001$) in obstructed kidneys from vehicle treated mice (Figure 15). Treatment with Ang-(1-7) was associated with a significant increase ($p < 0.001$) in apoptosis in obstructed kidneys compared to unobstructed kidneys. Furthermore, treatment with 6 and 62 µg/kg/hr Ang-(1-7) caused a further increase ($p < 0.001$) in apoptosis in obstructed kidneys compared to obstructed kidneys from vehicle treated mice.

3.4 Part 3: The effect of co-administration of A779 and Angiotensin-(1-7) in UUO

To determine whether A779 could block the deleterious actions of exogenousn Ang-(1-7) a third study was conducted in which A779 and Ang-(1-7) were co-administered during the 10 day UUO period.

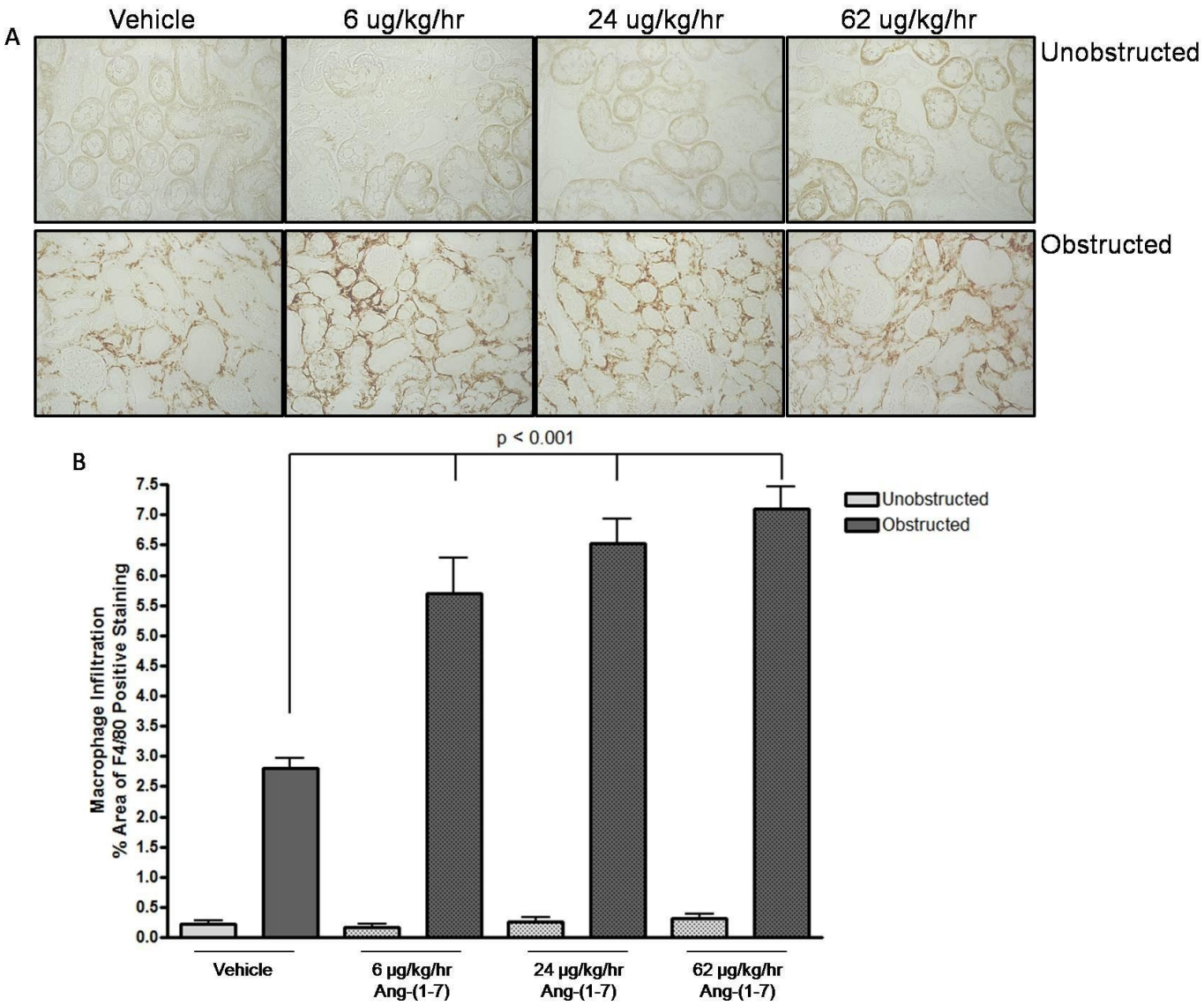

Figure 14: Effect of exogenous Angiotensin-(1-7) on macrophage infiltration in UUO. (A) Anti-F4/80 staining of paraffin embedded sections from renal sections of male C57Bl/6 mice that underwent UUO for 10 days and received vehicle or Ang-(1-7) (6, 24, or 62 µg/kg/hr) (B) Quantification of F4/80 positive area of obstructed and unobstructed kidneys. Values are means ± SEM (n = 6). Sections were evaluated blindly.

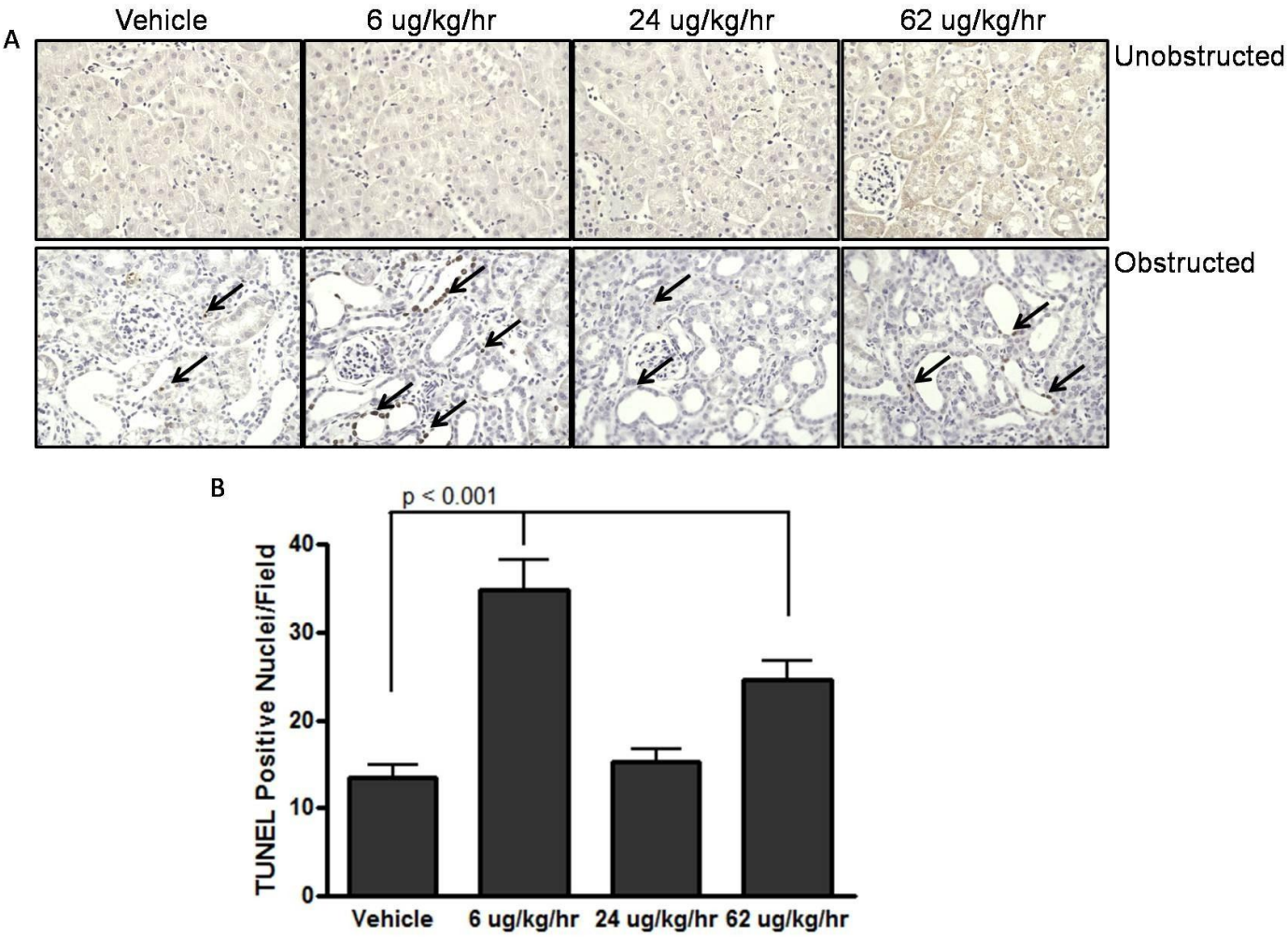

Figure 15: Effect of exogenous Angiotensin-(1-7) on apoptosis in UUO. (A) TUNEL staining of renal cortices from male C57Bl/6 mice that underwent UUO for 10 days and treatment with vehicle or Ang-(1-7) (6, 24, or 62 µg/kg/hr). Arows indicate apoptotic cells. (B) Quantification of apoptotic nuclei, as assessed by TUNEL assay, in obstructed kidneys of male C57Bl/6 mice that underwent UUO for 10 days. Values are means ± SEM (n = 6). Sections were evaluated blindly.

3.4.1 Whole animal data

At baseline, SBP and body weight were similar among all groups (Tables 14-15 Appendix 2). SBP and body weight were unaffected by UUO or any treatment. In addition, unobstructed and obstructed kidney and heart weight to body weight ratios were not different between groups.

3.4.2 Effect of co-administration of A779 and Angiotensin-(1-7) on renal cortical fibronectin, TGF-β and α-SMA expression after 10 days of UUO

Renal cortical fibronectin was increased in obstructed kidneys at 10 days post UUO compared to unobstructed kidneys (Figure 16). Treatment with either A779 or Ang-(1-7) caused a significant increase ($p < 0.01$) in renal cortical fibronectin expression in obstructed kidneys compared to unobstructed kidneys. Co-administration of A779 with Ang-(1-7) was also associated with a significant increase ($p < 0.001$) in renal cortical fibronectin expression in obstructed kidneys compared to unobstructed kidneys. Furthermore, co-administration of A779 with Ang-(1-7) caused a further significant increase ($p < 0.001$) in fibronectin expression in obstructed renal cortices compared to obstructed kidneys from vehicle treated mice. Fibronectin expression in obstructed kidneys was unaffected by any treatment.

UUO caused an increase in renal cortical TGF-β expression compared to unobstructed kidneys (see Figure 17). Treatment with A779 caused a significant increase in fibronectin expression in obstructed renal cortices compared to unobstructed renal cortices. As seen in Part 2, treatment with 62 µg/kg/hr Ang-(1-7) was associated with an increase in renal cortical TGF-β expression in obstructed kidneys compared to unobstructed kidneys, but this did not reach statistical significance. Co-administration of

A779 with Ang-(1-7) caused a significant reduction in TGF-β expression in obstructed renal cortices compared to mice that received A779 ($p < 0.001$) or Ang-(1-7) ($p < 0.01$). Treatment with Ang-(1-7) alone was associated with a small, but not significant, increase in fibronectin expression in unobstructed kidneys.

Renal cortical α-SMA expression was significantly elevated ($p < 0.05$) in obstructed kidneys from vehicle treated mice compared to unobstructed kidneys (see Figure 18). Treatment with A779 or Ang-(1-7) or both was associated with a significant increase ($p < 0.001$) in renal cortical fibronectin expression in obstructed kidneys compared to unobstructed kidneys. Co-administration of A779 with Ang-(1-7) was associated with a further significant increase in α-SMA expression in obstructed kidneys compared to obstructed kidneys from mice that received vehicle ($p < 0.001$) and A779 or Ang-(1-7) ($p < 0.05$). Co-administration of A779 with Ang-(1-7) did not affect α-SMA in unobstructed kidneys.

3.4.3 Effect of co-administration of A779 and Angiotensin-(1-7) on tubulointerstitial fibrosis

Unobstructed kidneys from all groups had tubulointerstitial fibrosis scores of zero (data not shown). UUO was associated with a significant increase ($p < 0.001$) in tubulointerstitial fibrosis scores in obstructed kidneys from all groups compared to unobstructed kidneys (Figure 19).

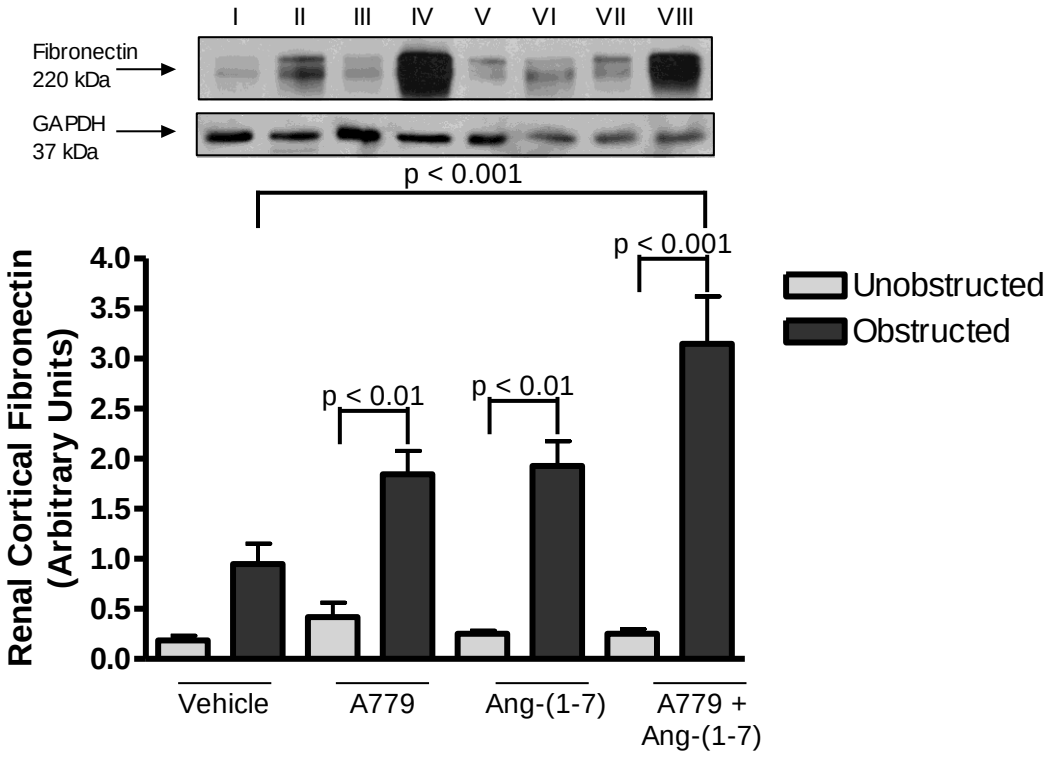

Figure 16: Effect of co-administration of A779 and high dose Ang-(1-7) on renal cortical fibronectin expression in UUO. Fibronectin expression in unobstructed and obstructed kidneys from male C57Bl/6 mice that underwent UUO for 10 days and received vehicle, A779 (83 µg/kg/hr), Ang-(1-7) (62 µg/kg/hr) or a combination via subcutaneous osmotic minipump. Representative immunoblot depicted above. Lane I: unobstructed, vehicle; Lane II: obstructed, vehicle; Lane III: unobstructed, A779; Lane IV: obstructed, A779; Lane V: unobstructed, Ang-(1-7); Lane VI: obstructed, Ang-(1-7); Lane VII: unobstructed, A779 + Ang-(1-7); Lane VIII: obstructed, A779 + Ang-(1-7). Data are means ± SEM (n = 6).

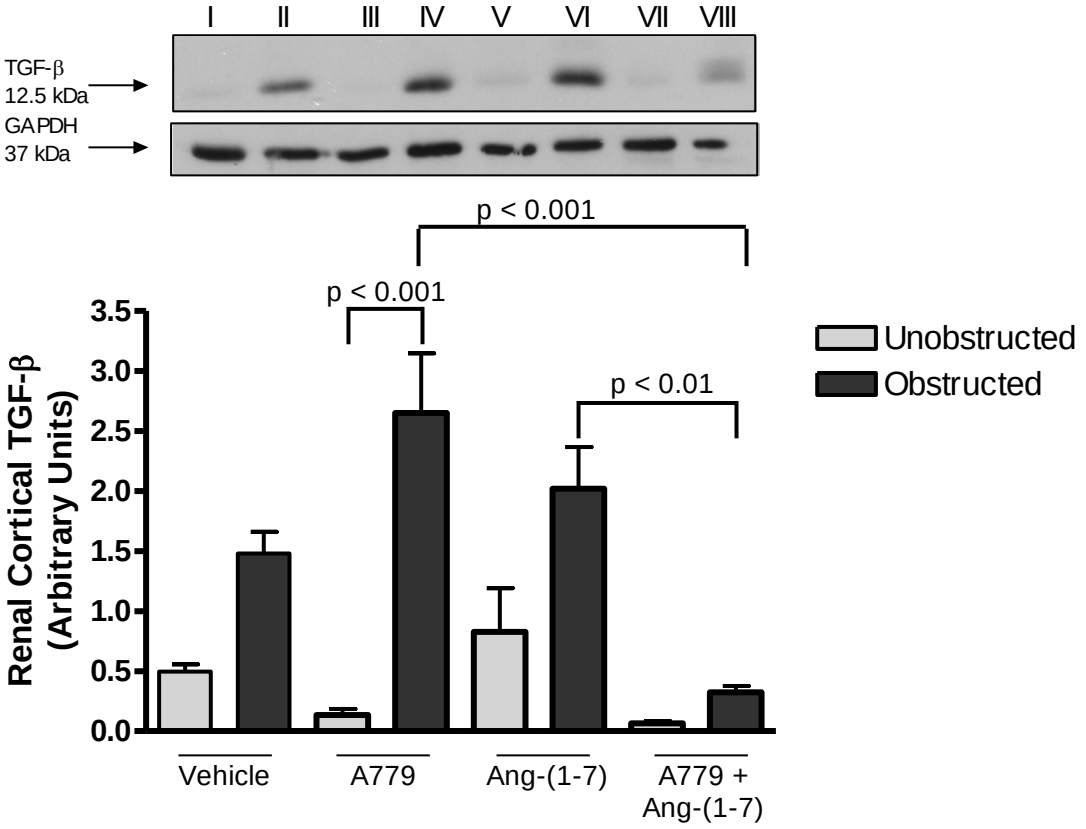

Figure 17: Effect of Co-administration of A779 and high dose Ang-(1-7) on renal cortical TGF-β expression in UUO. TGF-β expression in unobstructed and obstructed kidney cortex from male C57Bl/6 mice that underwent UUO for 10 days and received vehicle, 83 µg/kg/hr A779, 62 µg/kg/hr Ang-(1-7) or a combination via subcutaneous osmotic minipump. Representative immunoblot depicted above. Lane I: unobstructed, vehicle; Lane II: obstructed, vehicle; Lane III: unobstructed, A779; Lane IV: obstructed, A779; Lane V: unobstructed, Ang-(1-7); Lane VI: obstructed, Ang-(1-7); Lane VII: unobstructed, A779 + Ang-(1-7); Lane VIII: obstructed, A779 + Ang-(1-7). Data are means ± SEM (n = 6).

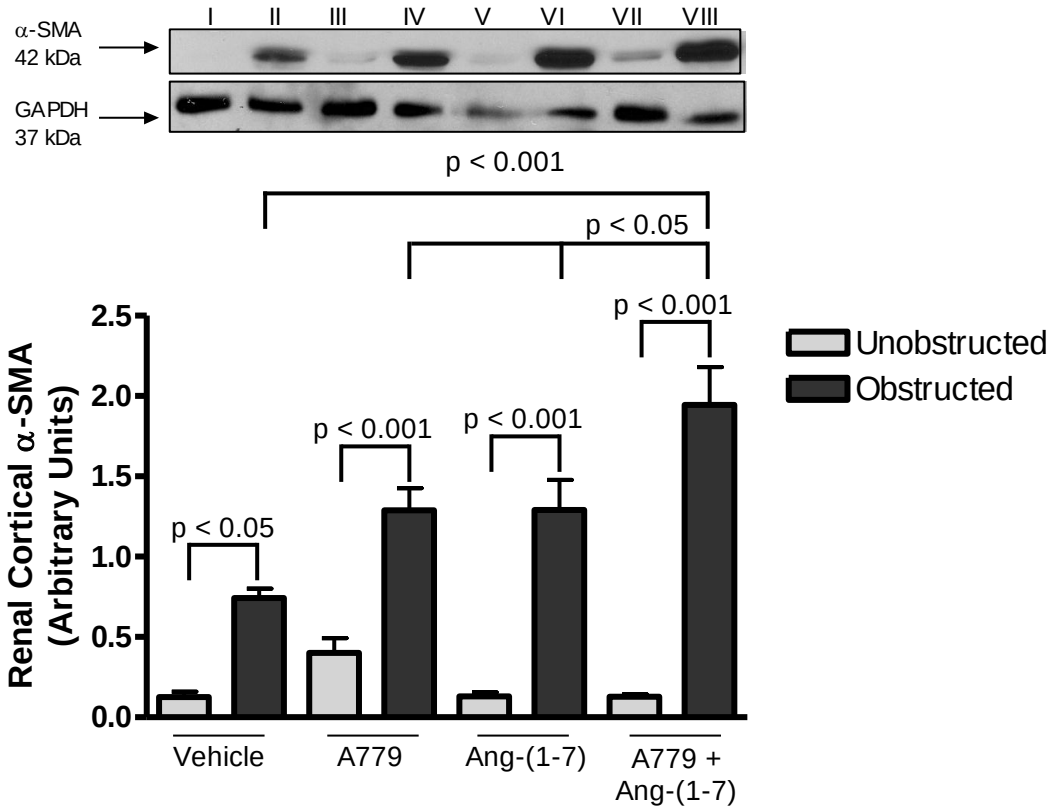

Figure 18: Effect of co-administration of A779 and high dose Ang-(1-7) on renal cortical α-SMA expression in UUO. α-SMA expression in unobstructed and obstructed kidney cortex from male C57Bl/6 mice that underwent UUO for 10 days and received vehicle, 83 µg/kg/hr A779, 62 µg/kg/hr Ang-(1-7) or a combination via subcutaneous osmotic minipump. Representative immunoblot depicted above. Lane I: unobstructed, vehicle; Lane II: obstructed, vehicle; Lane III: unobstructed, A779; Lane IV: obstructed, A779; Lane V: unobstructed, Ang-(1-7); Lane VI: obstructed, Ang-(1-7); Lane VII: unobstructed, A779 + Ang-(1-7); Lane VIII: obstructed, A779 + Ang-(1-7). Data are means ± SEM (n = 6).

Infusion of A779 (83 μg/kg/hr) or Ang-(1-7) alone was associated with a significant increase ($p < 0.05$ and $p < 0.001$, respectively) in tubulointerstitial fibrosis in obstructed kidneys compared to obstructed kidneys from vehicle treated mice.Co-administration of A779 with Ang-(1-7) was associated with a significant increase ($p < 0.05$) in tubulointerstitial fibrosis in obstructed kidneys compared to obstructed kidneys from vehicle treated mice. However, co-administration of A779 with Ang-(1-7) caused a slight reduction in tubulointerstitial fibrosis in obstructed kidneys compared to obstructed kidneys from mice that received Ang-(1-7) alone, though this reduction did not reach statistical significance.

3.5 Effect of Angiotensin-(1-7) antagonism or exogenous Angiotensin-(1-7) administration on AT1, AT2, and Mas receptor mRNA 3

3.5.1 Immunoblotting for AT1 and AT2 receptors

To determine if changes in RAS receptors played a role in exacerbation of renal injury seen with A779 or Ang-(1-7) treatment, immmunoblotting was initially performed for the AT1 and AT2 receptors (Figures 31-32 Appendix 2). However, based on concerns for the specificity of antibodies directed against G-protein coupled receptors, $AT1_{a/b}$ KO tissue was obtained to test several antibodies. All antibodies were found to detect a non-specific band at 42 kDa - the expected size for the AT1 receptor – in renal tissue from AT1 receptor KO mice (Figure 33, Appendix 2). Based on these findings, RT-PCR was performed to assess mRNA levels for AT1, AT2, and Mas receptors.

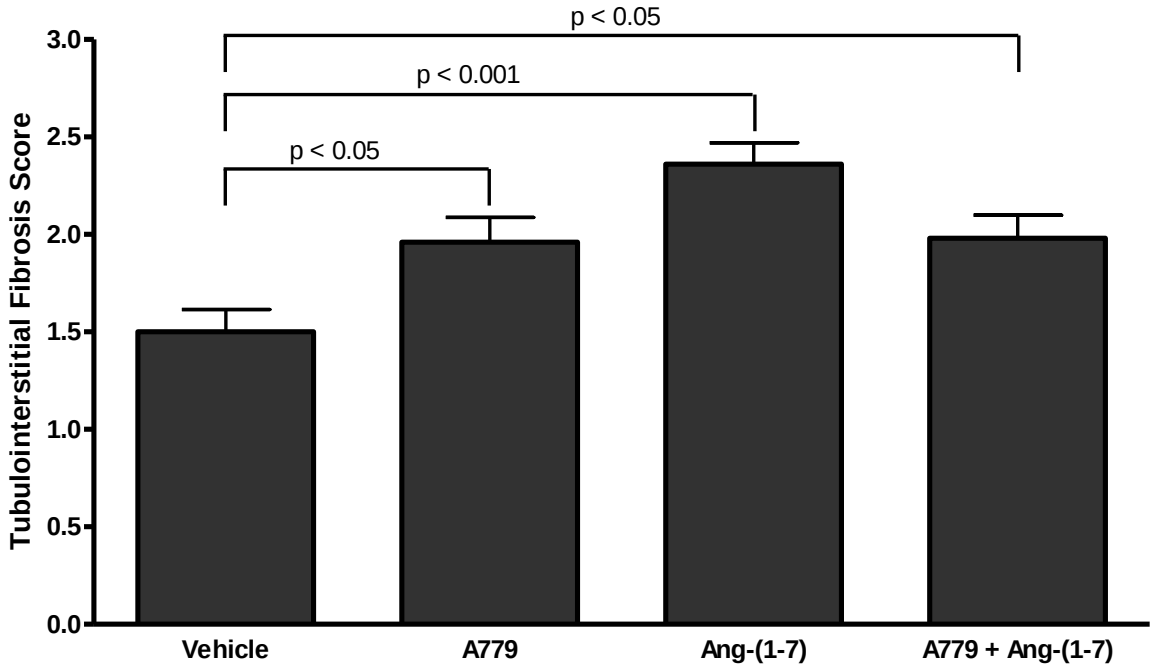

Figure 19: Effect of co-administration of A779 and high dose Ang-(1-7) on tubulointerstitial fibrosis scores in UUO. Tubulointerstitial fibrosis scores from PAS stained sections of obstructed kidneys. Values are means ± SEM (n = 6). Sections were evaluated blindly.

3.5.2 Effect of Angiotensin-(1-7) antagonism, via A779 on renal AT1, AT2 and Mas receptor mRNA

Obstruction was associated with a significant increase ($p < 0.05$) in renal cortical AT1 receptor mRNA compared to unobstructed renal cortices (Figure 20). Treatment with A779 was also associated with a significant increase ($p < 0.05$) in AT1 receptor mRNA levels in obstructed kidneys compared to unobstructed kidneys. However, AT1 receptor mRNA levels were not different between vehicle and A779 treatment groups in unobstructed or obstructed kidneys.

Given the low expression levels for the AT2 receptor within adult mouse kidneys (Reinhold et al., 2012), Real-time-PCR results for the AT2 receptor are presented as the mean CT values for the samples where a PCR product was detectable (Table 4). In unobstructed kidneys from vehicle treated mice, there were no samples with a detectable PCR product. In obstructed kidneys from vehicle treated mice, the average CT value was 38.8 ($n = 2$). Similarly, no renal cortical samples from unobstructed kidneys of mice that received A779 had a detectable PCR product for the AT2 receptor. The average CT value obtained for obstructed kidneys from mice that received A779 was 38.4 ($n = 2$).

Mas receptor mRNA levels were not significantly increased by obstruction in mice that received vehicle or A779 (Figure 21). Treatment with A779 caused a significant reduction in Mas receptor mRNA levels in unobstructed and obstructed kidneys compared to mice that received vehicle.

3.5.3 Effect of exogenous Angiotensin-(1-7) on renal AT1, AT2 and Mas receptor mRNA

Exogenous administration of Ang-(1-7) was associated with a significant reduction ($p < 0.001$) in AT1 receptor mRNA in obstructed kidneys compared to obstructed kidneys from vehicle treated mice (Figure 22). Furthermore, AT1 receptor mRNA levels were significantly decreased ($p < 0.05$ to $p < 0.01$) in unobstructed kidneys from mice that received exogenous Ang-(1-7) compared to unobstructed kidneys from mice that received vehicle.

AT2 receptor mRNA levels were detectable in three renal cortical samples from unobstructed kidneys of mice that received 6 µg/kg/hr Ang-(1-7), with an average CT value of 38.8 (Table 5). The average CT value for obstructed kidneys from mice that received 6 µg/kg/hr Ang-(1-7) was 37.5 ($n = 3$). None of the unobstructed kidneys from mice that received 24 µg/kg/hr Ang-(1-7) had a detectable AT2 receptor PCR product, while three obstructed renal cortical samples from mice that received 24 µg/kg/hr Ang-(1-7) were positive, giving an average CT value of 37.2. Treatment with 62 µg/kg/hr Ang-(1-7) was associated with a PCR product in only one obstructed renal cortical sample with a CT value of 38.2. Unfortunately, due to the high CT values and few samples from which a positive PCR product was obtained no statistical analyses could be performed for the data for AT2 receptor mRNA levels.

UUO was associated with a non-significant increase in Mas receptor mRNA levels compared to unobstructed kidneys from mice that received vehicle (Figure 23). Treatment with 6 µg/kg/hr or 24 µg/kg/hr Ang-(1-7) caused a significant reduction ($p < 0.001$ and $p < 0.05$, respectively) in Mas receptor mRNA levels in unobstructed kidneys compared to unobstructed kidneys from vehicle treated mice. Similarly, Mas receptor

mRNA levels were significantly decreased in obstructed kidneys from mice that received 6 µg/kg/hr or 24 µg/kg/hr Ang-(1-7) ($p < 0.001$) compared to obstructed kidneys from mice that received vehicle. Mas receptor mRNA levels were not affected in unobstructed or obstructed kidneys from mice that received 62 µg/kg/hr Ang-(1-7) compared to unobstructed and obstructed kidneys from mice that received vehicle.

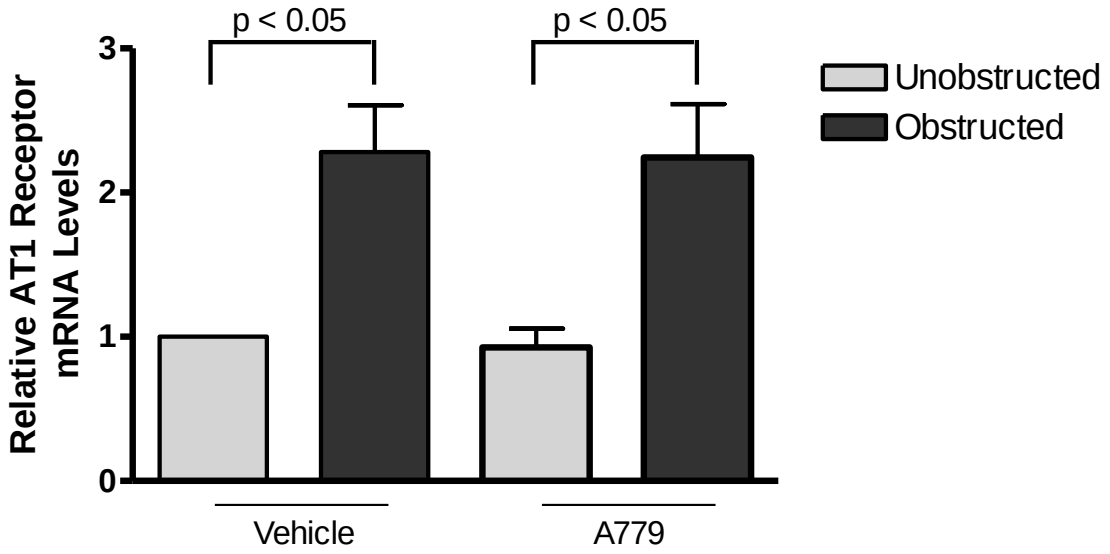

Figure 20: Effect of A779 on renal cortical AT1 receptor mRNA levels in UUO. Relative AT1 receptor mRNA levels in unobstructed and obstructed kidneys from male C57Bl/6 mice that underwent UUO for 10 days and received vehicle or A779 (31 µg/kg/hr). Data are means ± SEM (n = 12).

Table 4: Effect of A779 on detectable AT2 receptor mRNA in UUO

	Vehicle		**A779**	
	Unobstructed	Obstructed	Unobstructed	Obstructed
Detectable PCR Product	(0/6)	38.8±0.2 (2/6)	(0/6)	38.4±0.4 2/6

Mean CT values are indicated with the number of samples with a positive result for an amplification product using primers directed against the AT2 receptor indicated in parentheses.

Data are means ± SEM (n = 6)

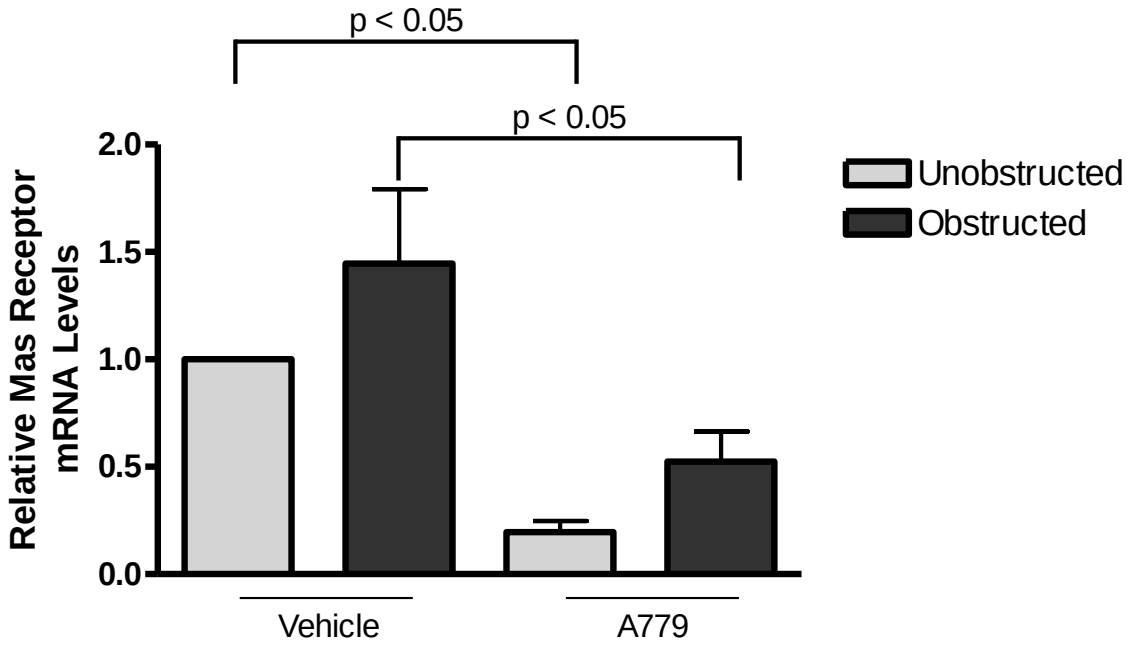

Figure 21: Effect of A779 on renal cortical Mas receptor mRNA levels in UUO. Relative Mas receptor mRNA levels in unobstructed and obstructed kidneys from male C57Bl/6 mice that underwent UUO for 10 days and received vehicle or A779 (31 µg/kg/hr). Data are means ± SEM (n = 12).

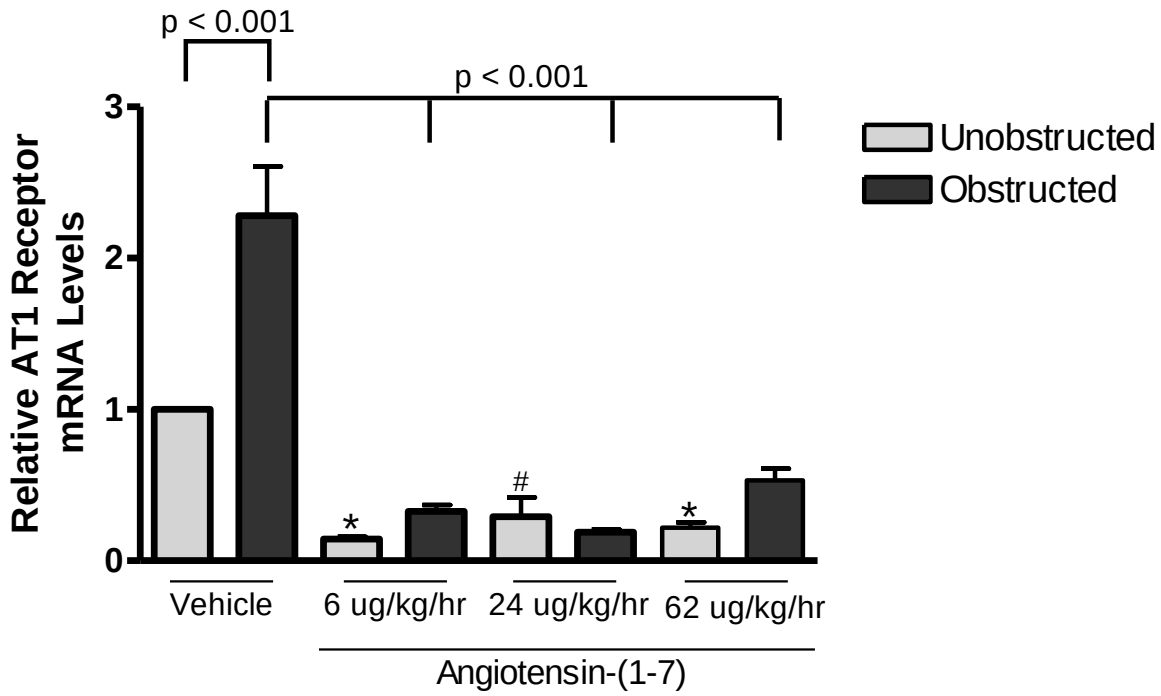

Figure 22: Effect of Exogenous Angiotensin-(1-7) on renal cortical AT1 receptor mRNA levels in UUO. Relative AT1 receptor mRNA levels in unobstructed and obstructed kidneys from male C57Bl/6 mice that underwent UUO for 10 days and received vehicle or Ang-(1-7) (6, 24, or 62 µg/kg/hr). Data are means ± SEM (n = 6). # $p < 0.05$ vs. vehicle unobstructed; * $p < 0.01$ vs. vehicle unobstructed

Table 5: Effect of exogenous Angiotensin-(1-7) on detectable AT2 receptor mRNA in UUO

					Angiotensin-(1-7)			
		Vehicle	**6 µg/kg/hr**		**24 µg/kg/hr**		**62 µg/kg/hr**	
	U	O	U	O	U	O	U	O
Detectable PCR Product	(0/6)	38.8±0.2 (2/6)	38.8±0.1 (3/6)	37.5±0.6 (3/6)	(0/6)	37.2±0.6 (3/6)	(0/6)	38.2 (1/6)

Mean CT values are indicated with the number of samples with a positive result for an amplification product using primers directed against the AT2 receptor indicated in parentheses.

Data are means ± SEM (n = 6)

Abbreviations

U: unobstructed

O: obstructed

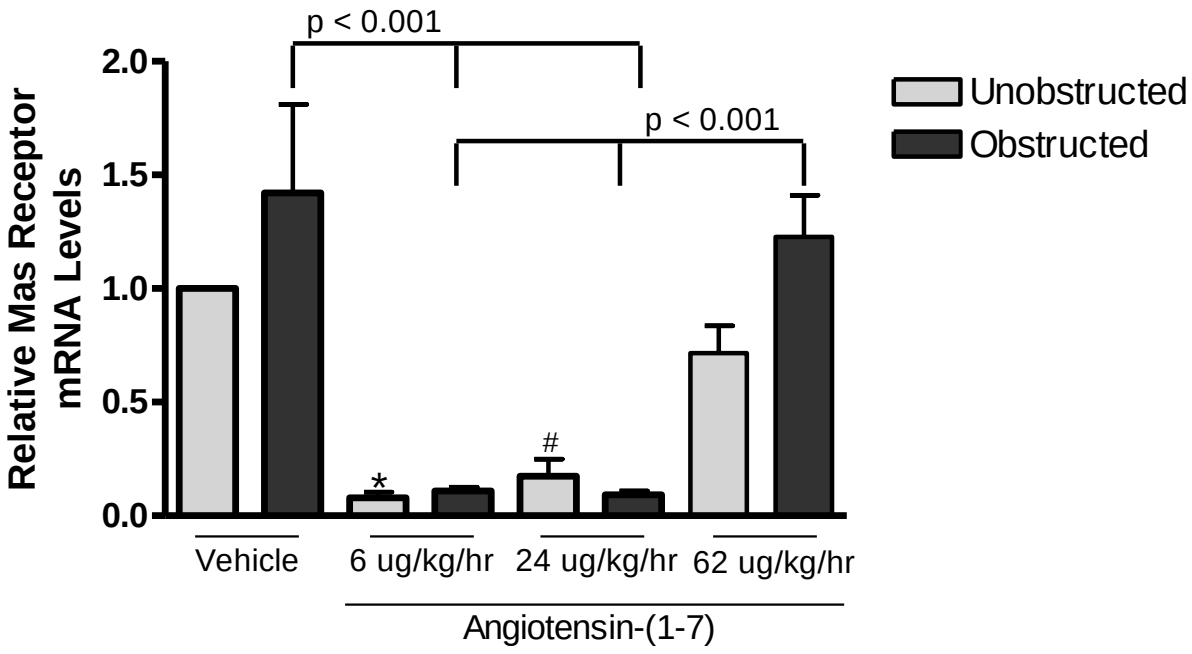

Figure 23: Effect of exogenous Angiotensin-(1-7) on renal cortical Mas receptor mRNA levels in UUO. Relative Mas receptor mRNA levels in unobstructed and obstructed kidneys from male C57Bl/6 mice that underwent UUO for 10 days and received vehicle or Ang-(1-7) (6, 24, or 62 µg/kg/hr). Data are means ± SEM (n = 6). # $p < 0.05$ vs. vehicle unobstructed; * $p < 0.001$ vs. vehicle unobstructed

3.6 Part 4: Effect of A779 in primary cultures of mouse proximal tubular cells

To evaluate whether increased renal injury in mice that received A779 or Ang-(1-7) was due to stimulation of potentially deleterious pathways, primary cultures of proximal tubular cells from male C57Bl/6 mice were incubated with 10^{-5} M A779 or 10^{-7} M Ang-(1-7) and p38 and ERK1/2 MAPK activation was assessed by immunoblot.

Incubation of primary cultures of mouse proximal tubular cells with Ang II (10^{-6} M) or PMA (10^{-5} M) was associated with a significant increase ($p < 0.01$) in p38 MAPK phosphorylation compared to vehicle (Figure 24). Incubation with A779 (10^{-5} M) or Ang-(1-7) (10^{-7} M) had no effect on p38 MAPK phosphorylation compared to vehicle. Furthermore, incubation with Ang-(1-7) (10^{-7} M) for 15 minutes prior to addition of Ang II (10^{-6} M) significantly attenuated ($p < 0.01$) p38 MAPK phosphorylation in primary cultures of mouse proximal tubular cells compared to Ang II alone.

ERK1/2 MAPK phosphorylation was increased in primary cultures of mouse proximal tubular cells stimulated with Ang II (10^{-6} M), although this did not reach statistical significance when compared to vehicle (Figure 25). Stimulation with PMA (10^{-5} M) was associated with a significant increase ($p < 0.05$) in ERK1/2 MAPK phosphorylation compared to vehicle. Stimulation with A779 (10^{-5} M) or Ang-(1-7) (10^{-7} M) had no effect on ERK1/2 MAPK phosphorylation compared to vehicle. Incubation with Ang-(1-7) (10^{-7} M) for 15 minutes prior to addition of Ang II (10^{-6} M) caused a significant reduction in ERK1/2 MAPK phosphorylation compared to Ang II alone.

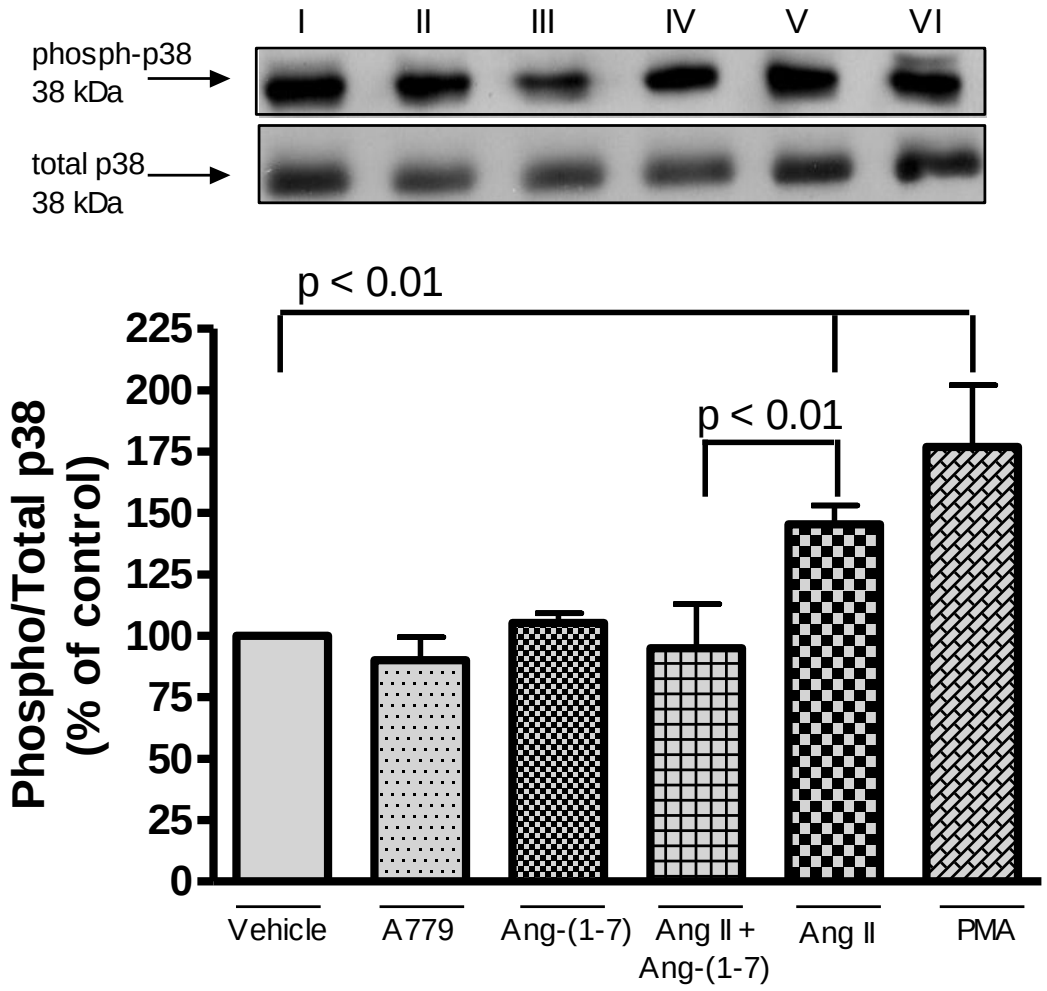

Figure 24: Effect of A779 on p38 MAPK phosphorylation *in vitro*. The effect of 10^{-5} M A779, 10^{-7} M Ang-(1-7), 10^{-6} M Ang II, Ang II + Ang-(1-7), or 10^{-5} M PMA on p38 MAPK phosphorylation. Cells were treated for 15 minutes and immunoblotting was performed for phosphorylated p38 and total p38 protein. Values are means ± SEM. (n = 5-8).

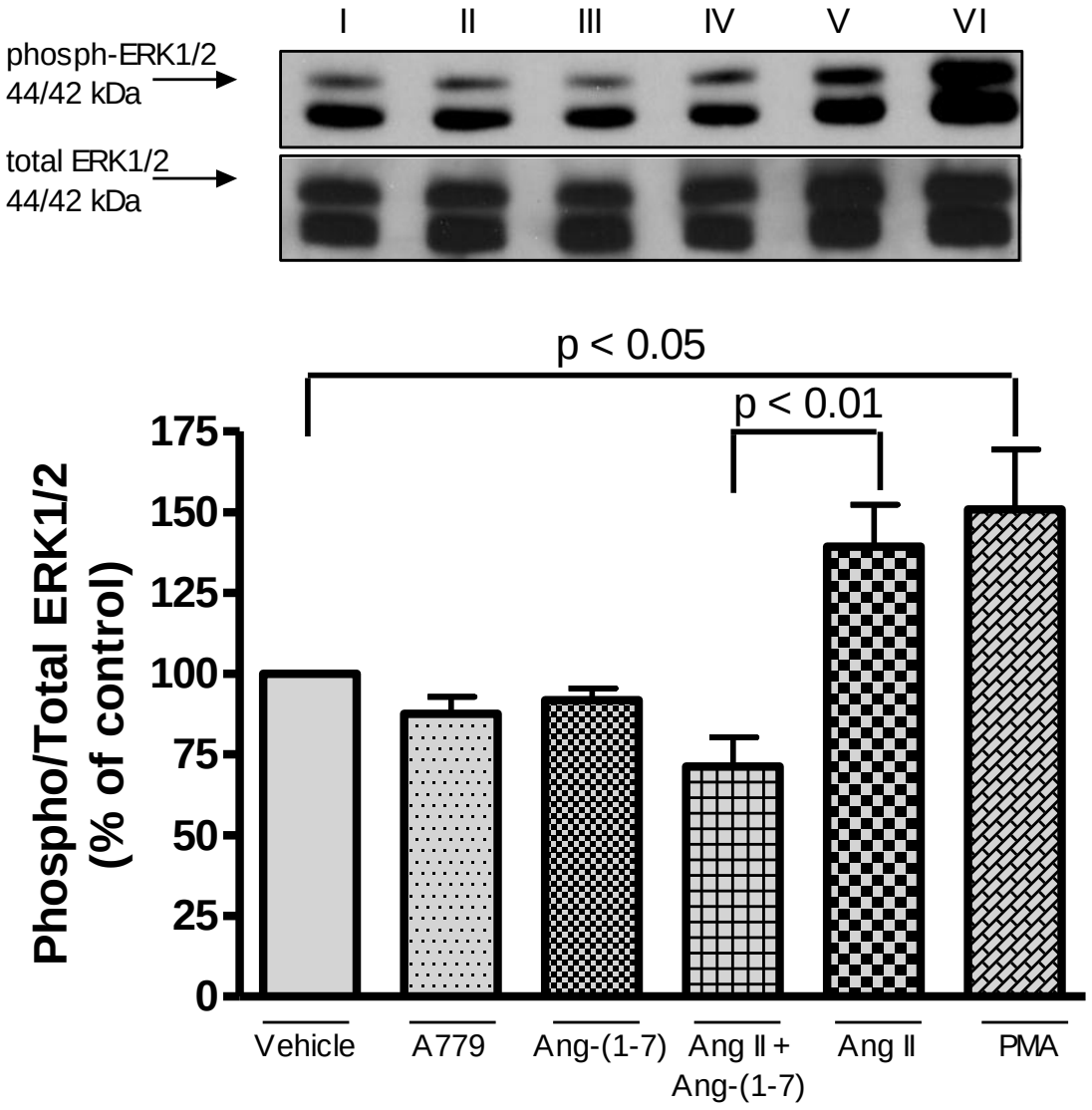

Figure 25: Effect of A779 on ERK1/2 MAPK phosphorylation *in vitro*. The effect of 10^{-5} M A779, 10^{-7} M Ang-(1-7), 10^{-6} M Ang II, Ang II + Ang-(1-7), or 10^{-5} M PMA on ERK1/2 MAPK phosphorylation. Cells were treated for 15 minutes and immunoblotting was performed for phosphorylated ERK1/2 and total ERK1/2 protein. Values are means ± SEM. (n = 5).

4.0 Discussion

The main objective of this study was to evaluate the effects of Ang-(1-7) in the UUO model of renal fibrosis. After 10 days of UUO, obstructed kidneys showed increased fibronectin, TGF-β, and α-SMA expression, increased NAPDH oxidase activity, tubulointerstitial fibrosis, inflammatory infiltrates, and apoptosis. Antagonism of endogenous Ang-(1-7), via A779, exacerbated all of these markers in obstructed kidneys suggesting an important role for endogenous Ang-(1-7) in the progression of UUO. Thus, it was hypothesized that delivery of Ang-(1-7) would attenuate the effects of UUO, at least at low dose. Surprisingly, treatment with exogenous Ang-(1-7) also exacerbated all markers of renal injury regardless of dose. Co-administration of A779 with high dose Ang-(1-7) was associated with increased fibronectin and α-SMA expression but partially decreased tubulointerstitial fibrosis scores compared to Ang-(1-7) alone and completely attenuated TGF-β expression compared to A779 or Ang-(1-7) alone.

4.1 Use of the pharmacological Angiotensin-(1-7) antagonist, A779, in UUO

The effects of endogenous Ang-(1-7) were investigated using A779, the antagonist to Ang-(1-7). This approach is useful as administration of the pharmacological antagonist of Ang-(1-7) to adult mice avoids any potential effect of either Mas or ACE2 KO on renal growth and development. Furthermore, the use of ACE2 KO mice does not clearly provide information on the role of Ang-(1-7) given that renal Ang II levels are also affected by ACE2 KO (Z. Liu, X. R. Huang, H. Y. Chen et al.,

2012). Santos et al (1994) have demonstrated that A779 is a selective antagonist of Ang-(1-7) that possesses no intrinsic agonistic activity or Ang II antagonist activity.

It is important to note that UUO did not have any effect on SBP, body weight, or any plasma parameters examined, as is typical of this model (Fern et al., 1999; L. J. Ma et al., 2003). In addition, treatment with A779 did not affect SBP, body weight, or plasma parameters. These findings indicate that any effect on renal injury is due to infusion of A779 and not secondary to alterations in SBP or overall animal health.

There was no effect of UUO on plasma electrolytes or markers of renal function, including plasma urea, as expected given the unobstructed kidney can compensate for the loss of function of the obstructed kidney (Chevalier et al., 2009). Treatment with A779 had no effect on plasma electrolytes or markers of renal function, suggesting the Ang-(1-7) antagonist did not impact function of the unobstructed kidney.

To assess renal injury in UUO immunoblotting was performed for fibronectin, TGF-β, and α-SMA, and tubulointerstitial fibrosis was scored according to a four point system. These markers of injury were chosen as they are commonly evaluated in the assessment of UUO-induced renal fibrosis (L. Liu et al., 2012; Z. Liu, X. R. Huang, H. Y. Chen et al., 2012; Tasanarong et al., 2012). UUO resulted in a significant increase in fibronectin, TGF-β, and α-SMA expression, and tubulointerstitial fibrosis scores in obstructed kidneys when compared to unobstructed kidneys. Antagonism of Ang-(1-7) was associated with an exacerbation of all markers of renal injury in obstructed kidneys, while minimal or no changes were noted in unobstructed kidneys suggesting an important role for endogenous Ang-(1-7) in the fibrotic response in UUO.

UUO has been associated with an increase in renal concentrations of both Ang-(1-7) and Ang II (Z. Liu, X. R. Huang, H. Y. Chen et al., 2012). Experiments are currently being performed in our lab to assess renal levels of Ang II and Ang-(1-7). Increased Ang II levels have been shown to play a major role in TGF-β and α-SMA expression in obstructed kidneys (Chevalier et al., 2009; Klahr et al., 1998). Elevations in Ang-(1-7) levels in the obstructed kidney likely represent a compensatory response and a play an important role in counteracting pro-fibrotic and pro-inflammatory signalling via Ang II/AT1 receptor pathways. In agreement with this, treatment of mice with the Ang-(1-7) antagonist caused a further increase in both TGF-β and α-SMA expression in obstructed kidneys indicating a loss of counter-regulatory signalling via Ang-(1-7)/Mas receptor pathways. Studies performed in primary cultures of mouse proximal tubular cells did not reveal any agonistic activity of A779 on MAPK signalling, suggesting increased renal injury is not due to stimulation of either the AT1 or Mas receptors by A779, at least in this cell type. Further studies in other cell types affected by UUO, including fibroblasts, may provide additional insight into potential off target effects of A779.

The inflammatory response in UUO has been linked to elevated Ang II and signalling via both AT1 and AT2 receptors, which leads to NF-kB activation and subsequent transcription of pro-inflammatory cytokines including tumour necrosis factor-α (TNF-α), MCP-1, and interleukin-6 (IL-6) (Esteban et al., 2004). Thus, as expected immunohistochemical analysis of renal cortical sections revealed a significant increase in inflammation in obstructed kidneys compared to unobstructed kidneys from vehicle treated mice. Obstructed kidneys from mice that received A779 showed no further

increase in inflammation compared to obstructed kidneys from mice that received vehicle. These data were unexpected given that pro-inflammatory signalling via Ang II/AT1 receptor pathways would go unchecked by Ang-(1-7)/Mas signalling in A779 treated mice. This suggests the anti-inflammatory pathways mediated by Ang-(1-7)/Mas may not act through inhibition of NF-kB signalling.

Apoptosis in UUO occurs rapidly post-obstruction and plays an important role in tubular atrophy and loss of functional renal mass (Truong et al., 1996). Accordingly, obstructed kidneys from mice that received vehicle showed increased numbers of apoptotic cells compared to unobstructed kidneys. Apoptosis was not confined to a specific cell type, with apoptotic cells being found in tubules, glomeruli, and the interstitium. There are many factors that have been implicated in the apoptotic pathways in UUO, including TGF-β. Furthermore, NO has been implicated as anti-apoptotic in UUO (Miyajima et al., 2001). Given that Ang-(1-7) is known to attenuate Ang II-induced TGF-β expression (Su et al., 2006) and to stimulate the production of NO (Gwathmey et al., 2010) in the kidney, it is not surprising that administration of the Ang-(1-7) antagonist was associated with a further increase in the number of apoptotic cells in the obstructed kidney. Therefore, these data indicate endogenous Ang-(1-7) may act as anti-apoptotic in the obstructed kidney to preserve functional renal tissue and delay the progression of fibrosis. These data stand in stark contrast to the data obtained by Esteban et al (2009) that suggest endogenous Ang-(1-7) acting via the Mas receptor stimulates pro-inflammatory and pro-apoptotic pathways. The data obtained in this study suggest a protective role for endogenous Ang-(1-7) in the obstructed kidney. These differences could be due to the activation of alternative pathways in the Mas KO

mice or alterations in other Mas related genes. Furthermore, the Ang-(1-7) antagonist may be acting in a non-specific manner and activating pro-fibrotic pathways yet to be determined. Further studies using the Ang-(1-7) antagonist in the Mas KO mice will yield further information about the potential role of A779 in the exacerbation of renal fibrosis seen in this study.

Oxidative stress has been identified as an important contributor in the progression of UUO (Kinter et al., 1999) and has been implicated in apoptosis (Kim et al., 2012; Sugiyama et al., 1996). Thus, we sought to determine whether NADPH oxidase activity was elevated in obstructed kidneys from vehicle or A779 treated mice. Using the lucigenin assay, NADPH oxidase activity was found to be slightly elevated in obstructed kidneys from vehicle treated mice, although this increase did not reach statistical significance. However, treatment with A779 was associated with a significant increase in renal NADPH oxidase activity compared to either unobstructed kidneys from mice that received A779 or obstructed kidneys from vehicle treated mice. These data suggest an important role for endogenous Ang-(1-7) in suppressing renal NADPH oxidase activity in the obstructed kidney. In agreement, Ang-(1-7) attenuates Ang II induced NADPH oxidase activity in experimental diabetic nephropathy (Moon et al., 2011). Taken together, these data suggest an important role for Ang-(1-7) in preventing pathological NADPH oxidase activation and subsequent ROS production.

Unfortunately, due to the non-specific nature of antibodies directed against GPCRs, the effect of A779 on AT1, AT2, and Mas receptor protein expression could not be reliably studied. However, real time RT-PCR was performed for all three receptors. Renal cortical AT1 receptor mRNA was elevated in obstructed kidneys from mice that

received vehicle or A779 compared to unobstructed kidneys. AT1 receptor mRNA levels were unaffected by treatment with A779, suggesting A779 has no effect on AT1 receptor transcription. AT2 receptor mRNA was either not detected or detected at too low a level to make any conclusions about the role of the AT2 receptor or the effects of A779 on AT2 receptor expression in UUO. Renal cortical mRNA for the Mas receptor was significantly decreased in unobstructed and obstructed kidneys from mice that received A779 compared to unobstructed and obstructed kidneys from mice that received vehicle. It is unclear if this effect is due to decreased Mas receptor degradation due to A779 binding or a direct effect of A779 on Mas gene transcription. If this decrease in Mas receptor mRNA levels correspond to a reduction in cell surface expression, combined with the presence of the Ang-(1-7) antagonist, the anti-fibrotic actions of Ang-(1-7) would be further limited.

4.2 Effect of exogenous Angiotensin-(1-7) in UUO

Whole animal characteristics, including SBP and body weight, were unaffected by treatment with exogenous Ang-(1-7). Furthermore, plasma electrolytes and markers of renal function, including urea and creatinine, were unchanged after 10 days of UUO and infusion of exogenous Ang-(1-7). A non-significant reduction in hematocrit was noted in all mice that received Ang-(1-7) regardless of dose. Anaemia is a common finding in patients with CKD that is secondary to a reduction in the failing kidney's ability to produce erythropoietin – a major factor in the production of red blood cells (Tsagalis, 2011). This suggests treatment with exogenous Ang-(1-7) caused considerable renal

injury in the obstructed kidney that may have led to reduced erythropoietin production, an effect that the unobstructed kidney may not have been able to compensate for.

Treatment with exogenous Ang-(1-7) exacerbated all markers of renal injury examined in this study. In most cases, a dose-dependent effect of Ang-(1-7) infusion was seen on renal injury, the only exceptions being renal cortical TGF-β expression and the number of TUNEL positive cells in the obstructed kidney. These data suggest a pro-fibrotic and pro-inflammatory role for Ang-(1-7) when delivered exogenously.

Renal cortical fibronectin and α-SMA showed a clear dose-dependent increase in expression in obstructed kidneys with exogenous Ang-(1-7) administration. TGF-β expression was slightly reduced at high dose (62 μg/kg/hr) compared to low (6 μg/kg/hr) or moderate (24 μg/kg/hr) dose Ang-(1-7), although this reduction did not reach statistical significance and was still elevated above control. It is possible that very high intra-renal concentrations of Ang-(1-7) within the obstructed kidney led to a more rapid activation of TGF-β compared to the lower doses. Thus, TGF-β expression may be returning to normal while other fibrotic pathways continue to promote fibronectin expression and the activation of myofibroblasts. In agreement with this, tubulointerstitial fibrosis scores were the highest in obstructed kidneys from mice that received high dose exogenous Ang-(1-7). Therefore, these data clearly suggest activation of pro-fibrotic pathways in response to exogenous Ang-(1-7). Whether the pro-fibrotic pathways are being activated via Ang-(1-7) acting on the Mas receptor or perhaps cross-reacting with the AT1 receptor or other unknown pathways is as yet unclear.

A dose-dependent increase in renal inflammatory infiltration was noted in obstructed kidneys from mice that received exogenous Ang-(1-7) compared to obstructed kidneys from mice that received vehicle. This suggests activation of pro-inflammatory pathways by exogenous administration of Ang-(1-7). Similarly, when Esteban et al (2009) infused Ang-(1-7) (25 µg/kg/hr) into mice subject to UUO for 5 days they found increased renal inflammatory infiltration and elevated NF-kB activity in obstructed kidneys compared to obstructed kidneys from mice that received saline. The pro-inflammatory effects of Ang-(1-7) were not attributed to cross-activation of AT1 receptors as inflammatory infiltration still occurred when high dose Ang-(1-7) (65 µg/kg/hr) was infused into healthy mice lacking AT1 and AT2 receptors. Taken together, these data suggest that at high doses, Ang-(1-7) activates NF-kB in obstructed kidneys leading to enhanced inflammation. However, the pathways through which Ang-(1-7) may activate NF-kB require further study.

Treatment with Ang-(1-7) resulted in a biphasic effect on apoptosis in UUO. Obstructed kidneys from mice that received low dose (6 µg/kg/hr) and high dose (62 µg/kg/hr) Ang-(1-7) had significantly more apoptotic cells than mice that received vehicle. Interestingly, obstructed kidneys from mice that received a moderate dose of Ang-(1-7) (24 µg/kg/hr) did not have increased numbers of apoptotic nuclei in obstructed kidneys compared to obstructed kidneys from mice that received vehicle. These results are difficult to interpret but indicate activation of pro-apoptotic pathways at low and high dose Ang-(1-7). Further studies into apoptotic pathways, including the roles of Bax and Bcl-xL, may provide additional information about the biphasic effect of Ang-(1-7) in apoptosis in UUO.

Exogenous Ang-(1-7) was associated with a 2.5 fold increase in renal cortical NADPH oxidase activity in obstructed kidneys compared to obstructed kidneys from vehicle treated mice. Interestingly, increasing the dose of Ang-(1-7) from 6 µg/kg/hr to 24 µg/kg/hr to 62 µg/kg/hr had no further effect on NADPH oxidase activity, suggesting a maximal activation of NADPH oxidase subunits in the obstructed kidney. Surprisingly, NADPH oxidase activity was also increased in unobstructed kidneys from mice that received 24 µg/kg/hr or 62 µg/kg/hr Ang-(1-7) suggestive of activation of oxidative stress pathways by Ang-(1-7) in the absence of any pathology. Ultimately, this suggests administration of exogenous Ang-(1-7) in UUO may promote renal injury via activation of NAPDH oxidases and oxidative stress pathways in both the unobstructed and obstructed kidney.

In contrast to the data obtained in first part of this study, these data are in agreement with those obtained by Esteban et al (2009). In their study, treatment of mice that had undergone UUO with Ang-(1-7) (24 µg/kg/hr) for 5 days was associated with enhanced apoptosis, renal inflammation, and NF-kB activation compared to mice that received saline. Taken together, the data obtained suggest a detrimental role for Ang-(1-7) in the UUO model of renal fibrosis through the activation of inflammatory and apoptotic pathways. The beneficial effects of Ang-(1-7) *in vivo* may be isolated to situations of elevated glucose as seen in studies of diabetic mice (Benter et al., 2007; Benter et al., 2008). Further studies in the UUO model need to be conducted to determine the pathways through which Ang-(1-7) may be promoting renal injury.

Administration of exogenous Ang-(1-7) was associated with a reduction in renal cortical mRNA for the AT1 receptor in unobstructed and obstructed kidneys. There are

several possible explanations for the reduction in renal cortical AT1 receptor mRNA. High concentrations of Ang-(1-7) have been shown to interact with the AT1 receptor and as such infusion of Ang-(1-7) may be promoting downregulation of the AT1 receptor (Bosnyak et al., 2011). Infusion of Ang-(1-7) has been shown to increase ACE activity (Velkoska, Dean, Griggs et al., 2010), which would promote Ang II generation which could also lead to reduced expression of the AT1 receptor. Furthermore, UUO-induced apoptosis could lead to loss of renal tubular cells that express the AT1 receptor. One might expect a reduction in renal cortical AT1 receptor mRNA expression to be beneficial to the kidney, but unfortunately we are unable to determine cell surface protein expression for the AT1 receptor. Interestingly, low dose Ang-(1-7) (6 µg/kg/hr) appears to increase renal cortical mRNA for the AT2 receptor. Due to high CT values obtained for the AT2 receptor, the results remain difficult to interpret. Mas receptor mRNA was significantly reduced in unobstructed and obstructed kidneys of mice that received low and moderate dose Ang-(1-7) (6 µg/kg/hr and 24 µg/kg/hr, respectively) but was unaffected by treatment with high dose Ang-(1-7) (62 µg/kg/hr). Unfortunately these data do not provide information on renal protein levels for the Mas receptor, but suggest that lower doses of Ang-(1-7) actually may downregulate transcription.

4.3 Effect of co-administration of A779 and Angiotensin-(1-7) in UUO

To investigate whether renal injury caused by Ang-(1-7) was mediated by the Mas receptor a group of mice received A779 (83 µg/kg/hr) with Ang-(1-7) (62 µg/kg/hr). For this portion of the study, the dose of A779 was increased in order to be in excess of Ang-(1-7).

Treatment with A779 or Ang-(1-7) alone was associated with similar effects on renal cortical fibronectin, TGF-β, and α-SMA expression, and tubulointerstitial fibrosis scores in obstructed kidneys as seen in Part1 and 2. Co-administration of A779 with Ang-(1-7) was associated with a further increase in fibronectin and α-SMA expression but a significant reduction in TGF-β expression in obstructed kidneys compared to obstructed kidneys from mice that received A779 or Ang-(1-7) alone. Furthermore, TGF-β expression in obstructed kidneys from mice that received A779 and Ang-(1-7) was decreased compared to obstructed kidneys from mice that received either agent alone, although this did not reach statistical significance. These data suggest that Ang-(1-7) may be stimulating TGF-β production via the Mas receptor but that other pathways are involved in the activation of myofibroblasts and the production of fibronectin. Whether these pathways involve cross-activation of the AT1 receptor due to high concentrations of Ang-(1-7) within the obstructed kidney or increased stimulation of the Mas receptor leading to pro-fibrotic and pro-inflammatory signalling is unclear.

Interestingly, co-administration of A779 with Ang-(1-7) was associated with a slight reduction in tubulointerstitial fibrosis scores in obstructed kidneys compared to obstructed kidneys from mice that received Ang-(1-7) alone. In fact, tubulointerstitial fibrosis scores from obstructed kidneys of mice that received A779 and Ang-(1-7) were similar to those scores from obstructed kidneys from mice that received A779 alone. These results are very similar to those obtained from mice that received Losartan. Treatment with Losartan completely reduced TGF-β expression while only partially attenuating fibronectin expression. Furthermore, Losartan treatment had no effect on α-

SMA expression. These data suggest these fibrotic markers may be mediated by several pathways not affected by AT1 receptor blockade or Ang-(1-7) antagonism.

In summary, co-administration of A779 with Ang-(1-7) completely prevented the increase in TGF-β expression and partially attenuated increased tubulointerstitial fibrosis scores. However, co-administration of A779 with Ang-(1-7) resulted in a further increase in both fibronectin and α-SMA expression in obstructed kidneys. These data suggest high intra-renal concentrations of Ang-(1-7) can act on the Mas receptor to promote TGF-β expression and subsequent pro-fibrotic signalling. However, the pathways by which exogenous Ang-(1-7) acts to stimulate fibronectin and α-SMA expression in the obstructed kidney remain unclear. Unfortunately, data are not available on the effect of co-administration of A779 with Ang-(1-7) on inflammation and apoptosis in the obstructed kidney.

4.4 Conclusions

In the UUO model of renal fibrosis, treatment with the Ang-(1-7) antagonist, A779, exacerbated all markers of renal injury including fibronectin , TGF-β, and α-SMA expression, tubulointerstitial fibrosis, apoptosis, and NADPH oxidase activity in the obstructed kidney. These data suggest an important role for endogenous Ang-(1-7) in counter-acting the pro-fibrotic pathways activated in the obstructed kidney and delaying the progression of renal fibrosis in UUO. Thus, it was hypothesized that delivery of exogenous Ang-(1-7) would provide a protective role in UUO and attenuate the fibrotic and inflammatory changes in the obstructed kidney associated with UUO. Paradoxically

however, infusion of exogenous Ang-(1-7) from low dose to high dose was associated with exacerbation of all markers of renal injury examined in this study. Some of these effects appear to be mediated by the Mas receptor as co-administration of A779 with Ang-(1-7) attenuated TGF-β production and partially reduced tubulointerstitial fibrosis scores. Exogenous Ang-(1-7) still appears to activate non-Mas-dependent pro-fibrotic pathways given that fibronectin and α-SMA expression remain significantly elevated in obstructed kidneys, despite co-administration of the Ang-(1-7) antagonist, A779. These data suggest that there are Mas-dependent pro-fibrotic pathways that may be mediated via TGF-β. It is as yet unclear how exogenous Ang-(1-7) stimulates pro-inflammatory pathways and EMT as suggested by elevated α-SMA levels. Possible mechanisms for the paradoxical effects of Ang-(1-7) in UUO are summarized in Figure 26 and Table 6. Additional studies in the Mas KO mouse may help to delineate whether A779 or Ang-(1-7) are acting on other receptors or through other pathways to promote renal inflammation and fibrosis in UUO.

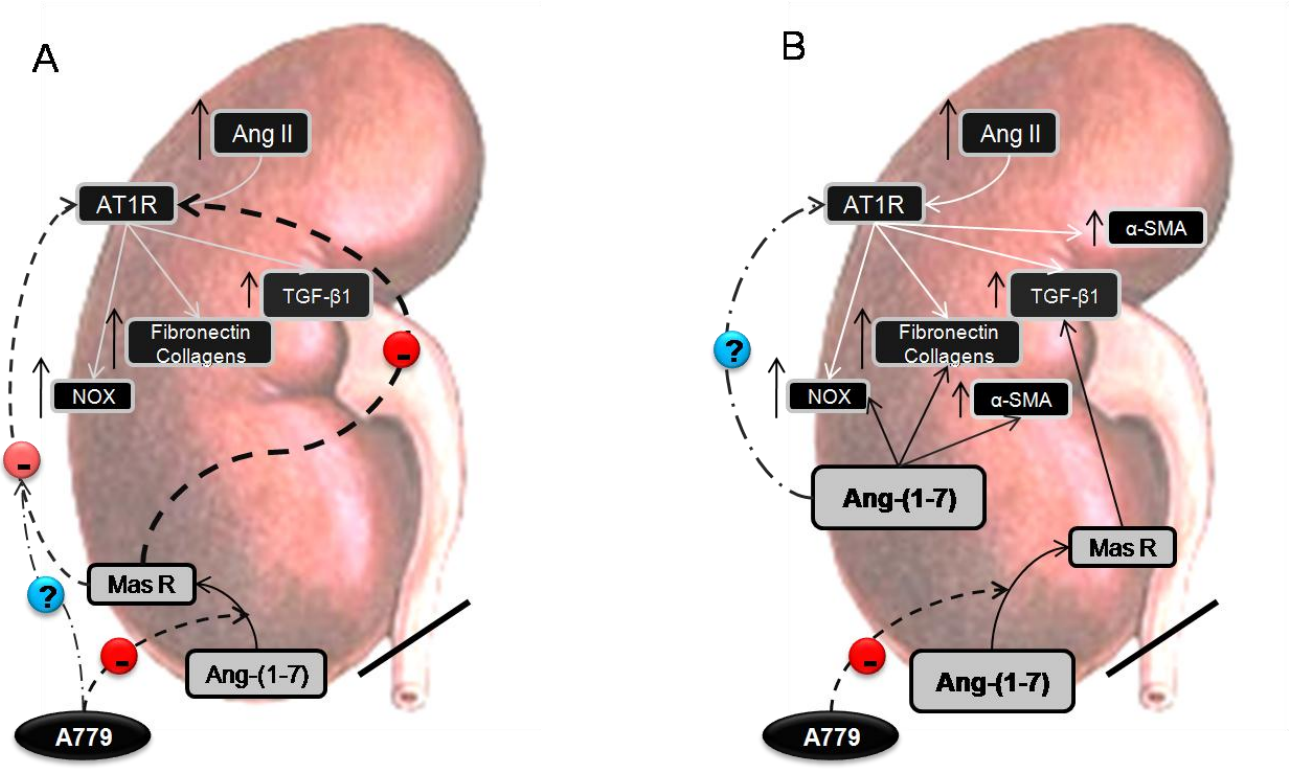

Figure 26: Potential mechanisms for the paradoxical effects of Angiotensin-(1-7) in UUO. (A) Endogenous Ang-(1-7) acts on the Mas receptor to attenuate Ang II-induced pro-fibrotic and pro-inflammatory signalling. A779 prevents the interaction of Ang-(1-7) with the Mas receptor and counter-regulatory signalling of Ang-(1-7) is inhibited. A779 may also prevent the Mas receptor from interacting with and inhibiting AT1 receptor signalling. (B) Delivery of exogenous Ang-(1-7) may lead to high intra-renal levels of Ang-(1-7) which may promote pro-fibrotic signalling via the Mas receptor or possible cross-activation of the AT1 receptor. The mechanisms behind Ang-(1-7) induced fibrosis and inflammation in UUO require further study.

Table 6: Possible mechanisms for the paradoxical effects of Angiotensin-(1-7) in UUO

Protective	Deleterious
Antagonism of AT1 receptor pathways	High dose Activation of AT1 receptor pathways
Stimulation of NO production	Mas receptor-dependent inflammatory pathways
Inhibition of renal NADPH oxidase activity	Mas receptor-dependent TGF-β activation
Mas receptor-dependent anti-inflammatory pathways	Non-Mas receptor-dependent fibrosis and EMT

5.0 References

Alenina, N., Xu, P., Rentzsch, B., Patkin, E. L., & Bader, M. (2008). Genetically altered animal models for Mas and angiotensin-(1-7). *Exp Physiol, 93*(5), 528-537.

Babelova, A., Avaniadi, D., Jung, O., Fork, C., Beckmann, J., Kosowski, J., Weissmann, N., Anilkumar, N., Shah, A. M., Schaefer, L., Schroder, K., & Brandes, R. P. (2012). Role of Nox4 in murine models of kidney disease. *Free Radic Biol Med, 53*(4), 842-853.

Basso, N., & Terragno, N. A. (2001). History about the discovery of the renin-angiotensin system. *Hypertension, 38*(6), 1246-1249.

Benter, I. F., Yousif, M. H., Cojocel, C., Al-Maghrebi, M., & Diz, D. I. (2007). Angiotensin-(1-7) prevents diabetes-induced cardiovascular dysfunction. *Am J Physiol Heart Circ Physiol, 292*(1), H666-672.

Benter, I. F., Yousif, M. H., Dhaunsi, G. S., Kaur, J., Chappell, M. C., & Diz, D. I. (2008). Angiotensin-(1-7) prevents activation of NADPH oxidase and renal vascular dysfunction in diabetic hypertensive rats. *Am J Nephrol, 28*(1), 25-33.

Bosnyak, S., Jones, E. S., Christopoulos, A., Aguilar, M. I., Thomas, W. G., & Widdop, R. E. (2011). Relative affinity of angiotensin peptides and novel ligands at AT1 and AT2 receptors. *Clin Sci (Lond), 121*(7), 297-303.

Burns, W. C., Velkoska, E., Dean, R., Burrell, L. M., & Thomas, M. C. (2009). Angiotensin II mediates epithelial-to-mesenchymal transformation in tubular cells by ANG 1-7/MAS-1-dependent pathways. *Am J Physiol Renal Physiol, 299*(3), F585-593.

Carey, R. M., & Siragy, H. M. (2003). The intrarenal renin-angiotensin system and diabetic nephropathy. *Trends Endocrinol Metab, 14*(6), 274-281.

Chappell, M. C., Brosnihan, K. B., Diz, D. I., & Ferrario, C. M. (1989). Identification of angiotensin-(1-7) in rat brain. Evidence for differential processing of angiotensin peptides. *J Biol Chem, 264*(28), 16518-16523.

Chappell, M. C., Pirro, N. T., Sykes, A., & Ferrario, C. M. (1998). Metabolism of angiotensin-(1-7) by angiotensin-converting enzyme. *Hypertension, 31*(1 Pt 2), 362-367.

Chevalier, R. L., Forbes, M. S., & Thornhill, B. A. (2009). Ureteral obstruction as a model of renal interstitial fibrosis and obstructive nephropathy. *Kidney Int, 75*(11), 1145-1152.

Dendooven, A., Ishola, D. A., Jr., Nguyen, T. Q., Van der Giezen, D. M., Kok, R. J., Goldschmeding, R., & Joles, J. A. (2011). Oxidative stress in obstructive nephropathy. *Int J Exp Pathol, 92*(3), 202-210.

Dilauro, M., Zimpelmann, J., Robertson, S. J., Genest, D., & Burns, K. D. (2010). Effect of ACE2 and angiotensin-(1-7) in a mouse model of early chronic kidney disease. *Am J Physiol Renal Physiol, 298*(6), F1523-1532.

Dong, X., Han, S., Zylka, M. J., Simon, M. I., & Anderson, D. J. (2001). A diverse family of GPCRs expressed in specific subsets of nociceptive sensory neurons. *Cell, 106*(5), 619-632.

Eddy, A. A. (2005). Progression in chronic kidney disease. *Adv Chronic Kidney Dis, 12*(4), 353-365.

Eddy, A. A., Lopez-Guisa, J. M., Okamura, D. M., & Yamaguchi, I. (2012). Investigating mechanisms of chronic kidney disease in mouse models. *Pediatr Nephrol, 27*(8), 1233-1247.

Esteban, V., Heringer-Walther, S., Sterner-Kock, A., de Bruin, R., van den Engel, S., Wang, Y., Mezzano, S., Egido, J., Schultheiss, H. P., Ruiz-Ortega, M., & Walther, T. (2009). Angiotensin-(1-7) and the g protein-coupled receptor MAS are key players in renal inflammation. *PLoS One, 4*(4), e5406.

Esteban, V., Lorenzo, O., Ruperez, M., Suzuki, Y., Mezzano, S., Blanco, J., Kretzler, M., Sugaya, T., Egido, J., & Ruiz-Ortega, M. (2004). Angiotensin II, via AT1 and AT2 receptors and NF-kappaB pathway, regulates the inflammatory response in unilateral ureteral obstruction. *J Am Soc Nephrol, 15*(6), 1514-1529.

Fern, R. J., Yesko, C. M., Thornhill, B. A., Kim, H. S., Smithies, O., & Chevalier, R. L. (1999). Reduced angiotensinogen expression attenuates renal interstitial fibrosis in obstructive nephropathy in mice. *J Clin Invest, 103*(1), 39-46.

Ferrario, C. M. (2011). ACE2: more of Ang-(1-7) or less Ang II? *Curr Opin Nephrol Hypertens, 20*(1), 1-6.

Ferrario, C. M., Jaiswal, N., Yamamoto, K., Diz, D. I., & Schiavone, M. T. (1991). Hypertensive mechanisms and converting enzyme inhibitors. *Clin Cardiol, 14*(8 Suppl 4), IV56-62; IV83-90.

Ferrario, C. M., Martell, N., Yunis, C., Flack, J. M., Chappell, M. C., Brosnihan, K. B., Dean, R. H., Fernandez, A., Novikov, S. V., Pinillas, C., & Luque, M. (1998). Characterization of angiotensin-(1-7) in the urine of normal and essential hypertensive subjects. *Am J Hypertens, 11*(2), 137-146.

Fink, H. A., Ishani, A., Taylor, B. C., Greer, N. L., MacDonald, R., Rossini, D., Sadiq, S., Lankireddy, S., Kane, R. L., & Wilt, T. J. (2012). Screening for, monitoring, and treatment of chronic kidney disease stages 1 to 3: a systematic review for the U.S. Preventive Services Task Force and for an American College of Physicians Clinical Practice Guideline. *Ann Intern Med, 156*(8), 570-581.

Fragiadaki, M., & Mason, R. M. (2011). Epithelial-mesenchymal transition in renal fibrosis - evidence for and against. *Int J Exp Pathol, 92*(3), 143-150.

Fraune, C., Lange, S., Krebs, C., Holzel, A., Baucke, J., Divac, N., Schwedhelm, E., Streichert, T., Velden, J., Garrelds, I., Danser, A. H., Frenay, A. R., van Goor, H., Jankowski, V., Stahl, R. A., Nguyen, G., & Wenzel, U. O. (2012). AT1 antagonism and renin inhibition in mice: pivotal role of targeting angiotensin II in chronic kidney disease. *Am J Physiol Renal Physiol, Epub ahead of print*.

Garcia, N. H., & Garvin, J. L. (1994). Angiotensin 1-7 has a biphasic effect on fluid absorption in the proximal straight tubule. *J Am Soc Nephrol, 5*(4), 1133-1138.

Gava, E., Samad-Zadeh, A., Zimpelmann, J., Bahramifarid, N., Kitten, G. T., Santos, R. A., Touyz, R. M., & Burns, K. D. (2009). Angiotensin-(1-7) activates a tyrosine phosphatase and inhibits glucose-induced signalling in proximal tubular cells. *Nephrol Dial Transplant, 24*(6), 1766-1773.

Gironacci, M. M., Adamo, H. P., Corradi, G., Santos, R. A., Ortiz, P., & Carretero, O. A. Angiotensin (1-7) induces MAS receptor internalization. *Hypertension, 58*(2), 176-181.

Grobe, J. L., Mecca, A. P., Lingis, M., Shenoy, V., Bolton, T. A., Machado, J. M., Speth, R. C., Raizada, M. K., & Katovich, M. J. (2007). Prevention of angiotensin II-induced cardiac remodeling by angiotensin-(1-7). *Am J Physiol Heart Circ Physiol, 292*(2), H736-742.

Guo, G., Morrissey, J., McCracken, R., Tolley, T., Liapis, H., & Klahr, S. (2001). Contributions of angiotensin II and tumor necrosis factor-alpha to the development of renal fibrosis. *Am J Physiol Renal Physiol, 280*(5), F777-785.

Gwathmey, T. M., Westwood, B. M., Pirro, N. T., Tang, L., Rose, J. C., Diz, D. I., & Chappell, M. C. (2010). Nuclear angiotensin-(1-7) receptor is functionally coupled to the formation of nitric oxide. *Am J Physiol Renal Physiol, 299*(5), F983-990.

Han, J. Y., Kim, Y. J., Kim, L., Choi, S. J., Park, I. S., Kim, J. M., Chu, Y. C., & Cha, D. R. (2010). PPARgamma agonist and angiotensin II receptor antagonist ameliorate renal tubulointerstitial fibrosis. *J Korean Med Sci, 25*(1), 35-41.

Higashi, K., Oda, T., Kushiyama, T., Hyodo, T., Yamada, M., Suzuki, S., Sakurai, Y., Miura, S., & Kumagai, H. (2010). Additive antifibrotic effects of pioglitazone and

candesartan on experimental renal fibrosis in mice. *Nephrology (Carlton), 15*(3), 327-335.

Horiuchi, M., Iwanami, J., & Mogi, M. (2012). Regulation of angiotensin II receptors beyond the classical pathway. *Clin Sci (Lond), 123*(4), 193-203.

Huang, Y. Y., Xu, A. P., Zhou, S. S., Fu, J. Z., & Du, H. (2011). Effect of losartan on renal expression of monocyte chemoattractant protein-1 and transforming growth factor-beta(1) in rats after unilateral ureteral obstruction. *Journal of Southern Medical University 31*(8), 1405-1410.

Iyer, S. N., Chappell, M. C., Averill, D. B., Diz, D. I., & Ferrario, C. M. (1998). Vasodepressor actions of angiotensin-(1-7) unmasked during combined treatment with lisinopril and losartan. *Hypertension, 31*(2), 699-705.

Jafar, T. H., Schmid, C. H., Landa, M., Giatras, I., Toto, R., Remuzzi, G., Maschio, G., Brenner, B. M., Kamper, A., Zucchelli, P., Becker, G., Himmelmann, A., Bannister, K., Landais, P., Shahinfar, S., de Jong, P. E., de Zeeuw, D., Lau, J., & Levey, A. S. (2001). Angiotensin-converting enzyme inhibitors and progression of nondiabetic renal disease. A meta-analysis of patient-level data. *Ann Intern Med, 135*(2), 73-87.

Kim, S. M., Kim, Y. G., Jeong, K. H., Lee, S. H., Lee, T. W., Ihm, C. G., & Moon, J. Y. (2012). Angiotensin II-Induced Mitochondrial Nox4 Is a Major Endogenous Source of Oxidative Stress in Kidney Tubular Cells. *PLoS One, 7*(7), e39739.

Kinter, M., Wolstenholme, J. T., Thornhill, B. A., Newton, E. A., McCormick, M. L., & Chevalier, R. L. (1999). Unilateral ureteral obstruction impairs renal antioxidant enzyme activation during sodium depletion. *Kidney Int, 55*(4), 1327-1334.

Klahr, S., & Morrissey, J. (1998). Angiotensin II and gene expression in the kidney. *Am J Kidney Dis, 31*(1), 171-176.

Klahr, S., & Morrissey, J. (2002). Obstructive nephropathy and renal fibrosis. *Am J Physiol Renal Physiol, 283*(5), F861-875.

Kostenis, E., Milligan, G., Christopoulos, A., Sanchez-Ferrer, C. F., Heringer-Walther, S., Sexton, P. M., Gembardt, F., Kellett, E., Martini, L., Vanderheyden, P., Schultheiss, H. P., & Walther, T. (2005). G-protein-coupled receptor Mas is a physiological antagonist of the angiotensin II type 1 receptor. *Circulation, 111*(14), 1806-1813.

Kumar, R., Thomas, C. M., Yong, Q. C., Chen, W., & Baker, K. M. (2012). The intracrine renin-angiotensin system. *Clin Sci (Lond), 123*(5), 273-284.

Lara, L. S., Bica, R. B., Sena, S. L., Correa, J. S., Marques-Fernandes, M. F., Lopes, A. G., & Caruso-Neves, C. (2002). Angiotensin-(1-7) reverts the stimulatory effect of angiotensin II on the proximal tubule Na(+)-ATPase activity via a A779-sensitive receptor. *Regul Pept, 103*(1), 17-22.

Lewis, E. J., Hunsicker, L. G., Bain, R. P., & Rohde, R. D. (1993). The effect of angiotensin-converting-enzyme inhibition on diabetic nephropathy. The Collaborative Study Group. *N Engl J Med, 329*(20), 1456-1462.

Li, N., Zimpelmann, J., Cheng, K., Wilkins, J. A., & Burns, K. D. (2005). The role of angiotensin converting enzyme 2 in the generation of angiotensin 1-7 by rat proximal tubules. *Am J Physiol Renal Physiol, 288*(2), F353-362.

Li, Y., Wu, J., He, Q., Shou, Z., Zhang, P., Pen, W., Zhu, Y., & Chen, J. (2009). Angiotensin (1-7) prevent heart dysfunction and left ventricular remodeling caused by renal dysfunction in 5/6 nephrectomy mice. *Hypertens Res, 32*(5), 369-374.

Liu, G. C., Oudit, G. Y., Fang, F., Zhou, J., & Scholey, J. W. (2012). Angiotensin-(1-7)-induced activation of ERK1/2 is cAMP/protein kinase A-dependent in glomerular mesangial cells. *Am J Physiol Renal Physiol, 302*(6), F784-790.

Liu, L., Kou, P., Zeng, Q., Pei, G., Li, Y., Liang, H., Xu, G., & Chen, S. (2012). CD4+ T Lymphocytes, especially Th2 cells, contribute to the progress of renal fibrosis. *Am J Nephrol, 36*(4), 386-396.

Liu, Z., Huang, X. R., Chen, H. Y., Penninger, J. M., & Lan, H. Y. (2012). Loss of angiotensin-converting enzyme 2 enhances TGF-beta/Smad-mediated renal fibrosis and NF-kappaB-driven renal inflammation in a mouse model of obstructive nephropathy. *Lab Invest, 92*(5), 650-661.

Liu, Z., Huang, X. R., & Lan, H. Y. (2012). Smad3 mediates ANG II-induced hypertensive kidney disease in mice. *Am J Physiol Renal Physiol, 302*(8), F986-997.

Loot, A. E., Roks, A. J., Henning, R. H., Tio, R. A., Suurmeijer, A. J., Boomsma, F., & van Gilst, W. H. (2002). Angiotensin-(1-7) attenuates the development of heart failure after myocardial infarction in rats. *Circulation, 105*(13), 1548-1550.

Ma, J., Nishimura, H., Fogo, A., Kon, V., Inagami, T., & Ichikawa, I. (1998). Accelerated fibrosis and collagen deposition develop in the renal interstitium of angiotensin type 2 receptor null mutant mice during ureteral obstruction. *Kidney Int, 53*(4), 937-944.

Ma, L. J., Yang, H., Gaspert, A., Carlesso, G., Barty, M. M., Davidson, J. M., Sheppard, D., & Fogo, A. B. (2003). Transforming growth factor-beta-dependent and -

independent pathways of induction of tubulointerstitial fibrosis in beta6(-/-) mice. *Am J Pathol, 163*(4), 1261-1273.

Manni, M. E., Bigagli, E., Lodovici, M., Zazzeri, M., & Raimondi, L. (2012). The protective effect of losartan in the nephropathy of the diabetic rat includes the control of monoamine oxidase type A activity. *Pharmacol Res, 65*(4), 465-471.

Meran, S., & Steadman, R. (2011). Fibroblasts and myofibroblasts in renal fibrosis. *Int J Exp Pathol, 92*(3), 158-167.

Miyajima, A., Chen, J., Poppas, D. P., Vaughan, E. D., Jr., & Felsen, D. (2001). Role of nitric oxide in renal tubular apoptosis of unilateral ureteral obstruction. *Kidney Int, 59*(4), 1290-1303.

Miyata, N., Park, F., Li, X. F., & Cowley, A. W., Jr. (1999). Distribution of angiotensin AT1 and AT2 receptor subtypes in the rat kidney. *Am J Physiol, 277*(3 Pt 2), F437-446.

Mizuiri, S., Hemmi, H., Arita, M., Aoki, T., Ohashi, Y., Miyagi, M., Sakai, K., Shibuya, K., Hase, H., & Aikawa, A. (2011). Increased ACE and decreased ACE2 expression in kidneys from patients with IgA nephropathy. *Nephron Clin Pract, 117*(1), c57-66.

Mizuno, S., Matsumoto, K., & Nakamura, T. (2001). Hepatocyte growth factor suppresses interstitial fibrosis in a mouse model of obstructive nephropathy. *Kidney Int, 59*(4), 1304-1314.

Moon, J. Y., Tanimoto, M., Gohda, T., Hagiwara, S., Yamazaki, T., Ohara, I., Murakoshi, M., Aoki, T., Ishikawa, Y., Lee, S. H., Jeong, K. H., Lee, T. W., Ihm, C. G., Lim, S. J., & Tomino, Y. (2011). Attenuating effect of angiotensin-(1-7) on angiotensin II-mediated NAD(P)H oxidase activation in type 2 diabetic nephropathy of KK-A(y)/Ta mice. *Am J Physiol Renal Physiol, 300*(6), F1271-1282.

Mordwinkin, N. M., Russell, J. R., Burke, A. S., Dizerega, G. S., Louie, S. G., & Rodgers, K. E. Toxicological and toxicokinetic analysis of angiotensin (1-7) in two species. *J Pharm Sci, 101*(1), 373-380.

Nadarajah, R., Milagres, R., Dilauro, M., Gutsol, A., Xiao, F., Zimpelmann, J., Kennedy, C., Wysocki, J., Batlle, D., & Burns, K. D. Podocyte-specific overexpression of human angiotensin-converting enzyme 2 attenuates diabetic nephropathy in mice. *Kidney Int*.

Nadarajah, R., Milagres, R., Dilauro, M., Gutsol, A., Xiao, F., Zimpelmann, J., Kennedy, C., Wysocki, J., Batlle, D., & Burns, K. D. (2012). Podocyte-specific

overexpression of human angiotensin-converting enzyme 2 attenuates diabetic nephropathy in mice. *Kidney Int, 82*(3), 292-303.

Oudit, G. Y., Liu, G. C., Zhong, J., Basu, R., Chow, F. L., Zhou, J., Loibner, H., Janzek, E., Schuster, M., Penninger, J. M., Herzenberg, A. M., Kassiri, Z., & Scholey, J. W. (2010). Human recombinant ACE2 reduces the progression of diabetic nephropathy. *Diabetes, 59*(2), 529-538.

Pendergrass, K. D., Pirro, N. T., Westwood, B. M., Ferrario, C. M., Brosnihan, K. B., & Chappell, M. C. (2008). Sex differences in circulating and renal angiotensins of hypertensive mRen(2). Lewis but not normotensive Lewis rats. *Am J Physiol Heart Circ Physiol, 295*(1), H10-20.

Pinheiro, S. V., Ferreira, A. J., Kitten, G. T., da Silveira, K. D., da Silva, D. A., Santos, S. H., Gava, E., Castro, C. H., Magalhaes, J. A., da Mota, R. K., Botelho-Santos, G. A., Bader, M., Alenina, N., Santos, R. A., & Simoes e Silva, A. C. (2009). Genetic deletion of the angiotensin-(1-7) receptor Mas leads to glomerular hyperfiltration and microalbuminuria. *Kidney Int, 75*(11), 1184-1193.

Reinhold, S. W., Kruger, B., Barner, C., Zoicas, F., Kammerl, M. C., Hoffmann, U., Bergler, T., Banas, B., & Kramer, B. K. (2012). Nephron-specific expression of components of the renin-angiotensin-aldosterone system in the mouse kidney. *J Renin Angiotensin Aldosterone Syst, 13*(1), 46-55.

Remuzzi, G., Ruggenenti, P., & Perico, N. (2002). Chronic renal diseases: renoprotective benefits of renin-angiotensin system inhibition. *Ann Intern Med, 136*(8), 604-615.

Ren, Y., Garvin, J. L., & Carretero, O. A. (2002). Vasodilator action of angiotensin-(1-7) on isolated rabbit afferent arterioles. *Hypertension, 39*(3), 799-802.

Santos, R. A., Ferreira, A. J., & Simoes, E. S. A. C. (2008). Recent advances in the angiotensin-converting enzyme 2-angiotensin(1-7)-Mas axis. *Exp Physiol, 93*(5), 519-527.

Santos, R. A., Simoes e Silva, A. C., Maric, C., Silva, D. M., Machado, R. P., de Buhr, I., Heringer-Walther, S., Pinheiro, S. V., Lopes, M. T., Bader, M., Mendes, E. P., Lemos, V. S., Campagnole-Santos, M. J., Schultheiss, H. P., Speth, R., & Walther, T. (2003). Angiotensin-(1-7) is an endogenous ligand for the G protein-coupled receptor Mas. *Proc Natl Acad Sci U S A, 100*(14), 8258-8263.

Shiota, A., Yamamoto, K., Ohishi, M., Tatara, Y., Ohnishi, M., Maekawa, Y., Iwamoto, Y., Takeda, M., & Rakugi, H. (2010). Loss of ACE2 accelerates time-dependent glomerular and tubulointerstitial damage in streptozotocin-induced diabetic mice. *Hypertens Res, 33*(4), 298-307.

Simoes e Silva, A. C., Diniz, J. S., Pereira, R. M., Pinheiro, S. V., & Santos, R. A. (2006). Circulating renin Angiotensin system in childhood chronic renal failure: marked increase of Angiotensin-(1-7) in end-stage renal disease. *Pediatr Res, 60*(6), 734-739.

Singh, K., Singh, T., & Sharma, P. L. (2011). Beneficial effects of angiotensin (1-7) in diabetic rats with cardiomyopathy. *Ther Adv Cardiovasc Dis, 5*(3), 159-167.

Soler, M. J., Wysocki, J., Ye, M., Lloveras, J., Kanwar, Y., & Batlle, D. (2007). ACE2 inhibition worsens glomerular injury in association with increased ACE expression in streptozotocin-induced diabetic mice. *Kidney Int, 72*(5), 614-623.

Su, Z., Zimpelmann, J., & Burns, K. D. (2006). Angiotensin-(1-7) inhibits angiotensin II-stimulated phosphorylation of MAP kinases in proximal tubular cells. *Kidney Int, 69*(12), 2212-2218.

Sugiyama, H., Kashihara, N., Makino, H., Yamasaki, Y., & Ota, Z. (1996). Reactive oxygen species induce apoptosis in cultured human mesangial cells. *J Am Soc Nephrol, 7*(11), 2357-2363.

Sugiyama, H., Kobayashi, M., Wang, D. H., Sunami, R., Maeshima, Y., Yamasaki, Y., Masuoka, N., Kira, S., & Makino, H. (2005). Telmisartan inhibits both oxidative stress and renal fibrosis after unilateral ureteral obstruction in acatalasemic mice. *Nephrol Dial Transplant, 20*(12), 2670-2680.

Tasanarong, A., Kongkham, S., Duangchana, S., Thitiarchakul, S., & Eiam-Ong, S. (2012). Vitamin E ameliorates renal fibrosis by inhibition of TGF-beta/Smad2/3 signaling pathway in UUO mice. *J Med Assoc Thai, 94 Suppl 7*, S1-9.

Truong, L. D., Petrusevska, G., Yang, G., Gurpinar, T., Shappell, S., Lechago, J., Rouse, D., & Suki, W. N. (1996). Cell apoptosis and proliferation in experimental chronic obstructive uropathy. *Kidney Int, 50*(1), 200-207.

Tsagalis, G. (2011). Renal anemia: a nephrologist's view. *Hippokratia, 15*(Suppl 1), 39-43.

Turner, J. M., Bauer, C., Abramowitz, M. K., Melamed, M. L., & Hostetter, T. H. (2012). Treatment of chronic kidney disease. *Kidney Int, 81*(4), 351-362.

van der Wouden, E. A., Henning, R. H., Deelman, L. E., Roks, A. J., Boomsma, F., & de Zeeuw, D. (2005). Does angiotensin (1-7) contribute to the anti-proteinuric effect of ACE-inhibitors. *J Renin Angiotensin Aldosterone Syst, 6*(2), 96-101.

Velkoska, E., Dean, R. G., Burchill, L., Levidiotis, V., & Burrell, L. M. (2010). Reduction in renal ACE2 expression in subtotal nephrectomy in rats is ameliorated with ACE inhibition. *Clin Sci (Lond), 118*(4), 269-279.

Velkoska, E., Dean, R. G., Griggs, K., Burchill, L., & Burrell, L. M. (2010). Angiotensin-(1-7) infusion is associated with increased blood pressure and adverse cardiac remodelling in rats with subtotal nephrectomy. *Clin Sci (Lond), 120*(8), 335-345.

Vinay, P., Gougoux, A., & Lemieux, G. (1981). Isolation of a pure suspension of rat proximal tubules. *Am J Physiol, 241*(4), F403-411.

Wong, D. W., Oudit, G. Y., Reich, H., Kassiri, Z., Zhou, J., Liu, Q. C., Backx, P. H., Penninger, J. M., Herzenberg, A. M., & Scholey, J. W. (2007). Loss of angiotensin-converting enzyme-2 (Ace2) accelerates diabetic kidney injury. *Am J Pathol, 171*(2), 438-451.

Xiong, M., Gong, J., Liu, Y., Xiang, R., & Tan, X. (2012). Loss of vitamin D receptor in chronic kidney disease: a potential mechanism linking inflammation to epithelial-to-mesenchymal transition. *Am J Physiol Renal Physiol*.

Yamada, K., Iyer, S. N., Chappell, M. C., Ganten, D., & Ferrario, C. M. (1998). Converting enzyme determines plasma clearance of angiotensin-(1-7). *Hypertension, 32*(3), 496-502.

Ye, M., Wysocki, J., William, J., Soler, M. J., Cokic, I., & Batlle, D. (2006). Glomerular localization and expression of Angiotensin-converting enzyme 2 and Angiotensin-converting enzyme: implications for albuminuria in diabetes. *J Am Soc Nephrol, 17*(11), 3067-3075.

Yogi, A., Mercure, C., Touyz, J., Callera, G. E., Montezano, A. C., Aranha, A. B., Tostes, R. C., Reudelhuber, T., & Touyz, R. M. (2008). Renal redox-sensitive signaling, but not blood pressure, is attenuated by Nox1 knockout in angiotensin II-dependent chronic hypertension. *Hypertension, 51*(2), 500-506.

Zhang, J., Noble, N. A., Border, W. A., & Huang, Y. (2010). Infusion of angiotensin-(1-7) reduces glomerulosclerosis through counteracting angiotensin II in experimental glomerulonephritis. *Am J Physiol Renal Physiol, 298*(3), F579-588.

Zhou, L., Xue, H., Wang, Z., Ni, J., Yao, T., Huang, Y., Yu, C., & Lu, L. (2012). Angiotensin-(1-7) attenuates high glucose-induced proximal tubular epithelial-to-mesenchymal transition via inhibiting ERK1/2 and p38 phosphorylation. *Life Sci, 90*(11-12), 454-462.

Zimmerman, D., & Burns, K. D. (2012). Angiotensin-(1-7) in kidney disease: a review of the controversies. *Clin Sci (Lond), 123*(6), 333-346.

Zimpelmann, J., & Burns, K. D. (2009). Angiotensin-(1-7) activates growth-stimulatory pathways in human mesangial cells. *Am J Physiol Renal Physiol, 296*(2), F337-346.

6.0 Appendices

6.1 Appendix 1: Primary and Secondary Antibodies

Table 7: List of primary and secondary antibodies used in this study and their dilutions.

Primary Antibodies		Secondary Antibodies	
Antibody	Dilution	Antibody	Dilution
Fibronectin (Sigma-Aldrich)	1:5000	Anti-rabbit IgG-HRP	1:2000
α-SMA (Sigma-Aldrich)	1:10 000	Anti-mouse IgG-HRP	1:2000
TGF-β	1:1000	Anti-rabbit IgG-HRP	1:2000
Phospho-p38 MAPK (Cell Signaling)	1:1000	Anti-rabbit IgG-HRP	1:2000
p38 MAPK (total) (Cell Signaling)	1:1000	Anti-rabbit IgG-HRP	1:2000
Phospho-ERK1/2 MAPK (Cell Signaling)	1:1000	Anti-rabbit IgG-HRP	1:2000
ERK1/2 MAPK (total) (Cell Signaling)	1:1000	Anti-rabbit IgG-HRP	1:2000
ACE (R&D Systems)	1:1000	Anti-goat IgG-HRP	1:2000
ACE2 (R&D Systems)	1:1000	Anti-goat IgG-HRP	1:2000
GAPDH (Sigma-Aldrich)	1:5000	Anti-mouse IgG-HRP	1:2000

Table 8: List of primary and secondary antibodies used in the detection of the AT1 receptor.

AT1 Receptor Antibodies		**Secondary Antibodies**	
Company	Dilution	Antibody	Dilution
Santa-Cruz sc-579	1:1000	Anti-rabbit IgG-HRP	1:2000
Santa-Cruz sc-31181	1:1000	Anti-rabbit IgG-HRP	1:2000
Santa-Cruz sc-1173	1:1000	Anti-rabbit IgG-HRP	1:2000
Sigma-Aldrich SAB3500209	1:1000	Anti-rabbit IgG-HRP	1:2000
Almone Labs AAR-011	1:1000	Anti-rabbit IgG-HRP	1:2000

6.2 Appendix 2: Supplementary Data

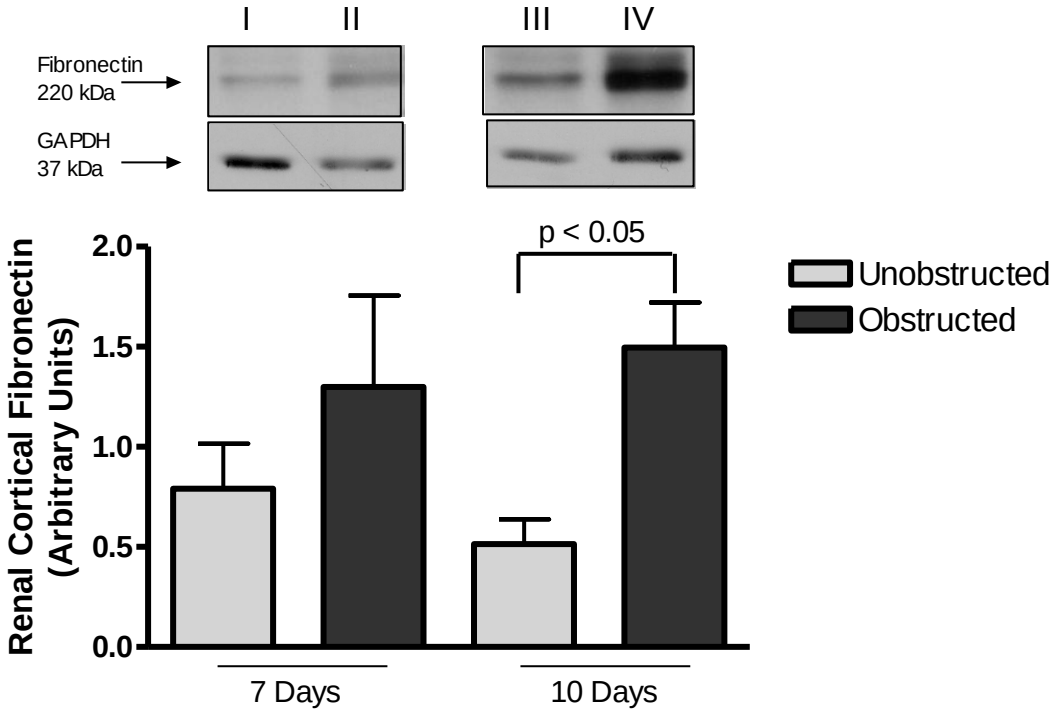

Figure 27: Effect of UUO on renal cortical fibronectin expression. Fibronectin expression in unobstructed and obstructed kidney cortex from female FVB/N mice that underwent UUO for 7 or 10 days. Representative immunoblot depicted above. Lane I: 7 day, unobstructed; lane II: 7 day, obstructed; lane III: 10 day, unobstructed; lane IV: 10 day obstructed. Values are means ± SEM (n = 3).

Table 9: Effect of Losartan on SBP in UUO

	Vehicle		**Losartan**	
	Baseline	UUO	Baseline	UUO
SBP (mmHg)	111.7±3.5	114.1±5.6	113.8±3.3	115.6±6.9

Abbreviations

SBP: systolic blood pressure

UUO: unilateral ureteral obstruction

Data are means ± SEM. (n = 8)

p = n.s. for all group comparisons.

Table 10: Effect of Losartan on body and organ weights in UUO.

	Vehicle	**Losartan**
	10 Days Post UUO	
Body Weight (g)	(25.3±0.3) 25.7±0.5	(25.6±0.3) 25.4±0.2
UKW/BW (mg/g)	8.5±0.2	8.7±0.3
OKW/BW (mg/g)	7.7±0.3	7.9±0.3
HW/BW (mg/g)	5.6±0.1	5.9±0.3

Baseline body weight indicated in parenthesis.

Abbreviations

UUO: unilateral ureteral obstruction

BW: body weight

UKW: unobstructed kidney weight

OKW: obstructed kidney weight

HW: heart weight

Data are means ± SEM. (n = 8)

p = n.s. for all group comparisons

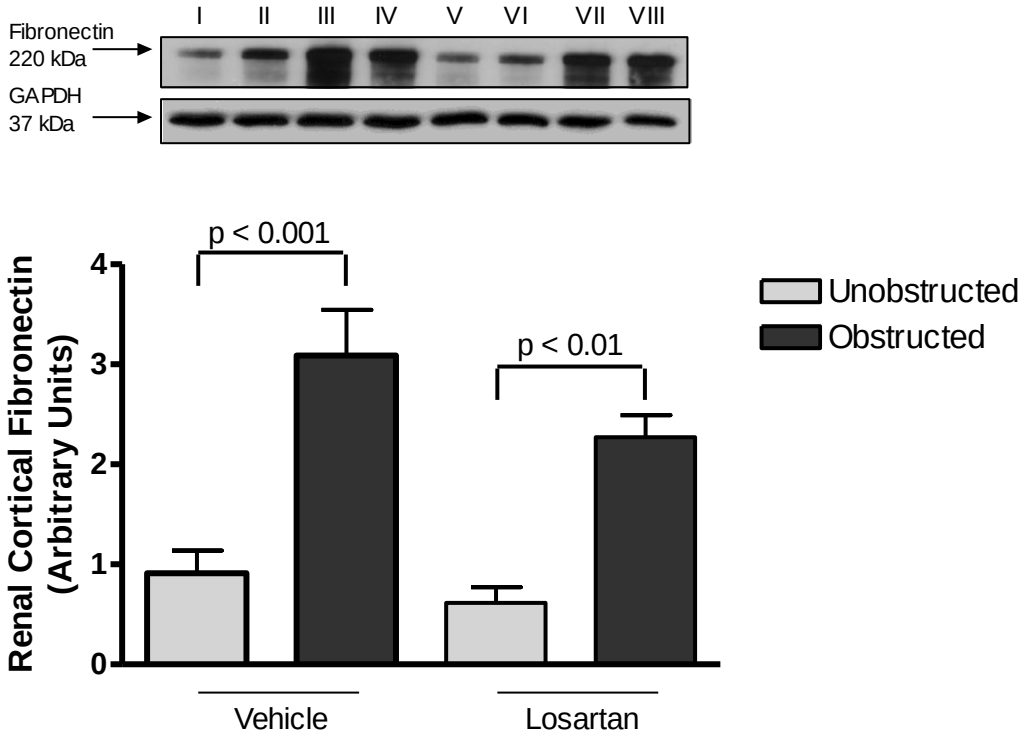

Figure 28: Effect of Losartan on renal cortical fibronectin expression in UUO. Fibronectin expression in unobstructed and obstructed kidney cortex from male C57Bl/6 mice that underwent UUO for 10 days and received vehicle or 25 mg/kg/day Losartan. Representative immunoblot depicted above. Lane I, II: unobstructed, vehicle; Lane III, IV: obstructed, vehicle; Lane V, VI: unobstructed, 25 mg/kg/day Losartan; Lane VII, VIII: obstructed, 25 mg/kg/day Losartan. Data are means ± SEM (n = 8).

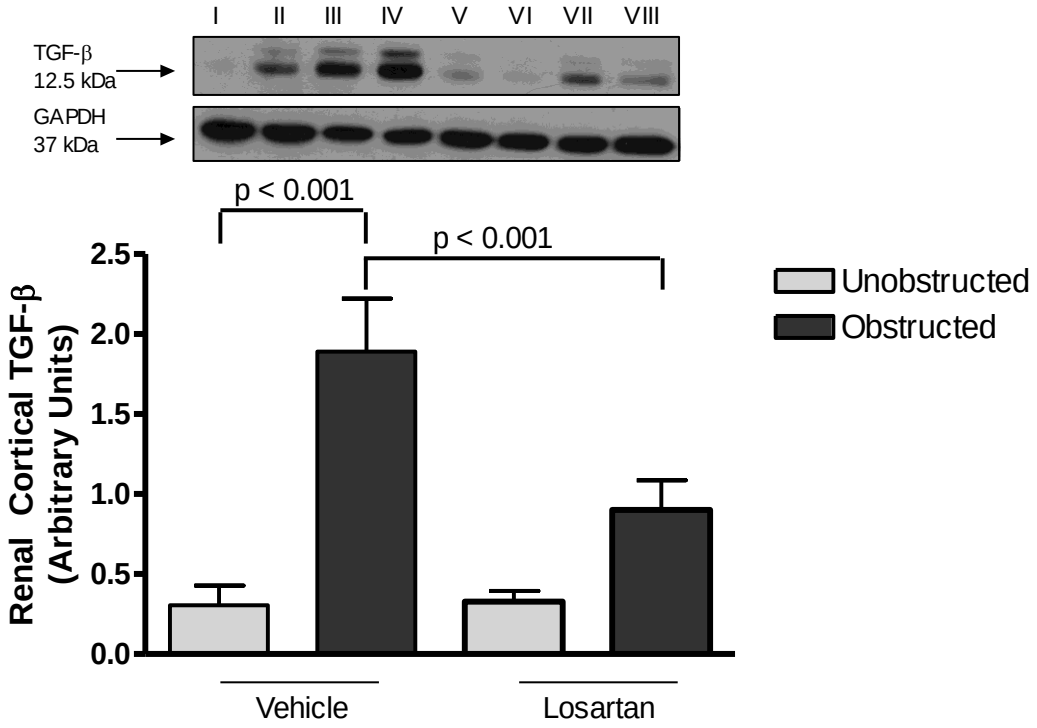

Figure 29: Effect of Losartan on renal cortical TGF-β expression in UUO. TGF-β expression in unobstructed and obstructed kidney cortex from male C57Bl/6 mice that underwent UUO for 10 days and received vehicle or 25 mg/kg/day Losartan. Representative immunoblot depicted above. Lane I, II: unobstructed, vehicle; Lane III, IV: obstructed, vehicle; Lane V, VI: unobstructed, 25 mg/kg/day Losartan; Lane VII, VIII: obstructed, 25 mg/kg/day Losartan. Data are means ± SEM (n = 8).

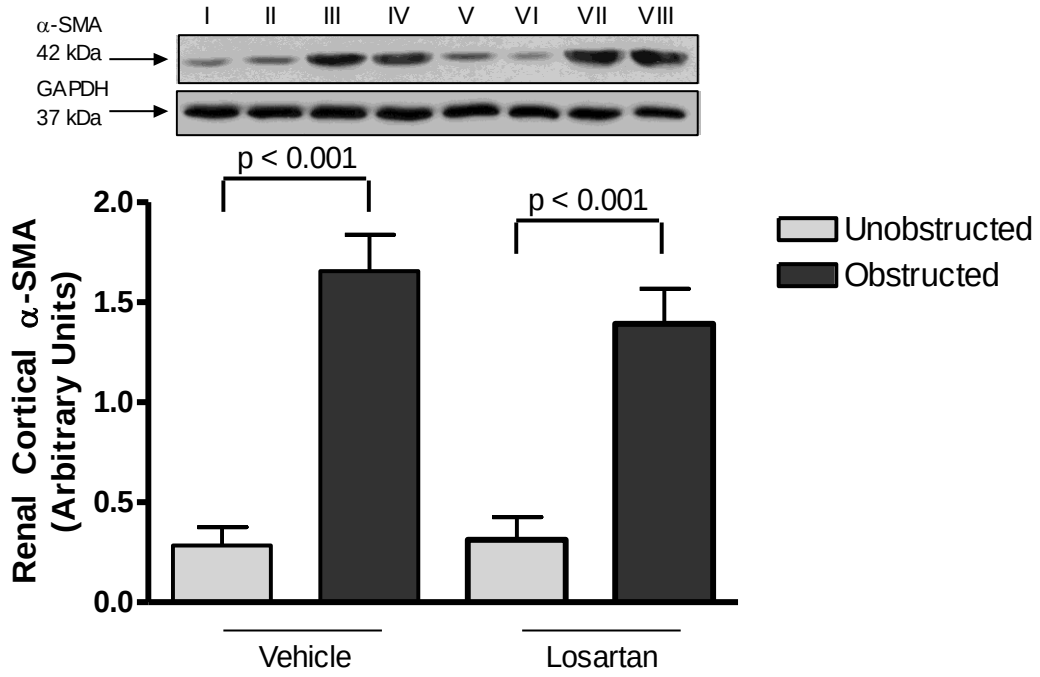

Figure 30: Effect of Losartan on renal cortical α-SMA expression in UUO. α-SMA expression in unobstructed and obstructed kidney cortex from male C57Bl/6 mice that underwent UUO for 10 days and received vehicle or 25 mg/kg/day Losartan. Representative immunoblot depicted above. Lane I, II: unobstructed vehicle; Lane III, IV: obstructed, vehicle; Lane V, VI: unobstructed, 25 mg/kg/day Losartan; Lane VII, VIII: obstructed, 25 mg/kg/day Losartan. Data are means ± SEM (n = 8).

Table 11: Effect of exogenous Ang-(1-7) on SBP in UUO

					Angiotensin-(1-7)			
		Vehicle	**6 µg/kg/hr**		**24 µg/kg/hr**		**62 µg/kg/hr**	
	Baseline	UUO	Baseline	UUO	Baseline	UUO	Baseline	UUO
SBP (mmHg)	105.0 ±4.7	109.3 ±5.1	113.1 ±5.3	115.0 ±4.3	105.3 ±6.5	106.3 ±6.4	114.7 ±3.2	114.3 ±4.0

Abbreviations

SBP: systolic blood pressure

UUO: unilateral ureteral obstruction

Data are means ± SEM. (n = 6)

p = n.s. for all group comparisons

Table 12: Effect of exogenous Ang-(1-7) on body and organ weights in UUO

		Angiotensin-(1-7)		
	Vehicle	**6 µg/kg/hr**	**24 µg/kg/hr**	**62 µg/kg/hr**
		10 Days Post UUO		
Body Weight (g)	(26.1±0.5) 27.1±0.6	(28.6±0.6) 27.4±0.6	(26.9±0.7) 26.8±0.8	(27.5±0.4) 27.9±0.4
UKW/BW (mg/g)	8.3±0.8	8.9±0.9	8.3±0.7	8.2±0.2
OKW/BW (mg/g)	7.8±0.8	7.3±0.6	7.5±0.2	7.3±0.2
HW/BW (mg/g)	6.6±0.2	6.5±0.3	7.8±0.6	6.4±0.3

Baseline body weight indicated in parenthesis.

Abbreviations

BW: body weight

UKW: unobstructed kidney weight

OKW: obstructed kidney weight

HW: heart weight

Data are means ± SEM. (n = 6)

p = n.s. for all group comparisons

Table 13: Effect of exogenous Ang-(1-7) on plasma characteristics in UUO

	Vehicle	**6 µg/kg/hr**	**24 µg/kg/hr**	**62 µg/kg/hr**
		10 Days Post UUO		
Hematocrit (%)	41.0±0.9	36.5±1.3	36.3±1.5	37.2±3.0
Na^+	146.2±1.0	145.8±0.6	145.7±0.6	144.8±1.4
K^+	4.9±0.2	4.5±0.2	4.7±0.2	4.3±0.2
Ca^{2+}	2.3±0.1	2.4±0.1	2.3	2.2±0.1
PO_4^{3-}	2.1±0.2	2.4±0.2	2.0±0.1	2.2±0.2
HCO_3^-	23.5±0.7	23.2±0.8	23.2±1.6	21.5±1.3
Mg^{2+}	0.9±0.1	1.0±0.1	1.0±0.1	0.9±0.1
Glucose	14.8±1.0	15.2±1.2	12.5±2.3	15.4±1.0
Cholesterol	2.4±0.3	2.8±0.1	2.1±0.4	2.6±0.2
Triglycerides (g/L)	0.7±0.2	1.3±0.1	0.7±0.2	1.1±0.1
Albumin (g/dL)	22.7±3.7	28.3±0.2	26.3±1.2	26.0±1.5
Urea	9.4±1.1	9.8±0.4	9.9±1.0	8.4±0.5
Creatinine (µM)	12.2±1.1	10.0±1.1	12.0±1.0	11.2±1.4

Values are in mM unless otherwise indicated.

Abbreviations

SBP: systolic blood pressure

UUO: unilateral ureteral obstruction

Data are means ± SEM. (n = 6)

p = n.s. for all group comparisons

Table 14: Effect of co-administration of A779 and Ang-(1-7) on SBP in UUO

	Vehicle		**A779**		**Angiotensin-(1-7)**		**A779 + Ang-(1-7)**	
	Baseline	UUO	Baseline	UUO	Baseline	UUO	Baseline	UUO
SBP (mmHg)	116.2 ±9.2	123.5 ±7.4	111.3 ±4.1	117.2 ±10.3	111.0 ±5.3	125. 6 ±8.2	103.5 ±2.0	108.3 ±4.4

Abbreviations

SBP: systolic blood pressure

UUO: unilateral ureteral obstruction

Data are means ± SEM. (n = 6)

p = n.s. for all group comparisons.

Table 15: Effect of co-administration of A779 and Ang-(1-7) on body and organ weights in UUO

	Vehicle	**A779**	**Angiotensin-(1-7)**	**A779 + Ang-(1-7)**
			10 Days Post UUO	
Body Weight (g)	(26.7±0.4) 27.6±0.3	(26.7±0.3) 27.1±0.4	(27.7±0.5) 27.3±0.4	(28.0±0.5) 28.5±0.7
UKW/BW (mg/g)	10.0±0.7	8.7±0.2	11.0±0.5	7.18±1.5
OKW/BW (mg/g)	9.2±0.7	7.5±0.2	8.4±0.2	7.5±0.2
HW/BW (mg/g)	7.8±0.4	6.8±0.2	7.9±0.7	7.0±0.2

Baseline body weight indicated in parentheses.

Abbreviations

BW: body weight

UKW: unobstructed kidney weight

OKW: obstructed kidney weight

HW: heart weight

Data are means ± SEM. (n = 6)

p = n.s. for all group comparisons

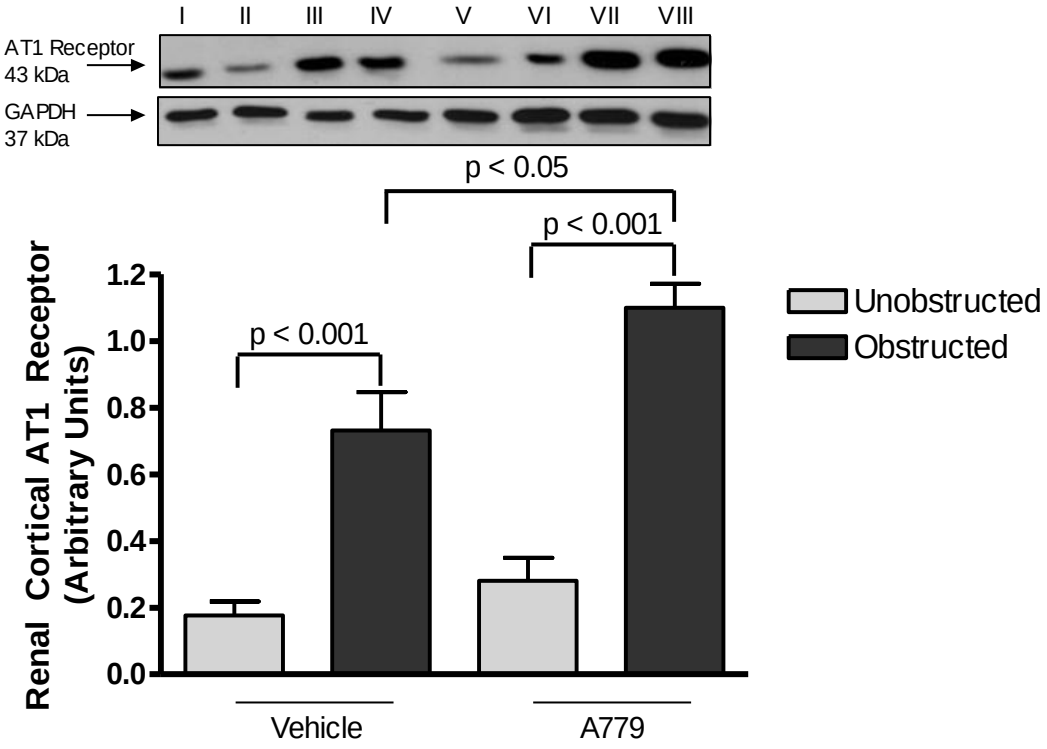

Figure 31: Effect of A779 on renal cortical AT1 receptor expression in UUO, as detected by immunoblot. AT1 receptor expression in unobstructed and obstructed kidney cortex from male C57Bl/6 mice that underwent UUO for 10 days and received either vehicle or A779 (31 µg/kg/hr). Representative immunoblot depicted above. Lane I, II: unobstructed, vehicle; Lane III, IV: obstructed vehicle; Lane V, VI: unobstructed, A779; Lane VII, VIII: obstructed A779. Data are means ± SEM (n = 12).

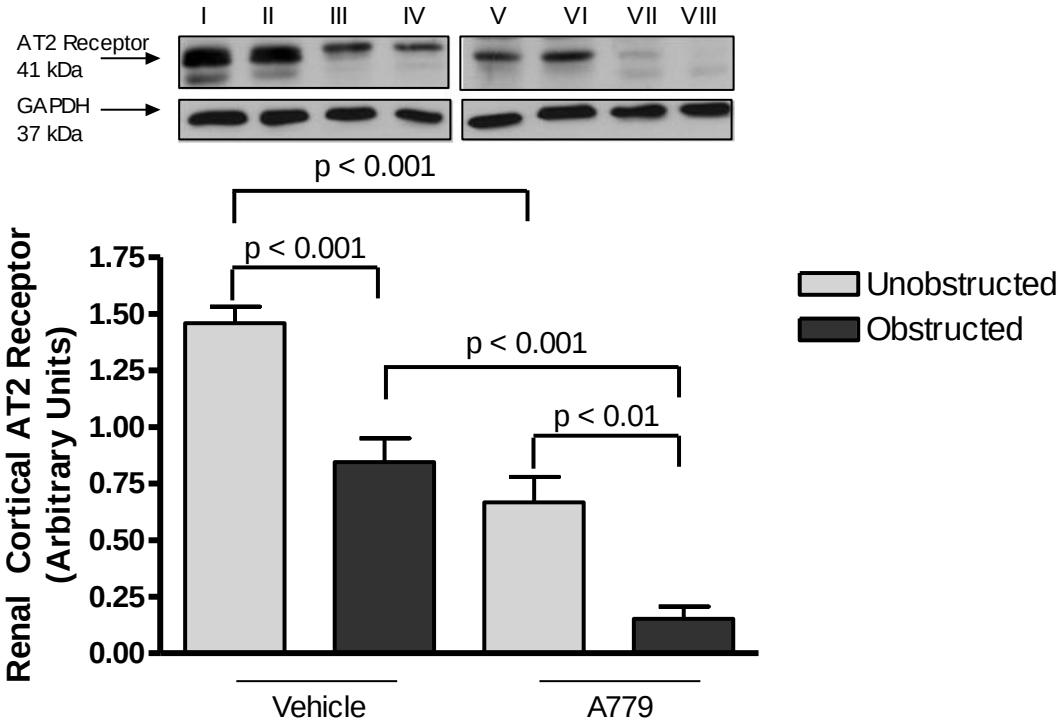

Figure 32: Effect of A779 on renal cortical AT2 receptor expression in UUO, as detected by immunoblot. AT2 receptor expression in unobstructed and obstructed kidney cortex from male C57Bl/6 mice that underwent UUO for 10 days and received either vehicle or A779 (31 µg/kg/hr). Representative immunoblot depicted above. Lane I, II: unobstructed, vehicle; Lane III, IV: obstructed vehicle; Lane V, VI: unobstructed, A779; Lane VII, VIII: obstructed A779. Data are means ± SEM (n = 12).

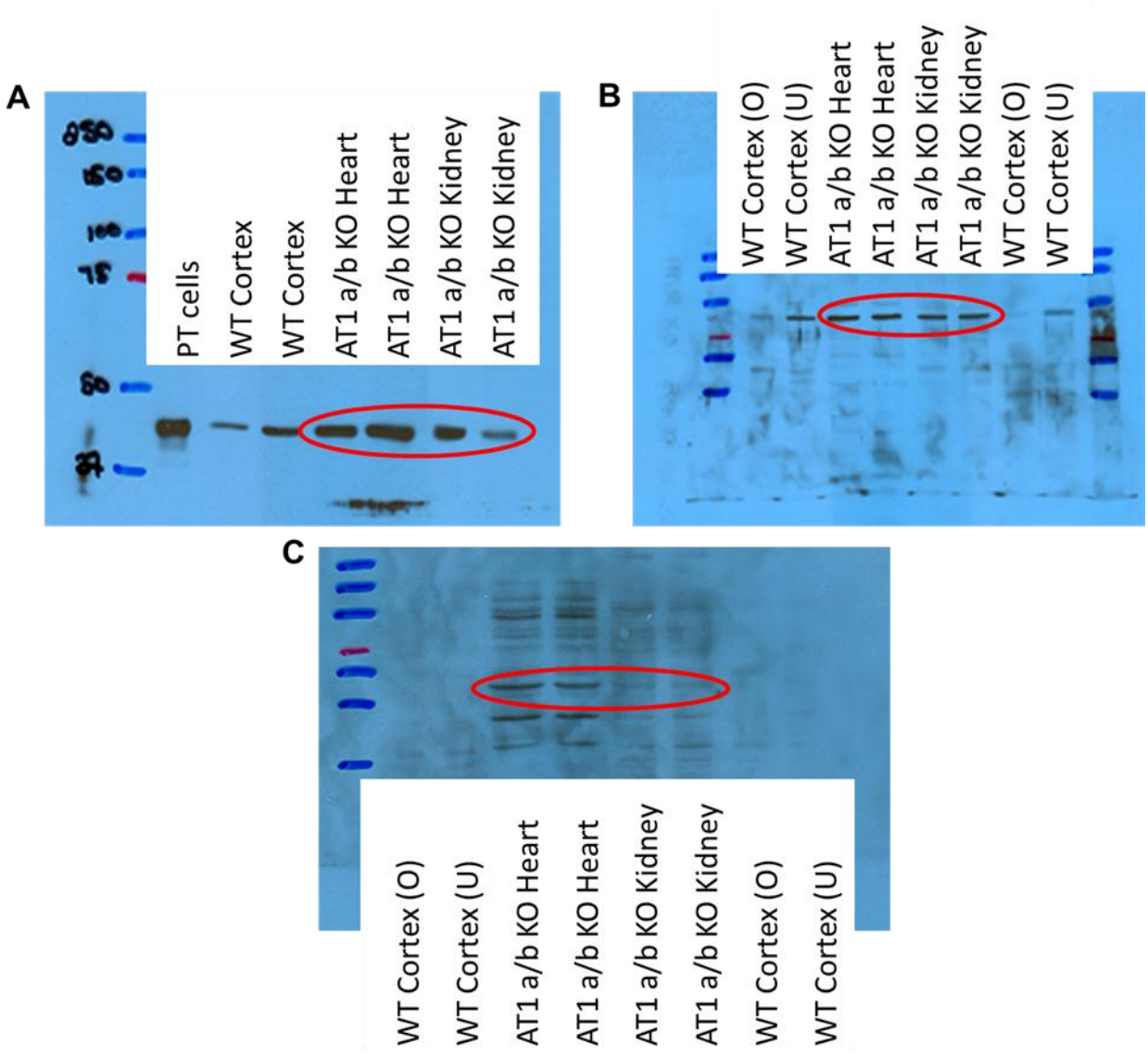

Figure 33: Representative immunblots indicating non-specific binding of AT1 receptor antibodies in AT1 receptor KO tissue. Five antibodies from Santa Cruz, Sigma-Aldrich, or Almone Labs were tested for AT1 receptor specificity. Antibody specificity was tested using $AT1_{a/b}$ KO tissue from mouse kidney and heart obtained from the laboratory of Dr. Coffman. Immunoblot depict results from antibodies from Santa Cruz: (A) SC-1173 (B) SC-579 (C) SC-31181. Non-specific bands that appeared at the expected size of the AT1 receptor protein (42 kDa) in KO tissue have been circled in red.